REVIEWS OF MODERN PHYSICS, VOLUME 76, JULY 2004

Mode-coupling theory and the glass transition in supercooled liquids

Shankar P. Das*

School of Physical Sciences, Jawaharlal Nehru University, New Delhi 110067, India

(Published 15 October 2004)

Mode-coupling theory is an approach to the study of complex behavior in the supercooled liquids which developed from the idea of a nonlinear feedback mechanism. From the coupling of slowly decaying correlation functions the theory predicts the existence of a characteristic temperature T_c above the experimental glass transition temperature T_g for the liquid. This article discusses the various methods used to obtain the model equations and illustrates the effects of structure on dynamics and scaling behavior over different time scales using a wave-vector-dependent model. It compares the theoretical predictions, experimental observations, and computer simulation results, and also considers phenomenological extensions of mode-coupling theory. Numerical solutions of the model equations to study the dynamics from a nonperturbative approach are also reviewed. The review looks briefly at recent observations from landscape studies of model systems of structural glasses and their relation to the mode-coupling temperature T_c. The equations for the mean-field dynamics driven by the p-spin interaction Hamiltonian are similar to those of mode-coupling theory for structural glasses. Related developments in the nonequilibrium dynamics and generalization of the fluctuation-dissipation relation for the structural glasses are briefly touched upon. The review ends with a summary of the open questions and possible future direction of the field.

CONTENTS

I. Introduction 786
II. Classical Liquids: Some Preliminaries 788
A. Equilibrium structure of the liquid 788
B. Time correlation functions 789
1. Neutron-scattering experiments 789
2. Light-scattering experiments 789
C. Linear response to perturbations 790
1. Fluctuation-dissipation theorem 790
2. Linear transport coefficients 790
III. Collective Modes in Classical Liquids 791
A. Hydrodynamic description 791
1. Conservation laws and balance equations 791
2. Macroscopic hydrodynamics 791
a. Local equilibrium distribution 791
b. Dissipative dynamics 792
c. Hydrodynamic fluctuations 792
B. Beyond conventional hydrodynamics 793
1. Generalized hydrodynamic modes 793
a. The projection operator 793
b. The hard-sphere liquid 794
2. Dynamics in the Markovian approximation 795
IV. Strongly Correlated Liquid 795
A. Mode-mode coupling: Some physical insight 795
B. The renormalized theory 796
1. Memory function approach 797
2. Nonlinear dynamics of collective modes 797
a. An example: Incompressible fluid 798
b. Compressible liquids 798
c. Renormalized transport coefficients 798
C. Dynamic density-functional model 800
V. Self-Consistent Mode-Coupling Theory 801
A. The one-component liquid 801
1. The schematic model 801
a. Relaxation over different time scales 801
b. The nonergodic phase $\Delta_0 \geqslant 0$ 802
c. The ergodic phase $\Delta_0 < 0$ 802
2. Effects of structure on the dynamics 802
a. The cusp behavior of the nonergodicity parameter 803
b. Scaling in power-law relaxations 804
c. The factorization property 804
d. Alpha-relaxation scaling 805
e. Viscoelastic behavior 805
3. Tagged-particle dynamics 806
B. Extensions to more complex systems 808
1. Mode-coupling theory for binary mixtures 808
2. The molecular liquid 809
a. The memory function 810
b. The glass transition scenario 811
VI. Absence of a Sharp Transition 812
A. Role of current fluctuations 812
B. Ergodicity-restoring and "hopping" processes 814
VII. Evidence from Experiments 816
A. The complex relaxation scenario 816
1. Signature of the dynamic transition 816
2. Power-law relaxations 817
a. The critical decay 817
b. von-Schweidler relaxation 817
3. The α-relaxation regime 820
a. The temperature dependence of the α peak 820
b. The scaling in the α regime 820
B. The Nagel plot and mode-coupling theory 821
C. Glass transition in colloids 822
VIII. Phenomenological Extensions of Mode-Coupling Theory 823
A. Hydrodynamics of solids 823
B. A model for structural relaxation 825
IX. Beyond Mode-Coupling Theory: Nonperturbative Approach 826

*Electronic address: shankar@mail.jnu.ac.in

 ©2004 The American Physical Society

A. Numerical solution of the Langevin equations 826
1. Nature of the relaxation 827
2. Dynamics in the free-energy landscape 827
B. Mapping onto a lattice gas model 828
X. Computer Simulation Results 830
A. Comparison with mode-coupling theory 830
B. Mode-coupling T_c: Landscape studies 831
C. Generalized fluctuation-dissipation relation 833
XI. Mode Coupling and Spin-Glass Models 834
A. p-spin interaction spin-glass model 834
B. Nonequilibrium dynamics: Spherical model 836
C. Generalization: Systems with intrinsic disorder 837
D. Comparison with the structural glass problem 838
XII. Conclusions and Outlook 839
Acknowledgments 841
Appendix: Deduction of the Self-Consistent Model 841
1. Analysis of the memory function 841
2. The field-theoretic formulation 842
a. The renormalized perturbation theory 842
b. Nonperturbative results 843
c. One-loop results 844
d. Simplified model in terms of the ρ field 844
References 845

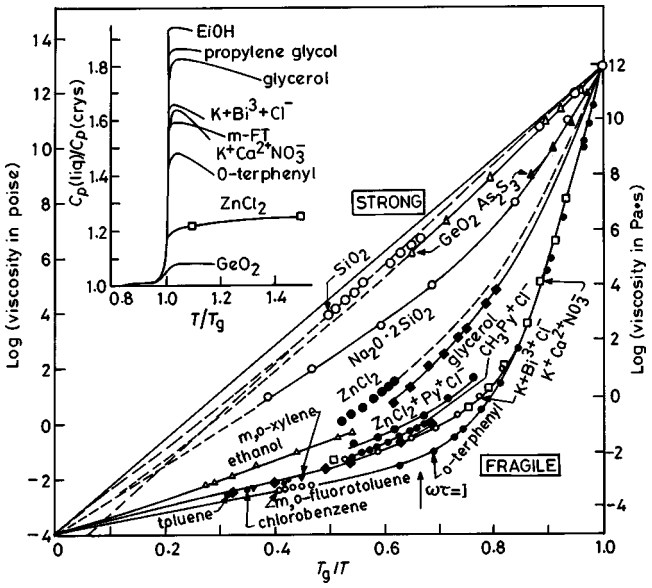

FIG. 1. Viscosity of various glass-forming liquids vs T_g/T. T_g is defined as the temperature at which the viscosity reaches 10^{14} P. From Angell, 1984.

I. INTRODUCTION

Almost every liquid undergoes a glass transition when supercooled below its freezing temperature, bypassing the formation of the crystalline state. The rapidly increasing viscosity of the liquid is a generic feature of the supercooled state. Many different expressions have been used to fit the experimentally observed temperature dependence of the viscosity. These include the standard Arrhenius form $\sim\exp(A/T)$, the Vogel-Fulcher form $\sim\exp[B/(T-T_{VF})]$, and the power-law behavior $\sim(T-T_o)^{-\gamma}$. Experimentally the temperature at which the viscosity reaches the value of 10^{14} P has usually been identified with the so-called calorimetric glass transition temperature T_g. An interesting plot of the data of glassy relaxation was made by Angell (1984) of viscosity η vs inverse temperature T_g/T scaled with T_g (see Fig. 1). The increase of viscosity in different materials occurs in different ways. One extreme is a slow growth of η with lowering of temperature T over the temperature range $T>T_g$ followed by a very sharp increase within a small temperature range close to T_g. In a number of systems described as *fragile liquids* a crossover in the temperature dependence of the viscosity η was observed. A more uniform increase is seen over the whole temperature range for strong liquids like B_2O_3 or SiO_2. This behavior has been quantified by defining a *fragility parameter* m as the slope of the viscosity-temperature curve as $m=d\ln\eta/dT$ at $T=T_g$ (Böhmer *et al.*, 1993). Thus, for example, $m=81$ (for o-terphenyl) and $m=20$ (for SiO_2) denote two extreme cases of fragile and strong systems.

Understanding the transformation of a normal liquid to an amorphous-solid-like state from the basic laws of statistical physics has been an area of strong research interest in recent times. The dynamics of the liquid state at the microscopic level are described by the classical equations of motion of a very large number of particles. Early theoretical work on the dynamics of the fluid state involved to a large extent the study of kinetic theories of hard spheres, following the approach of Maxwell and Boltzmann (Chapman and Cowling, 1970). Transport phenomena in the liquid were studied from the Boltzmann equation with Enskog corrections, which included only short-range uncorrelated binary collisions of the constituent particles. Theories of the fluid that consider only the time evolution of the microscopic states controlled by uncorrelated collisions lead to the conclusion that the fluctuations from equilibrium decay with an exponential dependence on time. Thus typical time-dependent measurements on the fluid could be understood in terms of simple exponential relaxations. Deviations from such behaviors appeared in subsequent studies. Typical examples of such cases are the density expansion of transport coefficients (Zwanzig, 1963; Kawasaki and Oppenheim, 1965; Ernst *et al.*, 1969) discovered to be nonanalytic, or computer simulation studies of hard-disk or hard-sphere fluids (Alder and Wainright, 1967, 1970) showing that the correlation of the velocity $v(t)$ of a tagged particle with the same quantity at an earlier time follows with a power-law decay ($t^{-d/2}$ in d dimensions). The traditional kinetic theories dealing with uncorrelated collisions of fluid particles were extended to study correlated motions in terms of ring and repeated-ring collision events between the fluid particles. The origin of these observed behaviors were collective or hydrodynamic effects (Zwanzig and Bixon, 1970; Pomeau and Résibois, 1975) on a semimicroscopic level. As the liquid is increasingly supercooled below its freezing point and approaches the glass transition, the role of correlated motions of the fluid particles becomes

dominant. One of the typical consequences of this process of slowing down, for example, is the fall of the self-diffusion coefficient of a tagged particle in the sea of identical particles. The motion of the tagged particle is delocalized in the normal liquid and, with increasing density, the cage formed by the surrounding particles becomes more persistent, tending to localize the tagged particle.

A related theoretical development for the dynamics of fluids came from the observation of very slow relaxation near the critical point (Hohenberg and Halperin, 1977). Following the initial work of Fixman (1962), Kawasaki (1966b) introduced the idea of including the nonlinear coupling of the slow modes in expressing the transport coefficients of the fluid. The time correlation functions of the slow modes are now expressed in terms of renormalized transport coefficients generalized to include frequency and wave-vector dependence, expressed in terms of correlation functions. Typically the renormalizing contributions are expressed as a functional $\mathcal{F}(C^0)$ of the correlation functions C^0 between the different hydrodynamic modes in the basic theory with exponential relaxations. Originally such mode-coupling models were used in the study of relaxation in systems near second-order phase-transition points (Fixman, 1962; Kadanoff and Swift, 1968; Kawasaki, 1970b). In the case of critical phenomena, the static correlations grow indefinitely near the transition point and through the mode-coupling terms the cooperative effects over different length and time scales are probed. For the normal-liquid state, mode-coupling contributions to transport coefficients (Alley *et al.*, 1983), and diffusivity (Curkier and Mehaffey, 1978) were computed at the lowest order to account for the substantial difference between computer simulation data and corresponding results obtained from the Enskog theory at the same density. More exotic results from inclusion of mode-coupling effects indicated the breakdown of conventional hydrodynamics, e.g., the long-time tails in the dynamic correlation functions (Forster *et al.*, 1977) or divergence of components of the dynamic viscosity tensor in smectic-*A* liquid crystals (Mazenko *et al.*, 1983).

The relevance of the mode-coupling theory to the theory of the glass transition emerged with the idea of expressing the mode-coupling terms, i.e., the functional $\mathcal{F}$ for the generalized transport coefficient, in terms of the full density autocorrelation function ψ. The functional $\mathcal{F}[\psi]$ and the defining relation for ψ in terms of the generalized transport coefficient thus obtained a closed equation for ψ. This provided a dynamic feedback mechanism self-consistently producing very slow dynamics for ψ (Geszti, 1983; Bengtzelius *et al.*, 1984; Leutheusser, 1984). A new approach to the study of supercooled liquid and the glass transition was thus initiated. As a result of this nonlinear feedback mechanism a dynamic transition of the liquid to a nonergodic state was predicted. In the long-time limit, the density correlation ψ freezes at a nonzero value beyond the transition point, while the thermodynamic properties of the liquid vary smoothly through the transition. The viscosity follows a power-law divergence approaching the dynamic transition point accompanied by a finite shear modulus in the glassy state. Subsequent work (Das and Mazenko, 1986) demonstrated that the sharp dynamic transition to an ideal glassy state predicted by Leutheusser (1984) and Bengtzelius *et al.* (1984) is finally removed due to coupling of the density and current fluctuations in a compressible fluid, and ergodicity is maintained at all densities. However, the above described feedback mechanism from the coupling of density fluctuations causes a substantial enhancement of the viscosity. Thus, although the sharp transition is suppressed, there are strong remnants of it causing a qualitative change in the supercooled liquid dynamics around a temperature T_c higher than the usual glass transition temperature T_g. Identification of the new temperature T_c ($>T_g$) for liquids, generally of the fragile type, has been one of the main outcomes of self-consistent mode-coupling theory. Subsequent theoretical and experimental work has focused on finding the signatures of the mode-coupling transition at T_c. The complex relaxation behavior predicted by mode-coupling theory has been observed in a wide number of experiments as well as computer simulations. Computer studies of the potential-energy landscape of simple model fragile systems has further enhanced our understanding of the complex nature of the dynamics. The recent advances in the dynamical theory of the supercooled liquid from self-consistent mode-coupling models will be the main focus of the present review. In our discussion of mode-coupling theory for the glass transition we shall follow a generalized hydrodynamic approach which we extend to the finite wave vector or corresponding short-length-scale regime. The glass transition is not intrinsically related to long distance and long time scales, which refer to hydrodynamics in the traditional sense. The transition to an amorphous-solid-like state is characterized by the freezing process occurring first over small or intermediate length scales. However, the effects of the jamming process should finally propagate to hydrodynamic regimes. In applying the continuum hydrodynamic description to liquids, it is useful to note that the length scale of the fluctuations does become comparable to the coarse-graining length. However as the density of the liquid increases, the mean free path becomes smaller than the particle size, and a continuum hydrodynamic treatment becomes more appropriate.

An outline of the review is as follows: A general background of the statics and the dynamics of the supercooled liquid in Sec. II is followed in Sec. III by a discussion of the generalized hydrodynamic approach. In Sec. IV we discuss how the mode-coupling models effectively describe strongly correlated motion in a dense liquid. In an associated Appendix we outline the different approaches to determining the self-consistent form of the model equations from the classical statistical mechanics of a many-particle system. Complex relaxation schemes and scaling predictions, as well as the corresponding corrections to the scaling laws, are reviewed in Sec. V. Here we also consider the implications of the feedback mechanism for other related properties of the

fluid like the response to shear or tagged-particle motion, and extend the mode-coupling theory to some complex situations. Work in which the ergodicity-restoring mechanism is included in the theory is discussed in Sec. VI. This is followed in Sec. VII by a review of the predictions of the mode-coupling theory that have been put to the test, with detailed analysis of data from experiments. Phenomenological extensions of mode-coupling theory, including further slow modes in the hydrodynamic description of the fluid, are reviewed in Sec. VIII. The basic equations of fluctuating hydrodynamics from which mode-coupling theory is obtained have been solved numerically and are reviewed in Sec. IX. The results of computer simulation studies of structural glasses with simple interaction potentials are discussed in Sec. X. The freezing of the liquid in the amorphous state, as seen in the structural glasses, occurs without the presence of any intrinsic disorder. This is in contrast to the so-called spin-glass systems, in which externally induced (quenched) disorderd is present. However, interesting analogies have been discovered between the two types of system, and these are reviewed in Sec. XI. We end this review with a discussion of the main achievements as well as the shortcomings of the mode-coupling theory and brief indications of the unresolved issues.

II. CLASSICAL LIQUIDS: SOME PRELIMINARIES

A liquid is a strongly interacting system intermediate between the vapor or gaseous state and the crystalline state of matter. In equilibrium it is characterized by time-independent thermodynamic properties like pressure P, or volume V, described in terms of the first derivatives of the Helmholtz (F) or Gibbs free energy (G), respectively, as $P=-(\partial F/\partial V)_T$ and $V=(\partial G/\partial P)_T$ at constant temperature T. Second derivatives of the free energy relate to experimentally measured quantities like isothermal compressibility χ_T or the thermal expansion coefficient α given, respectively, by

$$\chi_T = -V^{-1}(\partial V/\partial P)_T, \quad \alpha = V^{-1}(\partial V/\partial T)_P. \tag{2.1}$$

At the microscopic level a liquid is characterized by the elementary unit that it consists of. The basic unit characterizing a liquid varies from a single spherical atom, in an atomic liquid, to a complex molecule, in a molecular liquid. The interaction between these units is always the starting point of a theoretical model of the liquid. The mathematical formulation used to obtain a well-defined theory of the liquid state involves the hypothesis that the interatomic forces and energies in a classical liquid are dominated by a sum of pair interactions. Thus, if three or more atoms are close together in a dense liquid, the energy is the pairwise sum of the energies of the different atoms. An important feature of this pair potential in simple liquids is the harsh repulsive core that appears in the short range. It produces the characteristic short-range order of the liquid state. At long range the attractive part in the pair interaction is active and varies much more smoothly than the repulsive one. The simplest example is the hard-sphere model of a liquid with the interaction $u(r)=\infty$ for $r<\sigma$ and $=0$ for $r>\sigma$, where σ is the diameter of the hard spheres making up the liquid. Indeed the structure of a hard-sphere liquid is not significantly different from that of a liquid with a more complicated interaction potential. The hard-sphere liquid is the most commonly studied theoretical model used to understand the static, i.e., thermodynamic, as well as the dynamic properties of a liquid.

A. Equilibrium structure of the liquid

The description of the structure of a liquid begins with the pair correlation function or the radial distribution function $g(\mathbf{r}_1,\mathbf{r}_2)$. It is defined in terms of the conditional probability $\rho^{(2)}(\mathbf{r}_1,\mathbf{r}_2)$ of finding simultaneously a pair of atoms at $\mathbf{r}_1$ and $\mathbf{r}_2$, $\rho(\mathbf{r}_1,\mathbf{r}_2)=n^2g(\mathbf{r}_1,\mathbf{r}_2)$, where $n=N/V$ is the number of particles per unit volume. In equilibrium, translational invariance holds and for an isotropic system $g\equiv g(r_{12})$ is a function only of the distance between the two points. For small r, $g(r)$ is vanishing due to the repulsive core of the interaction potential, while for large r, $g(r)\to 1$, implying that the probability of two particles being at two widely separated points goes to the trivial limit n^2. In this description $g(r)$ is the most fundamental quantity in describing the equilibrium structure. Other thermodynamic properties like the pressure and the isothermal compressibility of the liquid are related to $g(r)$. $g(r)$ is often described in terms of the Fourier-transformed quantity called the *static structure factor* $S(k)$,

$$S(k) = 1 + n\int e^{i\mathbf{k}\cdot\mathbf{r}}h(r)d\mathbf{r}, \tag{2.2}$$

where $h(r)=g(r)-1$.

Theoretical calculation of $g(r)$ or $S(k)$ involves defining a new type of function, the *direct correlation function* $c(r)$, through the Ornstein-Zernike relation

$$h(r) = c(r) + n\int c(|\mathbf{r}-\mathbf{r}'|)h(r')d\mathbf{r}', \tag{2.3}$$

or equivalently $S(k)=[1-nc(k)]^{-1}$ in Fourier space. To solve for $g(r)$ and $c(r)$, for a given pair potential $u(r)$, we need to supplement Eq. (2.3) with a closure relation. Two standard prescriptions for this are, respectively, the Percus-Yevick (Percus and Yevick, 1958) solution and the hypernetted-chain closure (van Leeuwen *et al.*, 1959). The Percus-Yevick solution is most suitable for describing correlations between particles when the interaction potential is harshly repulsive or short range, e.g., a hard-sphere interaction. The hypernetted chain, on the other hand, is well suited for long-range potentials like those in Coulombic systems. However, for strongly coupled systems like the high-density or low-temperature liquids, both these closures lead to severe thermodynamic inconsistency (Hansen and McDonnald, 1986) since the virial and compressibility equations, respectively, lead to different equations of state (Carnahan and Starling, 1969). This problem was addressed by proposing bridge functions that interpolate between the

Percus-Yevick and hypernetted-chain schemes. The bridge function is adjusted to achieve full consistency between the two equations of state (Rogers and Young, 1984). For interaction potentials having an attractive potential well (a typical example is the Lennard-Jones interaction potential) the structure factors are also obtained by using the bridge function method mentioned above (Zerah and Hansen, 1986; Due and Haymet, 1995; Due and Henderson, 1996). The static structure factor for the liquid obtained through these schemes provides an accurate description of the thermodynamic properties at high density. Experimentally $S(k)$ and hence $g(r)$ is measured through scattering experiments with different types of incident radiation: electromagnetic (x rays, γ rays, light), electrons, neutrons, etc. The intensity from elastic scattering at a certain wave number k is related to the structure factor $S(k)$. The scattering centers in the sample liquid are different for different sources of radiation. The average scattered intensity $I(q)$ is proportional to the structure factor $S(k)$.

B. Time correlation functions

Time correlation of the dynamic variables averaged over the equilibrium ensemble forms an important ingredient in the study of the dynamics of a fluid (Onsager, 1931a, 1931b; Kadanoff and Martin, 1963). Let $\hat{\psi}_a$ and $\hat{\psi}_b$ denote some space-time-dependent dynamic properties of the fluid. The correlation function of the fluctuation of $\hat{\psi}_a$ and $\hat{\psi}_b$ around the corresponding equilibrium average is defined as

$$C_{ab}(r,r',t,t') = \langle \delta\hat{\psi}_a(\mathbf{r},t)\,\delta\hat{\psi}_b(\mathbf{r}',t')\rangle = C_{ab}(|r-r'|,t-t'), \tag{2.4}$$

where the angular brackets denote an average in the equilibrium ensemble in which time translational invariance and isotropy hold. The most important time correlation function for a fluid is that of the number density fluctuations denoted by $\delta n(\mathbf{r},t)=n(\mathbf{r},t)-n$, conveniently described in terms of the spatial Fourier transform,

$$F(\mathbf{k},t) = \frac{1}{V}\langle \delta n(\mathbf{k},t)\,\delta n(-\mathbf{k},0)\rangle. \tag{2.5}$$

The spectral quantity $S(k,\omega)$, which is the two-sided frequency transform of $F(k,t)$, is called the *dynamic structure factor*. In the equal-time limit, the correlation function $F(k,t=0)=nS(k)$ where $S(k)$ is the static structure factor defined in Eq. (2.2). In the theoretical models considered in the present review, the interaction potential between the particles of the fluid will influence its dynamic properties through the effect on the static structure factor.

Essentially all scattering experiments probing the dynamic properties of a fluid measure the time correlation functions. The frequency-dependent structure factors in this case are obtained from the intensity of the inelastic scattering. Let us consider some specific cases.

1. Neutron-scattering experiments

Neutron scattering usually accesses the liquid dynamics at time scales of 10^{-12}–10^{-7} s (Lovesey, 1984). For supercooled liquids the earliest studies of the dynamics were carried out at much lower frequencies corresponding to the very slow relaxations characteristic of such systems. However, more recent theoretical models probe the nature of the glassy dynamics (see Sec. V) over intermediate time and length scales. This is where neutron-scattering experiments have been very effective (Mezei, 1980, 1989). Several techniques have been employed for studying dynamic properties of the liquid using neutron scattering:

(a) A backscattering configuration geometry with the source and detector at 180° has achived high resolution. The corresponding Bragg angle $\theta=90°$ improves the energy resolution $\delta E/E=\cot\vartheta d\vartheta$.

(b) Time-of-flight experiments measure the flight time between the scattering event and the detection of cold (low-energy) neutrons. The time-of-flight data give the dynamic structure factor $S(2\theta,\omega)$ where 2θ is the scattering angle.

(c) The neutron spin-echo technique (Mezei, 1980; Lovesey, 1984) uses the number of Larmor precessions the neutron spin undergoes in a homogenous magnetic field to determine the neutron velocity change in the scattering event. This technique has been used to obtain the density autocorrelation function in the time-space domain (Mezei *et al.* 1987; Mezei, 1989).

2. Light-scattering experiments

Dynamic light-scattering techniques (Berne and Pecora, 1976) have also been used extensively in recent years for studying the dynamics of supercooled liquids (Pusey, 1991). The scattered speckle intensity carries information about the location of the particles in the liquid. The time correlation of this intensity obtains the dynamic density correlation function in time. Using scattering of monochromatic light beams, one studies the liquid dynamics over time scales of 10^{-12}–10^{2} s. A useful light-scattering technique for time domain measurements is *impulsive stimulated thermal scattering* (Yan and Nelson, 1987a, 1987b; Halalay *et al.*, 1994). It is applied in the study of supercooled liquids over time scales 10^{-12}–10^{-3} s. For optically isotropic liquids, the intensity of the scattered light having a transverse polarization with respect to the incident (depolarized) light is zero. However, a substantial intensity of the depolarized component is seen in the scattered light from an atomic liquid. Depolarized light scattering (Levine and Birnbaum, 1968) has been used extensively for studying the dynamic behavior of liquids and gases. Here scattering from a pair of density fluctuations results from interactions due to the dipole-induced-dipole mechanism (Berne and Pecora, 1976).

Besides the density autocorrelation, another important quantity often studied is the tagged-particle velocity autocorrelation, $\langle \mathbf{v}(t)\cdot\mathbf{v}(0)\rangle$, which is essential for understanding single-particle dynamics in the fluid (the angular brackets indicate an equilibrium average). In a dense fluid this correlation becomes negative for large t, signifying the rattling motion of a particle in the cage formed by its surrounding particles. This is generally termed the *cage effect*. The square of the displacement of the tagged particle from its initial position defines the *diffusion coefficient* D_s through the Einstein relation $\langle r^2(t)\rangle \sim D(t)t$. The corresponding frequency-dependent diffusion coefficient $D_s(\omega)$ of the tagged particle is obtained as an integral of the velocity autocorrelation,

$$D(\omega) = \frac{1}{3}\int_0^\infty dt e^{i\omega t}\langle \mathbf{v}(t)\cdot\mathbf{v}(0)\rangle. \tag{2.6}$$

$D_s(\omega\to 0)=D_s$ is the long-time limit of the tagged-particle diffusion coefficient. The velocity autocorrelation function develops a negative tail as a result of the cage effect, and this causes a fall in the diffusion coefficient, as can be seen from Eq. (2.6). In a normal liquid, D_s has an inverse dependence on the shear viscosity given by the Stokes-Einstein relation, $D_s=k_BT/(V\eta)$. The diffusion coefficient of a tagged particle in a dense fluid has been measured in real as well as computer experiments. Experimental techniques include measurement of tracer diffusion by inserting a dye molecule in the liquid and indirect calculation of self-diffusion from the van Hove correlation function using the incoherent part of the dynamic light scattering (van Megen *et al.*, 1998). Nuclear magnetic resonance (NMR) methods have also been used extensively in recent years for measuring the diffusion constant in supercooled liquids. In NMR experiments the change in the nuclear precession is monitored. The discrepancy in this phase caused by the motion of the fluid particle from a given point into another region, where the applied field is slightly different, has been used to measure the diffusion coefficient since the work of Carr and Purcell (1954).

C. Linear response to perturbations

The linear response of a dynamic variable $\hat{a}$ to an external time-dependent field $h_a(\mathbf{r},t)$ is induced by the interacting part of the Hamiltonian,

$$H'(t) = -\int \hat{a}(\mathbf{r})h_a(\mathbf{r},t)d\mathbf{r}. \tag{2.7}$$

The average change in a dynamic variable $\hat{b}$ at time t from the corresponding equilibrium average $\langle\hat{b}\rangle$ is obtained in terms of the linear-response function,

$$\langle\Delta\hat{b}(t)\rangle = \int_{-\infty}^{+\infty} dt' R_{ba}(t-t')h_a(t'), \tag{2.8}$$

such that $R_{ba}(t-t')$ is zero for $t'>t$ due to causality. A typical example is the measurement of the response function in dielectric experiments. The time-dependent polarization due to the dipoles lags behind the applied dynamic field—the time lag represents the dielectric relaxation and it results in an absorption of energy from the external field. The response of the system to a time-dependent external field has been used to study liquid dynamics (Williams and Watts, 1970). If $\tilde{\mathbf{P}}(\mathbf{r},t)$ is the polarization induced in a sample at the point $(\mathbf{r},t)$ where the electric field is $\mathbf{E}(\mathbf{r},t)$, then the corresponding linear-response function denoted by χ_{ij} is the dielectric susceptibility. The frequency and wave-vector transform of χ in the isotropic fluid, i.e., $\chi(q,\omega)$, is given by $\tilde{\mathbf{P}}=\chi(\omega)\mathbf{E}$. In the $q\to 0$ limit, this gives the dielectric susceptibility function $\chi(\omega)$ and is related to the corresponding complex dielectric permittivity, $\tilde{\epsilon}(\omega)=1+4\pi\chi(\omega)$. Here $\tilde{\epsilon}$ is a complex function whose real and imaginary parts are related through the Kramers-Kronig relation. The linear-response function corresponding to the external field is measured using different methods over various frequency ranges. The lowest frequency range of μHz–kHz is studied using time domain spectrometers (Mopsik, 1984), while the range of 1 MHz–10 GHz is covered with reflectometric techniques (Böhmer *et al.*, 1989). In recent times the linear dielectric response of a liquid has been measured over 18–20 decades of frequency (Schneider *et al.*, 1999).

1. Fluctuation-dissipation theorem

The equilibrium correlation function C_{ba} between the two dynamical variables a and b is related to the response function through the fluctuation-dissipation theorem,

$$R_{ba}(t-t') = -\Theta(t-t')\frac{1}{k_BT}\frac{\partial C_{ba}(t-t')}{\partial t'}. \tag{2.9}$$

The validity of the fluctuation dissipation theorem in the supercooled metastable state has been widely investigated in recent times and will be discussed in the present context of structural glasses in Sec. X.C and mean-field spin models in Sec. XI.B.

2. Linear transport coefficients

Fluctuations out of equilibrium occur in the fluid either spontaneously or due to an external perturbation, and their dissipation is an irreversible processes. The irreversible flux J_i of a physical property (mass, momentum, or energy) in the fluid is assumed to be linearly proportional to the gradient X_j of the conjugate thermodynamic property driving the flux. The matrix of linear transport coefficients is defined through the phenomenological constitutive relation

$$J_i = \sum_j L_{ij}X_j. \tag{2.10}$$

For heat conduction, Eq. (2.10) is Fourier's law with the constant of proportionality giving the thermal conductivity tensor λ_{ij}, whereas if J_i is the flux of matter this

describes Fick's law, and X_j corresponds to the concentration gradient, the corresponding transport coefficient being the diffusion coefficient tensor D_{ij}. In an isotropic fluid $\lambda_{ij}=\lambda\delta_{ij}$ and $D_{ij}=D_o\delta_{ij}$ where λ_o denotes the thermal conductivity and D_o is the diffusion coefficient. In a dense fluid, cooperative dynamics over different lengths and times are effective and hence the linear relation (2.10) is often generalized to a form that is nonlocal in both time and space. This results in frequency- and wave-number-dependent-generalized transport coefficients, which can be expressed in terms of equilibrium-averaged time correlation functions of suitable currents and are termed Green-Kubo relations. For example, the shear viscosity η of the fluid is expressed in terms of the time correlation of the transverse part of the flux corresponding to momentum density, i.e., the stress tensor σ_{ij},

$$\eta = n\beta\int_0^\infty d\tau\langle\sigma_{xy}(\tau)\sigma_{xy}(0)\rangle. \tag{2.11}$$

Microscopic expressions for σ_{xy} in terms of the interaction potential of the fluid particles are used to compute η from Eq. (2.11). This is particularly useful in computer simulations. A similar expression for the self-diffusion coefficient in terms of the velocity autocorrelation function is given by Eq. (2.6). In supercooled liquids direct measurements of the frequency-dependent transport coefficients have been made. For example, the frequency-dependent shear viscosity $\eta(\omega)$ was obtained by Menon *et al.* (1994), who applied a shear in the fluid between two plates and measured the balancing torque. Similarly the longitudinal viscosity of a supercooled liquid was measured from ultrasonic sound attenuation within it (Jeong *et al.*, 1986; Jeong, 1987), while the frequency-dependent specific heat was measured from the dynamic thermal response (Birge and Nagel, 1985; Dixon and Nagel, 1988).

III. COLLECTIVE MODES IN CLASSICAL LIQUIDS

A. Hydrodynamic description

The hydrodynamic description of a fluid involves a set of smoothly varying field variables which are obtained by coarse-graining the mass, momentum, and energy of the constituent particles over microscopic scales. A set of equations for the time evolution of these local densities describes the spatio-temporal behavior of the fluid over the corresponding length and time scales. The origin of these equations are microscopic conservation laws of the respective physical quantities. Thus in an isotropic fluid there are five conserved densities corresponding to the total mass, momentum, and energy.

1. Conservation laws and balance equations

At the microscopic level the conserved densities at a given space-time point $(\mathbf{r},t)$ are defined in terms of the phase-space coordinates, i.e., position and momentum $\{\mathbf{r}_\alpha,\mathbf{p}_\alpha\}\in\alpha=1,N$, of the N particles of the classical fluid as

$$\hat{\psi}(\mathbf{r},t)=\sum_\alpha \psi_\alpha\delta[\mathbf{r}-\mathbf{r}_\alpha(t)], \tag{3.1}$$

where $\psi_\alpha\equiv\{m,\mathbf{p}_\alpha,e_\alpha\}$ refers to the mass, momentum, and energy, respectively, of the αth particle. The significance of the above definitions for the microscopic variables is apparent in the coarse-grained picture. For example, the integral of the density $\hat{\rho}(\mathbf{r},t)$ over an elementary cell around the point $\mathbf{r}$ gives the total mass of the particles present inside it at time t. Each of these conserved densities in the set $\hat{a}(\mathbf{r})\equiv\{\hat{\rho}(\mathbf{r}),\hat{\mathbf{g}}(\mathbf{r}),\hat{e}(\mathbf{r})\}$ satisfies microscopic balance equations of the form $\partial_t\hat{\psi}+\nabla\cdot\mathbf{J}_\psi=0$ which retain time-reversal symmetry. For the five conserved densities $\{\hat{\rho},\hat{\mathbf{g}},\hat{e}\}$ the corresponding currents are, respectively, the mass current density $\hat{\mathbf{g}}$, the momentum current density or the stress tensor $\hat{\sigma}$, and the energy current $\hat{\mathbf{J}}_e$. Microscopic expressions for the currents $\hat{\mathbf{J}}_a$ in terms of the phase-space coordinates $\{\mathbf{r}_\alpha,\mathbf{p}_\alpha\}\in\alpha=1,N$ are obtained using the equations of Hamiltonian dynamics (Zubarev *et al.*, 1997).

2. Macroscopic hydrodynamics

a. Local equilibrium distribution

The nonequilibrium state of the fluid described in hydrodynamics corresponds to the time regime where it has reached a state of local equilibrium. At this stage the local densities $\{\hat{a}(\mathbf{r})\}$ are sufficient to describe the state of the system. The probability function for the local equilibrium state is obtained in analogy with that of the equilibrium state. For an equilibrium state with a set of conserved quantities $\mathbf{A}=\{N,H,\mathbf{P},\ldots\}$, the probability density of the grand ensemble is $f_{eq}(\mathbf{x}^N)\sim\exp[-\beta(H-\mu N+\mathbf{P}\cdot\mathbf{v})]$, with the respective thermodynamic variables being given by the set $\mathbf{b}=\{\beta,\mu,\mathbf{v}\}$ referring to the inverse temperature, chemical potential, and velocity. Analogously, the local equilibrium state f_{le} is characterized by the set of local thermodynamic variables $\{\beta(\mathbf{r},t),\mu(\mathbf{r},t),\mathbf{v}(\mathbf{r},t)\}$, now dependent on the space and time.

The average of the microscopic density $\langle\hat{\psi}(\mathbf{r},t)\rangle_{le}$ over the local equilibrium distribution function f_{le} gives the corresponding hydrodynamic field $\psi(\mathbf{r},t)$ with smooth spatio-temporal dependence. The dynamical equations for $\psi(\mathbf{r},t)$ are obtained in the form $\partial_t\psi+\nabla\cdot\bar{\mathbf{J}}_\psi=0$, where the $\bar{\mathbf{J}}_\psi$ denote the average microscopic current $\hat{\mathbf{J}}_\psi$ with respect to the local equilibrium distribution. By a canonical transformation to a locally moving frame defined through $\mathbf{p}_\alpha=\mathbf{p}'_\alpha+m\mathbf{v}(\mathbf{r}'_\alpha)$ and $\mathbf{r}_\alpha=\mathbf{r}'_\alpha$, the average currents are obtained as (Zubarev *et al.*, 1997)

$$\bar{\mathbf{J}}_\rho=\mathbf{g}=\rho\mathbf{v};\quad \bar{\mathbf{J}}_e=\left(\epsilon+\frac{\rho v^2}{2}+P\right)\mathbf{v},$$
$$\bar{\sigma}_{ij}=P\delta_{ij}+\rho v_i v_j. \tag{3.2}$$

Here we have used the definitions $\bar{\sigma}'_{ij}=P(\mathbf{x},t)\delta_{ij}$ and $\bar{\epsilon}'=\epsilon(\mathbf{x},t)$ for the pressure $P(\mathbf{x},t)$ and the internal energy

density $\epsilon(\mathbf{x},t)$, respectively, in the local rest frame. These currents given by Eq. (3.2) constitute the Euler equations for the hydrodynamics representing reversible dynamics. The entropy of the fluid in the local equilibrium state, defined as $S(t)=-\langle \ln f_{le}(t)\rangle$, remains unchanged for an isolated system.

b. Dissipative dynamics

Dissipative processes due to irreversible transport in the fluid are included in the equations of motion for the local densities in a phenomenological manner. There is no dissipative part in the mass current $\mathbf{g}$, which itself is a conserved quantity. The other dissipative currents are expressed in terms of the gradients of the local temperature $T(\mathbf{r},t)=\beta^{-1}(\mathbf{r},t)$ and velocity $\mathbf{v}(\mathbf{r},t)$,

$$\sigma_{ij}^{D}=\sum_{k,l}\eta_{ijkl}\nabla_k v_l, \quad [\mathbf{J}_{\epsilon}^{D}]_i=\sum_j \lambda_{ij}\nabla_j T. \tag{3.3}$$

The tensor η_{ijkl} and λ_{ij} refer to the viscosity and thermal conductivity, respectively, of the liquid. The forms for the dissipative currents (3.3) follow from general thermodynamic considerations like positive entropy production in an irreversible process (Martin *et al.*, 1972). For an isotropic fluid the transport matrices can be further simplified as follows: The fourth-rank tensor η_{ijkl} is expressed in terms of two independent coefficients, η_o and ζ_o, called the shear and bulk viscosities, respectively. The thermal conductivity λ is given by $\lambda_{ij}=\lambda\delta_{ij}$. The set of hydrodynamic equations for the averaged local densities $\{\rho(\mathbf{r},t),\mathbf{g}(\mathbf{r},t),\epsilon(\mathbf{r},t)\}$ is thus

$$\begin{aligned}
&\partial_t\rho+\nabla\cdot\mathbf{g}=0,\\
&\partial_t g_i+\nabla_j[g_i g_j/\rho]=-\nabla_i P+L_{ij}^{o}v_j,\\
&\partial_t\epsilon+\mathbf{v}\cdot\nabla\epsilon=-h\nabla\cdot\mathbf{v}+\lambda\nabla^2 T,
\end{aligned} \tag{3.4}$$

where $h=e+P$ is the enthalpy density, with e the energy density, and P the pressure in equilibrium. The dissipation matrix L_{ij}^{o} relates to the viscosities as

$$L_{ij}^{o}=\eta_o'\delta_{ij}\nabla^2+\eta_o\nabla_i\nabla_j \tag{3.5}$$

with the longitudinal viscosity $\eta_o'=\zeta_o+\eta_o/3$. Conventional hydrodynamics as described by Eq. (3.4) considers only slow processes occurring over long length and time scales. At what is known as the Navier-Stokes order, the dissipative terms are considered to be linearly proportional to the gradients of the local thermodynamic fields. The macrodynamic equations including the terms up to second order in the gradients are called the Burnett equations. The transport coefficients appearing in the hydrodynamic equations are system-dependent constants and are treated as inputs. Transport coefficients for a given interaction potential are computed in the kinetic theory of fluids.

To compute the transport coefficients for a given liquid in terms of the basic interactions of the particles, a suitable kinetic equation is used to describe the irreversible dynamics of the system at the microscopic level. The starting point of such a theory is the Liouville equation (Hansen and McDonald, 1986) for the N-particle distribution function $f^{(N)}(\mathbf{r}_\alpha,\mathbf{p}_\alpha,t)$, from which the equation for the reduced distribution function $f^{(n)}$ is obtained by integrating out the rest of the $(N-n)$ degrees of freedom. The set of equations of motion for $n=1,N$ constitute the BBGKY hierarchy equations. The basic kinetic equation in terms of the one-particle reduced probability distribution function $(n=1)$ is obtained with a suitable closure of this hierarchy. In the simplest form the dynamics are taken into account at the level of uncorrelated two-body collisions. At higher densities Enskog corrections are included in the kinetic theory to obtain density-dependent transport coefficients (Chapman and Cowling, 1970; Résibois and de Leener, 1977).

c. Hydrodynamic fluctuations

The hydrodynamics variables, e.g., the density field $\rho(\mathbf{x},t)$, fluctuate due to chaotic motion of the actual fluid particles (or due to a random external field). Conventional hydrodynamics refers to properties of the fluid over length and time scales long compared to the corresponding characteristic microscopic ranges. The corresponding hydrodynamic fluctuations (Landau and Lifshitz, 1963) are those of low frequency ω and small wave number k, so that $\omega\tau_c\ll 1$ and $kl\ll 1$, where τ_c is the mean time between collisions and l is the average particle spacing in the liquid. The equations satisfied by the fluctuations are similar to Eq. (3.4), which involves nonlinear coupling of the modes. Let us consider first the linearized dynamics of the fluctuations. The hydrodynamic equations are not in a closed form with the field variables $\psi(\mathbf{x},t)$. Equations (3.4) involve local properties (like local pressure P, temperature T, and velocity v) which are generalizations of the corresponding thermodynamic properties of the equilibrium state. When we Fourier-transform the first two equations in Eq. (3.4) (we ignore energy fluctuations for simplicity) in the small k-limit, we obtain

$$\begin{aligned}
&\partial_t\delta\rho(k,t)+i\mathbf{k}\cdot\mathbf{g}(k,t)=0,\\
&\partial_t\mathbf{g}(k,t)+i\mathbf{k}c_o^2+\eta_o^K k^2\mathbf{g}(k,t)+\eta'^{K}_{o}\mathbf{k}k\cdot\mathbf{g}(k,t)=0,
\end{aligned} \tag{3.6}$$

where $\eta_o'^{K}=\eta_o'/\rho_o$ and $\eta_o^K=\eta_o/\rho_o$, with $\rho_o=mn$ being the average mass density. The dissipative equations given by Eq. (3.6) are applicable for length and time scales long compared to the microscopic scales. The constant transport coefficients like η_o^K, etc., are input parameters in the theory. In reaching the closed form of those equations we have used a generalization of the corresponding thermodynamic relation $\nabla P=c_o^2\nabla\delta\rho$, where $c_o^2=(\partial P/\partial\rho)_T$ is the isothermal speed of sound.

In an isotropic fluid the four equations (3.6) split into (a) two coupled longitudinal equations consisting of the mass density ρ and the longitudinal component of momentum current g and (b) two identical equations for the transverse components of momentum g. The linearized dynamical equations for the fluctuations of the hydrodynamic fields obtain exponentially decaying modes

$[\sim\exp(z_\mu t)]$. For the longitudinal case $z_\mu(k)=\pm ic_o k+\Gamma_o k^2$ for $\mu=1,2$ constitutes a complex-conjugate pair, signifying two propagating sound modes with speed c_o and attenuation $\Gamma_o=\eta_o'+\eta_o$. The two transverse modes are degenerate, $z_{T1}(k)=z_{T2}(k)=\eta_o k^2$, corresponding to shear fluctuations decaying through diffusion. If the equation for the energy fluctuation is included in the set (3.6), there is an extra decay mode in the longitudinal part with decay rate $z_H=-ik^2D_o$, where D_o is the heat diffusion constant in the isotropic fluid. This third decay mode (in addition to the two sound modes) represents the energy diffusion over the hydrodynamic length and time scales and is termed the *heat mode*.

B. Beyond conventional hydrodynamics

A theoretical formulation of the dynamics of dense fluids going beyond the Enskog approximation (see Sec. III.A.2.b) is possible in several ways. An important step in this direction is the revised Enskog theory of van Beijeren and Ernst (1973) for hard-sphere fluids at high density. Here the dependence of the local structure of the fluid on the nonequilibrium density is included in the collision term describing the two-body interaction process. Thus the pair correlation function $g^{ne}(r_{12})$ of the nonequilibrium fluid is treated as a functional of the local density $\rho(t)$. The revised Enskog theory for dense liquids was used by de Schepper and Cohen (1980, 1982) to consider short-wavelength and short-time phenomena beyond the hydrodynamic range. These collective modes are extensions of the corresponding hydrodynamic modes at small wave number and frequency and are useful in understanding the neutron-scattering results for the dynamic structure factor $S(k,\omega)$ in this wave-number and frequency domain. A similar approach was taken in molecular dynamics computer simulations of hard spheres (Alley *et al.*, 1983). Here wave-vector-dependent (generalized) transport coefficients were used in the hydrodynamic expressions for the correlation functions in order to obtain agreement of the theory with simulation results.

Although the assumption of slow variations used in obtaining the hydrodynamic equations is not valid at short length and time scales, the above results indicate that the deviations occur in a subtle and gradual manner. Therefore, instead of following the fully kinetic approach of distribution functions outlined above (see Sec. III.A.2.b), one can also consider the dynamic evolution of the fluid in terms of hydrodynamic equations generalized to include short-wavelength, short-time phenomena. While retaining the basic structure of the equations one can extend the hydrodynamic description by replacing the relevant thermodynamic properties or transport coefficients by functions that can vary in space or in both space and time (Chung and Yip, 1969; Akcasu and Daniels, 1970; Ailawadi *et al.*, 1971). The resulting theory, which describes the dynamical behavior of the fluid over a wider range of spatial and temporal variations, is termed *generalized hydrodynamics* (Kadanoff and Martin, 1963; Boon and Yip, 1991). We first consider the extension of the theory to short wavelengths still at the level of uncorrelated binary collisions. This is comparable to many-body kinetic theory, in that it focuses on the dynamics of a small set of slow modes.

1. Generalized hydrodynamic modes

The generalized hydrodynamic approach was used (Kirkpatrick, 1985b) to obtain time correlation functions for a hard-sphere fluid at finite k and ω outside the domain of conventional hydrodynamics. The results were similar to those obtained by the kinetic theory work using the revised Enskog model. In the generalized hydrodynamic approach (Lutsko *et al.*, 1989) the equations of motion for the conserved densities of mass, momentum, and energy were obtained following the projection operator technique of Mori and Zwanzig (Zwanzig, 1961; Mori, 1965a, 1965b).

a. The projection operator

In the deterministic equations of hydrodynamics the conserved density refers to the corresponding fluctuating quantity averaged over some suitable statistical ensemble. The projection operator technique is applied to obtain equations of motion that apply to the time evolution of the corresponding fluctuating property in any single member of the ensemble. Let us consider a set of dynamical variables $\{A_i(\mathbf{r},t)\}$ whose time evolution follows from the Liouville equation, i.e., $A_i(t)=\exp(i\mathcal{L}t)A_i$ in terms of the Liouville operator $\mathcal{L}$ (Hansen and McDonald, 1986). We define A_i such that its equilibrium average is equal to zero and use the notation $A_i(t=0)\equiv A_i$. The *projection operator* $\mathcal{P}$ is defined through its action on a dynamical variable $B(t)$,

$$\mathcal{P}B(t)=\sum_{j,k}\langle B(t)A_j^*\rangle\langle A_j^*A_k\rangle^{-1}A_k, \tag{3.7}$$

where the angular brackets denote an average over the equilibrium distribution. The operator $\mathcal{Q}=1-\mathcal{P}$ denotes the projection in the orthogonal subspace. The equations for the time evolution of the dynamic variables A_i are obtained (Hansen and McDonald, 1986) in the matrix form,

$$\dot{\mathbf{A}}(t)-\mathbf{i\Omega}\cdot\mathbf{A}(t)+\int_0^t\mathbf{M}(t-s)\cdot\mathbf{A}(s)ds=\mathbf{R}(t), \tag{3.8}$$

where $\mathbf{A}$ here refers to the column vector with the A_i's. The frequency matrix $\mathbf{\Omega}$ and the random force vector $\mathbf{R}$ are given by

$$\Omega_{ij}=\sum_k\langle A_i^*i\mathcal{L}A_k\rangle\chi_{kj}^{-1},$$
$$R_i(t)=\exp(i\mathcal{Q}L\mathcal{Q}t)K_i \tag{3.9}$$

with $K_i=\mathcal{Q}\dot{A}_i$ and χ denoting the equilibrium correlation function matrix $\langle A_i^*A_j\rangle=\chi_{ij}$. $\mathbf{R}(t)$ on the right-hand side of (3.8) remains at all times orthogonal to the space of

$\mathbf{A}$, $\langle A_i^* R_j(t)\rangle = 0$. The kernel matrix $\mathbf{M}$ relates $\dot{\mathbf{A}}$ to the $\mathbf{A}$'s at earlier times and is called the *memory function*. $\mathbf{R}$ is expressed in terms of the correlation of the force $\mathbf{R}(t)$ in the subspace of $\mathcal{Q}$ through a Green-Kubo-type relation,

$$M_{ij} = \sum_k \langle R_i R_k(t)\rangle \chi_{kj}^{-1}. \tag{3.10}$$

The chosen set of variables $\{\mathbf{A}\}$ is termed "slow" and the remaining large numbers of degrees of freedom other than $\{\mathbf{A}\}$ for the system are spanned by the operator $\mathcal{Q}$. Their role in the dynamics given by $\mathbf{R}(t)$ in Eq. (3.8) is to be treated as "noise." The corresponding autocorrelation is related to the generalized transport coefficients $\mathbf{M}$ in Eq. (3.10). The dynamical equation for the time evolution of the correlation functions [defined in Eq. (2.4)] of the slow modes is reached in a matrix form by multiplying Eq. (3.8) from the right with $\mathbf{A}^* \cdot \langle \mathbf{A}^* \mathbf{A}\rangle^{-1}$ and averaging to obtain

$$\frac{\partial \mathbf{C}}{\partial t} - \mathbf{i}\boldsymbol{\Omega}\mathbf{C}(t) + \int_0^t \mathbf{M}(t-s)\cdot\mathbf{C}(s)ds = 0, \tag{3.11}$$

where it is taken that $\langle A R(t)\rangle = 0$. The one-sided Laplace transform of the memory function equation (3.11) reduces to the form

$$[z\mathbf{I} + \boldsymbol{\Omega} + \mathbf{M}]\mathbf{C}(z) = \chi, \tag{3.12}$$

where we have used the definition

$$f(z) = -i\int_0^\infty e^{izt} f(t)dt, \quad \mathrm{Im}(z) > 0 \tag{3.13}$$

for the Laplace transform. $\chi \equiv C(t=0)$ represents the initial conditions for Eq. (3.11).

The projection operator scheme described above provides us a way of describing the dynamics of the many-particle system in terms of a reduced set of variables given a proper definition of their inner product. In the present context of the dynamics of fluids we use the set of conserved local densities of mass, momentum, and energy to constitute the chosen set while the average equilibrium ensemble is taken as the inner product. These collective modes are deviations from the equilibrium state, whose properties are assumed to be known. For the chosen variables there is a vast difference in the time scales of variation in comparison to those of the large number of microscopic variables of the fluid. The origin of these slow variables for a specific system can be different, e.g., microscopic conservation laws as in the present case, heavy mass of a Brownian particle, or breaking of a continuous symmetry (Forster, 1975) of the many-particle system. The fluctuating equations for the conserved densities are treated as plausible generalizations of the macroscopic hydrodynamic laws and describe the actual motion of the hydrodynamic variables and not just their mean values. These equations can be used to study phenomena at microscopic frequencies and wavelengths.

b. The hard-sphere liquid

For a hard-sphere liquid the chosen set of variables consists of $\{\rho, \mathbf{g}, T\}$ denoting the density, momentum, and the kinetic energy, respectively (there is no potential energy in this case). The equations for the fluctuations thus obtained are assumed to be valid even at short wavelengths (finite k). For an isotropic system the correlation functions involving the momentum current $\mathbf{g}$ split into (a) the longitudinal component g_l and (b) the two transverse components g_t. The equal-time correlation function matrix χ in this case is diagonal with the nonzero elements, $\chi_{\rho\rho} = m^2 nS(k)$, $\chi_{ee} = 3n/(2\beta^2)$, and $\chi_{g_l g_l} = \chi_{g_t g_t} = mn/\beta$. From the matrix Eq. (3.12) correlation functions are computed in the crucial short-time approximation. In this limit the contribution from the memory function term $\mathbf{M}$ in Eq. (3.11) is set equal to zero. For a hard-sphere system with instantaneous collisions this is still a reasonable approximation for studying the dynamics even up to long times. The frequency matrix $\boldsymbol{\Omega}$ is computed from Eq. (3.9) involving the Liouville operator $\mathcal{L}$. For the special case of discontinuous hard-sphere potentials, the time dependence of the dynamic variable $A(t) = e^{i\mathcal{L}_\pm t} A$ is generated by operators $\mathcal{L}_+$ and $\mathcal{L}_-$ for $t > 0$ and $t < 0$, respectively (Résibois and de Leener, 1977). Note that $\mathcal{L}_\pm$ are identical for fluids with continuous interaction potentials. Straightforward calculation obtains for Ω,

$$\boldsymbol{\Omega} = \begin{bmatrix} 0 & ik & 0 \\ -ikc_o^2(k) & \Gamma_o(k) & ikw(k) \\ 0 & -kw(k) & D_H(k) \end{bmatrix}, \tag{3.14}$$

where $c_o^2(k) = 1/\beta m S(k)$. The different wave-vector-dependent functions are given by $w(k) = 1 + 3yj_1(k\sigma)/(k\sigma)$, $D_H(k) = \nu_o[1 - j_o(k\sigma)]$, and $\Gamma_o(k) = \nu_o[1 - j_o(k\sigma) + 2j_2(k\sigma)]$, with the j_l's denoting a spherical Bessel function of order l and $y = 4\pi\varphi g(\sigma)$. $D_H(k)$ corresponds to the generalized heat diffusion constant and sound attenuation. $\nu_o = 2/(3t_E)$ represents a microscopic frequency, t_E being the Enskog time between collisions (Résibois and de Leener, 1977). The density autocorrelation function $F(k,t)$ at large k is obtained in terms of the three exponentially relaxing modes,

$$F(k,t) = \sum_{\mu=1}^{3} A_\mu(k) e^{-z_\mu(k)t}, \tag{3.15}$$

where $z_\mu(k)$ are the three eigenvalues of the matrix (3.14). These z_μ's in the small-k limit reduce to the three hydrodynamic modes described in Sec. III.A.2. The wave-number-dependent functions $D_H(k)$, $\Gamma_o(k)$, and $\eta_o(k)$ play the role of generalized transport coefficients representing dissipative effects over short length scales. These generalized transport coefficients in the small-wave-number limit reduce to the corresponding Enskog values obtained from a kinetic theory calculation (in which only the collisional contribution has been kept; see Kirkpatrick, 1984). Similarly the eigenvalue for the transverse shear mode is at $z = -\eta_o(k)$, where $\eta_o(k)$

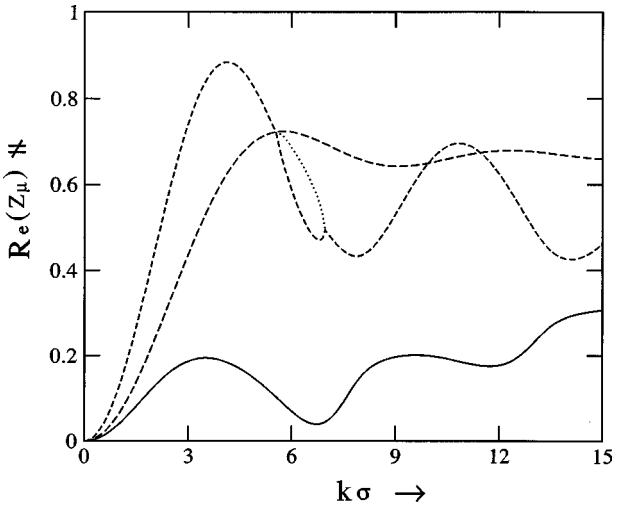

FIG. 2. Real part of the eigenvalues $-z_\mu(k)$ $(\mu=1,\ldots,5)$ vs k for a hard-sphere fluid at packing fraction $\varphi=\pi n\sigma^3/6=0.471$: dotted curve, the pair of complex-conjugate sound modes; solid curve, the heat mode; dashed curves, two degenerate shear modes. From Das and Dufty, 1992.

$=\nu_o\{1-j_o(k\sigma)-j_2(k\sigma)\}$ is the generalized shear viscosity.

In Fig. 2 we show the real part of the eigenvalues $-z_\mu(k)$ $(\mu=1,\ldots,5)$ extended to large k, for a hard-sphere system at packing fraction $\varphi=\pi n\sigma^3/6=0.471$. The Percus-Yevick solution (Ashcroft and Lekner, 1966) with Verlet-Weiss correction (Verlet and Weiss, 1972; Henderson and Grundke, 1975) for the structure factor $S(k)$ has been used in computing the matrix elements of Eq. (3.14). The propagating pair of sound modes (shown by dotted lines) crosses over to a pair of real modes for an intermediate wave-number range. The most interesting feature is the behavior of the heat mode (solid line), which becomes soft near the peak of the structure factor of the liquid, since $S^{-1}(k)$ is small there. Analysis of the amplitude factors at the peak indicate that the soft mode corresponds mostly to a density fluctuation. At high density the softening is pronounced and it corresponds to very slow dynamics near the diffraction peak (de Gennes, 1959). The two transverse shear modes (dashed lines) are identical in the isotropic liquid.

2. Dynamics in the Markovian approximation

Unlike the case of hard spheres, for continuous potentials, $\mathbf{\Omega}$ would not give rise to dissipative terms. From general considerations of the conservation laws $\Omega_{\rho g_i}=ik_i$, $\Omega_{g_i\rho}=-ik_ic_o^2(k)$, and $\Omega_{g_ig_i}=0=\Omega_{\rho\rho}$. In order to keep the description simple we have here considered the reduced set of dynamic variables consisting of the set $\{\rho,\mathbf{g}\}$ and ignored the energy variable e. For the matrix $\mathbf{M}$ of the transport coefficients, the elements are $M_{\rho\rho}=M_{\rho g_i}=M_{g_i\rho}=0$ to ensure that the continuity equation follows from Eq. (3.11). Let us assume that the nonzero elements $M_{g_ig_j}$ are supposed to have only short-time contributions idealized in terms of a delta function. For the isotropic liquid, the $M_{g_ig_j}$ are expressed in terms of longitudinal and transverse components,

$$M_{g_ig_j}(t)=[\hat{q}_i\hat{q}_jm_o^L(q)+(\delta_{ij}-\hat{q}_i\hat{q}_j)m_o^T(q)]\delta(t), \qquad (3.16)$$

where $\hat{q}$ denote the unit vector in the direction of $\mathbf{q}$. Memory effects in time are ignored here, and hence the resulting transport coefficients are frequency independent. The Langevin equations take a Markovian form. In the present context the dynamics are treated only at the level of uncorrelated collisions such that the wave-number-dependent transport coefficients go smoothly to constants in the long-time limit. The correlation functions are now obtained from Eq. (3.12). The most important of these, the density correlation function and transverse current correlation function, each normalized with respect to their equal-time values, are

$$\phi(q,z)=\left[z-\frac{\Omega_q^2}{z+im_o^L(q)}\right]^{-1}, \qquad (3.17)$$

$$\phi_T(q,z)=\frac{1}{z+im_o^T(q)}, \qquad (3.18)$$

where $\Omega_q=qc_o(q)$ represents a fundamental time scale in liquid-state dynamics. Here $m_o^L(q)=q^2\Gamma_o(q)$ relates to the generalized longitudinal viscosity $\Gamma_o(q)$, and $m_o^T(q)=q^2\eta_o(q)$ relates to the shear viscosity $\eta_o(q)$. In the long-wavelength and low-frequency hydrodynamic limit $c_o(q)$ reduces to the hydrodynamic speed of sound. Similarly, $\eta_o(q)$ and $\Gamma_o(q)$ reduce to the macroscopic shear and longitudinal viscosities η_o and $\Gamma_o=4\eta_o/3+\zeta_o$, respectively. The dynamic structure factor $S(q,\omega)$ [Eq. (3.17)] consists of the standard Brillouin sound doublet seen in light-scattering experiments. Such a theory leads to correlation functions that decay exponentially with time to the equilibrium value. The approximation of ignoring the memory effects and replacing the transport coefficients by short-time contributions is good at low densities at which cooperativity is low.

IV. STRONGLY CORRELATED LIQUID

A. Mode-mode coupling: Some physical insight

The Markovian equations for the collective modes involving frequency-independent transport coefficients constitute a model for the dynamics of fluids with exponential relaxation of fluctuations. However, exceptions occur in certain situations, in which the description of the dynamics cannot be reduced to a set of linearly coupled fluctuating-equations with frequency-independent transport coefficients. The striking anomalies seen in the transport properties near critical points are an example. In order to explain the observed phenomena, Kawasaki (1966b) introduced the idea of including in the dynamical description nonlinear coupling of the collective modes. Another case in which frequency-independent transport coefficients are not appropriate is the observation of long-time tails which refer to power-law behavior in the asymptotic decay of correlation function in a fluid, e.g., $1/t$ decay of the velocity correlation of a tagged particle seen in computer

simulations of hard disks (Alder and Wainright, 1967, 1970). Using Green-Kubo relations similar to Eq. (2.11) implies that the frequency-dependent self-diffusion coefficient varies as $1/\omega$ at low frequency, i.e., diverges in the zero-frequency limit. The origin of such observations lies in collective effects over semihydrodynamic length scales. Indeed, by measuring the hydrodynamic flow field around a tagged particle, Alder and Wainright (1970) showed that the initial momentum of this particle was partially transferred to the surrounding liquid, thereby setting up vortices around it. The flow field in turn transferred some of its momentum to the tagged particle by producing a backflow reaction and this resulted in a positive tail in the correlation of $\langle \mathbf{v}(t)\cdot\mathbf{v}(0)\rangle$ extending up to hydrodynamic time scales. A simple estimate of the above cooperative process can be made as follows: The initial velocity of the tagged particle is shared with the surrounding particles, producing vortices in a volume Ω_t of radius R_t. After a short time the tagged particle is moving at velocity $v(t)\sim v(0)/n\Omega_t$, n being the number of particles in a unit volume. This length R_t grows as $t^{1/2}$ through diffusion of vortices, so that $\Omega_t \sim t^{d/2}$, producing the $t^{-d/2}$ power-law tail.

The above described cooperative process was analyzed from a rigorous theoretical approach using nonlinear kinetic equations. The hard-sphere kinetic theory with Boltzmann-level description of random binary collisions was improved (Dorfman and Cohen, 1972, 1975) to include the so-called ring- and repeated-ring-type collisions between the particles. For a dense liquid, a general formalism for including the effects of correlated collisions was proposed through the fully renormalized kinetic theory (Mazenko, 1973a, 1973b, 1974; Mazenko and Yip, 1977; Sjögren and Sjölander, 1978). Here the treatment of the dynamics of dense fluids was separated into a binary collision part and a contribution from ring collisions represented by memory functions. These methods provided reasonable explanations of the features of dense-fluid dynamics as seen in computer simulations and scattering experiments. It was demonstrated that the self-diffusion coefficient of a tagged fluid particle in a sea of similar particles decreases as the density increases. For very high densities, however, pursuing the traditional kinetic theory models has not proved to be very effective, though they are as an important precursor to more innovative models for the dynamics in a strongly correlating liquid state.

An alternative way of studying the correlated dynamics in a fluid came from introducing nonlinear coupling of the hydrodynamic modes in the dynamic description (Kawasaki, 1970a, 1971; Ernst *et al.*, 1971, 1976; Ernst and Dorfman, 1976). These theories predicted a decay of $t^{-d/2}$ in d dimension for a variety of correlation functions connected with viscosity, diffusion, and thermal conductivity. The implication of including products of nonlinear modes in the description of the dynamics as slow modes can be clarified from the following simple analysis (Kim and Mazenko, 1990). Let us consider the slow variable ψ_i which is related to the corresponding current J_i through the balance equation $\partial_t\psi_i + \nabla\cdot\mathbf{J}_i = 0$. Since $\psi_i(\mathbf{x},t)$ is the local density corresponding to a globally conserved property, the integral $I_i = \int d\mathbf{x}\psi_i(\mathbf{x},t)$ is independent of time. It is relevant to ask whether the product of the slow variables $\psi_i(\mathbf{x},t)\psi_j(\mathbf{x},t)$ should be treated as slow or not. To apply the above test, the time derivative of the integral $I_{ij}(t) = \int d\mathbf{x}\psi_i(\mathbf{x},t)\psi_j(\mathbf{x},t)$ is obtained as

$$\int \frac{d\mathbf{k}}{(2\pi)^3}(i\mathbf{k})\cdot[\mathbf{J}_i(\mathbf{k},t)]\psi_j(-\mathbf{k},t) + \mathbf{J}_j(\mathbf{k},t)\psi_i(-\mathbf{k},t) \quad (4.1)$$

using the balance equations for the slow modes. Since ψ_i, ψ_j are hydrodynamic variables, for long time t, the value of Eq. (4.1) is dominated by the small-k part of the integral, and this is obviously small due to the factor of k in the integrand. Thus the nonlinear couplings of the slow variables in the equations of motion essentially include collective effects in the dense systems extending up to long length and time scales.

The various types of long-time tails are observed in the asymptotic behavior of correlation functions, which are associated with different types of mode-coupling models. The power-law decay in the velocity correlation function has been experimentally observed in low-viscosity liquids like molten sodium (Morkel *et al.*, 1987). This behavior is explained as a consequence of the coupling of tagged-particle motion with hydrodynamic velocity fields (Pomeau and Résibois, 1975). The power-law decay is present at arbitrary low densities, for which the Boltzmann equation (which predicts an exponential decay) is expected to hold. The Boltzmann equation becomes exact only at a fixed time in the limit of low density, but not at a fixed density (no matter how small) in the limit of long times. On the other hand, a stronger $t^{-3/2}$ tail is seen in stress correlation functions in dense liquids (Evans, 1980; Erpenbeck and Wood, 1981) with amplitudes 500 times larger than expected from the conventional models described above. This behavior is valid for the intermediate times considered in computer experiments. These tails are understood as consequences of dense-liquid effects through a generalization of the mode-coupling model (Kirkpatrick, 1984), taking into account the finite wave-vector modes (described in Sec. III.B), especially the soft heat mode.

B. The renormalized theory

A renormalized theory including the coupling of collective modes in the description of the dynamics can be obtained in several ways (Zwanzig, 1972). One approach is to consider the linear equations of motion for a set of collective modes, using the projection operator formalism outlined in the previous section but including memory effects through generalized transport coefficients. The frequency-dependent memory function is analyzed in the projected space of the nonlinear modes through suitable approximations. Alternatively we can treat the dynamics of collective modes with nonlinear Langevin equations involving bare transport coefficients. The consequences of the nonlinearities in the

equations of motion, i.e., renormalization of bare transport coefficients, are then obtained using graphical methods. The field-theoretic techniques developed in the context of dynamic critical phenomena or other disordered systems are particularly suitable for obtaining a self-consistent form of the mode-coupling theory. While the former approach with memory function is simpler, it is somewhat arbitrary. The field-theoretic approach, though formal, is more systematic. In the following we shall briefly outline both approaches, with details given in the Appendix as well as in the cited references.

1. Memory function approach

The dynamical equations (3.8), which are linear in the fluctuations A_i, involve the matrix of non-Markovian transport coefficients $\mathbf{M}(t)$ which are also expressed in the Green-Kubo form in Eq. (3.10). The collective effects that influence the long-time dynamical behavior are now included in the memory function matrix $\mathbf{M}$. The frequency- and wave-number-dependent functions in $\mathbf{M}$ are obtained in terms of the products of time correlation functions (Götze and Lücke, 1975; Munakata and Igarashi, 1977, 1978). The memory effects are thus computed in terms of the correlation functions themselves rather than being approximated through phenomenological time-dependent functions (Boon and Yip, 1991). An analysis of the memory function in the projected space of an extended set of slow modes (involving coupling of slow modes) obtains the frequency-dependent part in terms of hydrodynamic correlation functions. We outline this deduction and the related Kawasaki approximation in Appendix A.1. A recent development due to Zaccarelli *et al.* is also discussed in this regard.

The Laplace transform of the density correlation function $\phi(q,z)$ is now expressed in the form (3.17) with a generalization of the memory function $m^L(q,z)$, in the form

$$\frac{\phi(q,z)}{z\phi(q,z)-1} = z + im^L(q,z), \tag{4.2}$$

where we have rescaled time to dimensionless form with a characteristic microscopic frequency $\Omega_o \equiv cq$. The memory function is expressed as a sum of two parts,

$$m^L(q,z) = m_o^L(q) + \int_o^\infty dt e^{izt} \tilde{m}^L(q,t), \tag{4.3}$$

where the mode-coupling contribution $m^L(q,t)$ in Eq. (4.2) is obtained (with the approximations outlined in the Appendix) as

$$\tilde{m}^L(q,t) = \frac{n}{2m\beta}\int \frac{d\mathbf{k}}{(2\pi)^3}[V_L(\mathbf{q},\mathbf{k})]^2 S(k_1) \times S(k)\phi(k_1,t)\phi(k,t), \tag{4.4}$$

with the notation $\mathbf{k}_1 = \mathbf{q} - \mathbf{k}$. The vertex function is defined as

$$V_L(\mathbf{q},\mathbf{k}) = (\hat{\mathbf{q}}\cdot\mathbf{k})c(k) + (\hat{\mathbf{q}}\cdot\mathbf{k}_1)c(k_1). \tag{4.5}$$

The renormalization of the transport coefficients in terms of density correlation functions is expressed in a self-consistent form. This is essential for the dynamic feedback mechanism discussed in the next section. In an intuitive picture this self-consistent treatment is justified by appealing to the nature of the single-particle motion in a strongly correlated liquid: the tagged particle rattles in the cage formed by its surrounding particles, which are also trapped. The tagged particle thus needs to be treated in the same manner as those forming the cage around it, and hence the renormalized transport coefficient is taken to be a self-consistent functional of the density correlation function. The feedback process is a manifestation of the fact that the motion of the particles in a dense medium influences the surroundings, which in turn react and influence subsequent motion. The self-consistent approach used in mode-coupling theory is similar to the more refined version of the Hartree approximation known as the "self-consistent screening approximation" (Bray, 1974).

2. Nonlinear dynamics of collective modes

The equations of motion for the collective modes including nonlinear couplings are obtained through a generalization of the linear equations. These equations are treated as the equations of motion for the actual hydrodynamic variables, and may be considered a plausible generalization of the standard hydrodynamic laws. For a set of variables $\{\psi_i\}$ the nonlinear Langevin equation has the generalized form (Ma and Mazenko, 1975)

$$\frac{\partial \psi_i(\mathbf{r},t)}{\partial t} + [Q_{ij} + L_{ij}^o]\frac{\delta F}{\delta \psi_j} = \zeta_i(\mathbf{r},t), \tag{4.6}$$

where $F[\psi]$ is the effective free-energy functional in terms of the slow variables $\{\psi\}$. The reversible part of the dynamics is represented as $Q_{ij}(\delta F/\delta\psi_j) \equiv V^i[\psi]$ in terms of the Poisson bracket $Q_{ij} = \{\psi_i, \psi_j\}$ (Dzyaloshinskii and Volovick, 1980) between the slow variables ψ_i and ψ_j. L_{ij}^o refers to the matrix of bare transport coefficients, which are different from those appearing in linear transport laws. For the most part we shall treat F as a quadratic functional of ψ corresponding to a Gaussian theory for the statics. Complementary to the Langevin approach of Eq. (4.6), the dynamics may also be described in terms of the probability density function $g_\varphi(t) = \Pi_{i,\mathbf{r}}\, \delta[\varphi_i(\mathbf{r}) - \psi_i(\mathbf{r},t)]$, defined in terms of the fields $\varphi_i(\mathbf{x})$. The time evolution of $g_\varphi(t)$ is given by the Fokker-Planck equation,

$$\frac{\partial \bar{g}_\varphi}{\partial t} + \sum_i \left[V^i - L_{ij}\left(\frac{\delta}{\delta\varphi_j} + \beta\frac{\delta F}{\delta\varphi_j}\right)\right]\bar{g}_\varphi = 0. \tag{4.7}$$

The stationary probability distribution function for the system is given by $e^{-\beta F}$. The condition

$$\sum_i \frac{\delta}{\delta\psi_i}[V_i e^{-\beta F}] = 0 \tag{4.8}$$

ensures that the probability current vector, which is equal to the product of probability density ($e^{-\beta F}$) and the streaming velocity (V_i), is divergence-free in the space of ψ_i. The noise ζ_i in the generalized Langevin equation is assumed to be Gaussian with the following fluctuation-dissipation relation with the bare transport coefficients L^o_{ij}:

$$\langle \zeta_i(\mathbf{r},t)\zeta_j(\mathbf{r}',t')\rangle = 2k_B T L^o_{ij}\delta(t-t'). \tag{4.9}$$

The bare transport coefficients are not determined from the theory and are regarded as input parameters in the theory.

a. An example: Incompressible fluid

Before we turn to the full analysis of the equations for a compressible liquid with the nonlinear constraint, let us take a brief look at the case of an incompressible fluid, i.e., one of constant density. Here $\nabla\cdot\mathbf{g}=0$, that is. $\mathbf{k}\cdot\mathbf{g}(\mathbf{k})=0$, so that the momentum field is transverse to the direction of the wave vector $\mathbf{k}$ and is denoted by $\mathbf{g}^T$. The equation for the momentum conservation reduces to the form

$$\frac{\partial g_i^T}{\partial t} = -P_{ij}^T\left[\frac{g_k}{\rho_o}\nabla_k g_j\right] + \eta_o\nabla^2 g_i^T + \theta_i^T, \tag{4.10}$$

where θ_T^j is the transverse component of the noise. The nonlinear term in Eq. (4.10) is due to convective nonlinearity, which in this case will be the transverse part of $(\mathbf{g}\cdot\nabla)\mathbf{g}$. The transverse projection is done by the operator $P_{ij}^T(\mathbf{x})$, whose Fourier transform is given by $P_{ij}^T(\hat{k}) = \delta_{ij} - \hat{k}_i\hat{k}_j$. The effect of this nonlinearity on the bare viscosity η_o was studied using standard theoretical techniques (Forster *et al.*, 1977). The shear viscosity η developed a long-time tail of power-law decay $\eta(t) = A_\eta t^{-d/2}$, with the exponent of power-law behavior, i.e., $d/2$ was the same as that obtained in computer simulations and kinetic theory models. Moreover, the exponent A_η was computed to be the same as the corresponding result obtained from a detailed microscopic kinetic theory calculation (Pomeau and Résibois, 1975). The convective nonlinearity in the fluctuating hydrodynamic equation thus accounted for the long-time tails, which were a consequence of correlated motion of the fluid particles.

b. Compressible liquids

We consider the dynamics of a set of collective variables for the liquid $\{\rho(\mathbf{r},t),\mathbf{g}(\mathbf{r},t)\}$. In the supercooled state, density fluctuations are most dominant and hence, in order to keep the analysis simple, we ignore the energy fluctuations (Kim and Mazenko, 1991) here. The deduction of the fluctuating hydrodynamic equations for a liquid has been dealt with in detail in the literature (Das and Mazenko, 1986). The streaming velocities V_ρ and $V^i_{\mathbf{g}}$ are computed from the Poisson brackets Q_{ij} for the hydrodynamic variables $\rho(\mathbf{r},t)$ and $\mathbf{g}(\mathbf{r},t)$. The driving free-energy functional F used in the construction of the dynamic equations, is expressed in terms of the hydrodynamic fields, ρ and $\mathbf{g}$, and is separated into two parts, $F=F_K[\mathbf{g},\rho]+F_U[\rho]$. The dependence of F on $\mathbf{g}$ is entirely in the kinetic part F_K, in the form (Langer and Turski, 1973)

$$F_K[\mathbf{g},\rho] = \int d\mathbf{x}\frac{g^2(\mathbf{x})}{2\rho(\mathbf{x})}. \tag{4.11}$$

The potential part F_U is treated as a functional of the density only. The dissipative matrix, $L_{\rho\psi}=0$ so that the continuity equation for ρ is obtained for the fluctuating variables in the same form as Eq. (3.4),

$$\frac{\partial\rho}{\partial t} + \nabla\cdot\mathbf{g} = 0. \tag{4.12}$$

The nonlinear equation for the momentum density is a generalized form of the Navier-Stokes equation,

$$\frac{\partial g_i}{\partial t} = -\nabla_j\left[\frac{g_i g_j}{\rho}\right] - \rho\nabla_i\frac{\delta F_u}{\delta\rho} - \sum_j L^o_{ij}\frac{g_j}{\rho} = \theta_i. \tag{4.13}$$

The noise θ_i is assumed to be Gaussian, with a variance given by Eq. (4.9). For an isotropic liquid, this damping matrix is obtained in terms of two independent bare viscosities similar to Eq. (3.5).

On the right-hand side of Eq. (4.13) both the first and second terms refer to the reversible part of the dynamics. The first one is the Galilean term representing the well-known Navier-Stokes nonlinearity and is a result of coupling of currents. The most important nonlinearity for producing the slow dynamics in a supercooled liquid is the second term in Eq. (4.13). This term relates to the pressure gradient term in the momentum conservation equation. This nonlinearity in the pressure term appears as a coupling of density fluctuations and is of dynamic origin since it is quadratic in density fluctuations $\delta\rho$, even for a completely Gaussian free-energy functional $F_u[\rho]$. For compressible liquids, in the generalized equation (4.13), both the convective term (the second term) and the dissipative term (the third term) contain a $1/\rho$ nonlinearity. The appearance of this nonlinearity in the hydrodynamic equations can be avoided (Das and Mazenko, 1986) by introducing an extra fluctuating field $\mathbf{V}(\mathbf{x},t)$,

$$\mathbf{g}(\mathbf{x},t) = \rho(\mathbf{x},t)\mathbf{V}(\mathbf{x},t). \tag{4.14}$$

For an incompressible liquid this is a trivial relation, since $\rho(\mathbf{x},t)=\rho_o$ is a constant. However, for a compressible liquid this imposes a nonlinear constraint on the fluctuating fields and is essential for understanding the dynamics. The nonlinearities in Eq. (4.13) are computed with a properly defined free-energy functional $F_U[\rho]$.

c. Renormalized transport coefficients

The bare transport coefficients in the nonlinear Langevin equations are corrected with additional contributions from the nonlinearites, and the renormalized

transport coefficient corresponds to the experimentally measured quantity. The renormalization is done in a perturbative manner using standard methods for dealing with nonlinear equations of motion (Ma and Mazenko, 1975; Mazenko *et al.*, 1983; Das *et al.*, 1985b). In this formalism the dynamic correlation functions between the collective variables are obtained in a perturbative expansion in $O(k_BT)$. A straightforward approach is to simply iterate the equations of motion. Such direct methods for computing the corrections due to the nonlinearities have been used extensively in studying the dynamics of critical phenomena (Ma, 1976). However, the renormalized perturbation theory for compressible liquids is constructed more appropriately with a formalism that is now standard and was first described by Martin *et al.* (1973).

The Martin-Siggia-Rose field theory is a general scheme applied to compute the statistical dynamics of classical systems. The theory is constructed with a generating functional from which both the time correlation and the response functions are obtained. The graphical methods of field theory can be conveniently used in this approach for deriving earlier results on mode-coupling models for transport near the critical point (Kadanoff and Swift, 1968; Kawasaki, 1970b) or on turbulence (Kraichnan, 1959b, 1961a; Edwards, 1964). The original Martin-Siggia-Rose theory (Martin *et al.*, 1973; Deker and Haake, 1975; Phythian, 1975, 1976; Anderson, 2000) was developed within an operator formalism involving the field variables ψ and an additional set of corresponding adjoint operators $\hat{\psi}$. The ψ operators do not commute with their hatted counterparts. The correlation between ψ and $\hat{\psi}$ corresponds to the response functions that are now computed together with the usual correlation functions between the ψ's. When applied to the case of classical continuous fields satisfying a linear or nonlinear Langevin equation, this theory is formulated in the functional-integral approach (Bausch *et al.*, 1976; Janssen, 1976; Phythian, 1977; de Dominicis and Pelti, 1978). The construction of the theory now includes, in addition to the field variable, an associated hatted field in the same manner as the operator approach. For studying the coupling of strong density fluctuations in a dense liquid approaching the glass transition, a renormalized theory has been developed (Das and Mazenko, 1986). This involves sets of fields $\{\rho, \mathbf{g}, \mathbf{V}\}$ and their corresponding hatted counterparts. Corrections to the transport coefficients are obtained in a diagrammatic expansion, and the renormalization of the transport coefficients (at one-loop order) is the same as that from the Kawasaki approximation of the memory function, described in the previous subsection.

The full implication of the nonlinearities of the Langenvin equations is realized with the Martin-Siggia-Rose theory for the set of field equation (4.12)–(4.14). However, the technicalities involved in the construction of this theory with multiple fields is quite involved. We therefore review the main features of this renormalization procedure in the Appendix and limit our discussion here to the main results that will be useful for a discussion of slow dynamics near the glass transition. The renormalization scheme for the linear theory depends crucially on the form of the nonlinearities in the Langevin equations (termed the vertex functions). The structure of these nonlinearities depends on the driving free-energy functional F_U for the system. A useful choice (Kirkpatrick and Nieuwoudt, 1986a; Das, 1990) is to take the expansion of F_U in terms of the direct correlation functions for the liquid, in the same form as used in static density-functional theories (Ramakrishnan and Yussouff, 1979). The potential part F_U is split into two parts, $F_U[\rho(x)] = F_{\rm id}[\rho] + F_{\rm int}[\rho]$ where $F_{\rm id}$ is the ideal-gas entropy term,

$$\beta F_{\rm id}[\rho] = m^{-1} \int \mathbf{d}x \rho(\mathbf{x}) \{\ln[\rho(\mathbf{x})/\rho_o] - 1\}, \tag{4.15}$$

with $\beta = 1/(k_BT)$ the inverse Boltzmann factor. The interaction term $F_{\rm int}$ is given (up to a constant) to lowest order in the density fluctuations as

$$\beta F_{\rm int}[\rho] = \beta F_l[\rho_o] - \frac{1}{2m^2} \int d\mathbf{x} \times \int d\mathbf{x}' c^{(2)}(\mathbf{x}-\mathbf{x}') \delta\rho(\mathbf{x}) \delta\rho(\mathbf{x}'), \tag{4.16}$$

where F_l is the interaction free energy of the uniform liquid state with density ρ_o. The equilibrium two particle correlation function $c^{(2)}(\mathbf{x}) \equiv c(x)$ was introduced in Sec. II through Eq. (2.3). Higher-order terms, beyond the level of the two-point direct correlation function, are ignored in the expansion on the right-hand side of Eq. (4.16). The model is thus restricted to a quadratic coupling of density fluctuations, and hence the crucial density nonlinearity (quadratic) from $\rho\nabla_i \delta(F_U/\delta\rho)$ in the momentum equation is of entirely dynamic origin. It is worth noting that $F_{\rm id}$ in (4.15) is not strictly Gaussian. Since our main interest is in the dynamic properties of the fluid, to avoid technical complications we assume that these higher-order terms do not affect the statics in any serious way. In the equation of motion for $\mathbf{g}$ the contribution from the ideal-gas part $F_{\rm id}$ to the force term $\rho\nabla_i \delta(F_U/\delta\rho)$ is only linear in $\delta\rho$. We obtain the streaming velocity $V^i_{\mathbf{g}}$ as

$$V^i_{\mathbf{g}} = -\nabla_i \int d\mathbf{x}' V^{(1)}(\mathbf{x},\mathbf{x}') \delta\rho(\mathbf{x},t) - \int d\mathbf{x}_1 d\mathbf{x}_2 \times V^{(2)}_i(\mathbf{x},\mathbf{x}_1,\mathbf{x}_2) \delta\rho(\mathbf{x}_1,t) \delta\rho(\mathbf{x}_2,t), \tag{4.17}$$

where the linear kernel is given by $(\beta m) V^{(1)}(\mathbf{x},\mathbf{x}') = [\delta(\mathbf{x}-\mathbf{x}') - nc(|\mathbf{x}-\mathbf{x}'|)]$ and the quadratic vertex $V^{(2)}_i$ is given by

$$(\beta m^2) V^{(2)}_i(\mathbf{x},\mathbf{x}_1,\mathbf{x}_2) = \delta(\mathbf{x}-\mathbf{x}_2) \nabla^i_x c(|\mathbf{x}-\mathbf{x}_1|) + \delta(|\mathbf{x}-\mathbf{x}_1|) \nabla^i_x c(|\mathbf{x}-\mathbf{x}_2|). \tag{4.18}$$

The one loop contribution to the transport coefficients is obtained from evaluation of the renormalized theory following Eqs. (A12)–(A14). The wave-vector-

dependent mode-coupling integrals for the renormalization of the longitudinal viscosity obtained are identical to Eq. (4.4). It is useful to note the simplifications and approximations that are implied in reaching a model for the glassy dynamics. First, in the supercooled state the slow decay of the density fluctuations is assumed to produce the dominant contribution to the transport properties. Second, the contributions from self-energy graphs involving convective nonlinearities [due to coupling of currents in Eq. (4.13)] are relatively small and are absorbed by redefining of the bare transport coefficient. In low-dimensional systems, however, such terms give diverging contributions (Forster *et al.*, 1977). In a similar way the renormalization of the transverse current correlation function also obtains the mode-coupling contribution to the shear viscosity [see Eq. (5.29)]. In the present context the dependence of the theoretical predictions on the interaction potential or on thermodynamic properties like temperature or density enter in terms of the equilibrium correlation functions. The structure factor which is an input in the model is determined from theories of equilibrium statistical mechanics.

The different routes for reaching a self-consistent model have sometimes created confusion as to which scheme is more "microscopic." Both the methods outlined in the two subsections above obtain the same results. The approximations made in either also have similar implications. In the memory function approach of projecting onto the density pair subspace leading to the mode-coupling expression (4.4) one must choose at the outset certain couplings through "selection rules" based on physical considerations. In the field-theoretic approach the same is done when those one-loop diagrams involving slowly decaying density correlations are picked up. However, in the Martin-Siggia-Rose approach we can express corrections that occur due to nonlinearities in the equations of motion, as renormalization of transport coefficients. The field-theoretic treatment includes both correlation and response functions, and one can obtain nonperturbative expressions for the renormalization using the available fluctuation-dissipation relations (see the Appendix). Thus the theory is controlled in a formal sense. For practical calculations diagrammatic loop expansions for the renormalized quantities are used in a perturbative manner. A convenient starting point for computing the corrections is the one-loop level. Indeed, it was through such diagrammatic analysis that the full implications of the mode-coupling terms at one-loop order was realized. The procedure of making the approximations (taking only coupling of density fluctuations as dominant) at the outset missed some important aspects of the corrections to the basic model and led to incomplete conclusions (Bengtzelius *et al.*, 1984; Das *et al.*, 1985b). This will be discussed in Sec. VI, subsequent to the discussion of the basic model in Sec. V.

C. Dynamic density-functional model

The fluctuating hydrodynamic description of a dense fluid discussed so far starts with a basic set of slow variables including the mass and momentum densities. A somewhat simplified approach is to describe the dynamics only in terms of the density variable ρ. This approach has sometimes been referred to in the literature as the dynamical extension of the density-functional theory of crystallization. By integrating out the momentum density, we are able to reduce the fluctuating hydrodynamic description to a form involving only density fluctuations. The relaxation of the density fluctuations slows at a wavelength corresponding to the peak of the structure factor (see Sec. VI). In the supercooled state strong density fluctuations play the most dominant role in producing the slow dynamics. At short wavelengths, energy and momentum fluctuations in the fluid can be quickly transferred among the particles, while the individual density fluctuations may still be decaying much more slowly. A similar formulation of the dynamics of density fluctuations was used earlier in studying the kinetics of fluid undergoing a transition into an ordered phase (Bagchi, 1987a, 1987b; Munakata, 1989, 1990).

The time evolution of the probability density functional $P[\rho,t]$ of the density distribution $\rho(\mathbf{r})$ in the fluid is described by the Fokker-Planck equation (Kawasaki, 1994),

$$\frac{\partial}{\partial t}P[\rho,t] = -\mathcal{D}_\rho P[\rho,t]. \tag{4.19}$$

The operator $\mathcal{D}_\rho$ is given by

$$\mathcal{D}_\rho = D_o \int d\mathbf{r} \frac{\delta}{\delta\rho(\mathbf{r})} \nabla \cdot \rho(\mathbf{r}) \nabla \left[\frac{\delta}{\delta\rho(\mathbf{r})} + \beta \frac{\delta F_U[\rho]}{\delta\rho(\mathbf{r})} \right], \tag{4.20}$$

where the positive constant D_o is treated as a bare transport coefficient. The stationary solution of Eq. (4.19) is given by $\exp[-\beta F_U]$, where $F_U[\rho]$ is the free-energy functional of the density ρ. The above equation for the dynamics of the density distribution was obtained (Kawasaki, 1994, 1998) from two different microscopic approaches: first, from the Smoluchowski equation for interacting colloidal particles without hydrodynamic interactions, using a suitable coarse-graining procedure; second, from Eqs. (4.12) and (4.13) for fluctuating hydrodynamics, adiabatically eliminating $g(\mathbf{r},t)$ being treated as a fast variable. The dynamics are described only in terms of the fluctuating variable ρ in that case.

A self-consistent mode-coupling model of the feedback mechanism leading to a dynamic transition (Bengtzelius *et al.*, 1984; Kirkpatrick, 1985a) has also been obtained within the present formulation (Kawasaki and Miyazima, 1997), though in a somewhat different form. This involves mainly integrating out from the model equations the momentum density, which is assumed to relax very fast. The density autocorrelation function is then obtained, in terms of the renormalized quantity D_R, as

$$\phi(q,z) = \frac{1}{z + D_R(q,z)}. \tag{4.21}$$

The bare transport coefficient D_o^{-1} is renormalized to $D_R^{-1}(q,z)$ with the result at one-loop order

$$D_R^{-1}(q,\omega) = D_o^{-1} + \Omega_q^2 \int dt e^{i\omega t} \tilde{m}^L(q,t), \tag{4.22}$$

where $\tilde{m}^L(q,t)$ is given by Eq. (4.4). Thus the one-loop contribution to the renormalization of the longitudinal viscosity in terms of products of the density correlation functions is identical to that for D_o^{-1}. In the present case the effects of the mode-coupling appear in the form of a lifetime renormalization. The implications of the model equations (4.21) and (4.22) are similar to those of the model described by Eqs. (4.2) and (4.3).

V. SELF-CONSISTENT MODE-COUPLING THEORY

A. The one-component liquid

1. The schematic model

In order to focus on the dynamic feedback mechanism that forms the basis of the mode-coupling theory for glassy dynamics, we consider a single q-independent $\phi(q,t) \equiv \phi(t)$ and ignore all wave-vector dependences. The corresponding Laplace transform $\phi(z)$ of the density correlation function $\phi(t)$ is obtained from Eq. (4.2) as

$$\phi(z) = \left[z - \frac{1}{z + im(z)} \right]^{-1}. \tag{5.1}$$

The renormalized longitudinal viscosity $m^L(q,z)$ is written here as $m(z)$, dropping all wave-vector dependences. We keep the analysis here at a more general level by considering the memory function as

$$m(z) = m_0 + \int_0^\infty dt e^{izt} H[\phi(t)], \tag{5.2}$$

with $H[\phi(t)]$ being a local polynomial functional of the density correlation function $\phi(t)$ (Das *et al.*, 1985b; Götze, 1991; Kim and Mazenko, 1992),

$$H[\phi(t)] = \sum_{n=1}^{M} c_n \phi^n(t). \tag{5.3}$$

The constants c_n depend on the thermodynamic state of the liquid, to be determined by including proper wave-vector dependence in the model. This will be considered in the next section. Equations (5.1) and (5.2) form a coupled set of nonlinear equations for ϕ and they are expressed as one closed nonlinear integro-differential equation for $\phi(t)$ in time,

$$\ddot{\phi}(t) + m_o \dot{\phi}(t) + \phi(t) + \int_0^t ds H[\phi(t-s)] \dot{\phi}(s) = 0. \tag{5.4}$$

Equation (5.4) was first proposed by Leutheusser (1984) for $H[\phi] = c_2 \phi^2$ using a simple physical picture of supercooled liquid dynamics. This is as follows: A deeply supercooled liquid has fairly large density fluctuations corresponding to wave numbers near the structure factor peak, which in turn correspond to length scales of order a molecular size at which the system tends to crystallize. These fluctuations, moreover, are slower than those at nearby wave numbers. The hydrodynamic velocity field scatters off these slow thermally excited density fluctuations, acquiring an enhanced viscosity. This increase in the viscosity further slows down these slow density fluctuations. The dynamical transport coefficients at high density are thus strongly influenced by correlated motion of the fluid particles, expressed through mode-coupling terms involving products of strong density fluctuations. This constitutes a feedback process, which is an essentially dynamic mechanism, not accompanied by sharp changes in the thermodynamic properties of the liquid. A similar enhancement was also argued for the shear viscosity by Geszti (1983). These developments for modeling supercooled liquid dynamics are closely related to earlier work on the diffusion localization problem (Götze *et al.*, 1981a, 1981b). Simultaneously Bengtzelius *et al.* (1984) developed a model in which the feedback mechanism for the liquid was considered in greater detail. In this theory the proper structure factor of a real liquid was included in the model equations.

The complex relaxation scenario that results from the nonlinear feedback mechanism of density fluctuations is effective even in terms of the above schematic model without any wave-vector dependence. This simple model is described next and is followed by a discussion of the effects of including wave-vector dependence.

a. Relaxation over different time scales

Let us now consider the multistep relaxation scenario for $\phi(t)$ that follows from Eq. (5.4). The basic assumption in the analysis of Eq. (5.1) is that depending on the kernel $H[\phi]$, i.e., the coefficients c_n, there is a time range over which $\phi(t)$ is approximately time independent. It has the form

$$\phi(t) = f + (1-f)\phi_\nu(t), \tag{5.5}$$

where f is the value of $\phi(t)$ in some metastable state. We consider time scales in which the inequality $|z\phi_\nu(z)| \ll 1$ is valid for the Laplace transform $L_z[\phi_\nu(t)]$. Using Eq. (5.5) in Eq. (5.1) and keeping terms to $O[\phi_\nu^2(z)]$ we obtain

$$\frac{\Delta_0}{z} + \Delta_1 \phi_\nu(z) - (1-f)H'(f) z \phi_\nu^2(z) + \frac{(1-f)^2}{2} H''(f) L_z[\phi_\nu^2(t)] = 0, \tag{5.6}$$

where $\Delta_0 = H(f) - f/(1-f)$, and $\Delta_1 = \partial_f[(1-f)H(f) - f]$. In Eq. (5.6) primes denote derivatives with respect to f. An ideal metastable state is obtained when both Δ_0 and Δ_1 are zero, giving a solution for the decaying function $\phi_\nu(t)$. $\Delta_1 = 0$ for $H(f) = (C_o + f)/(1-f)$ where C_o is a constant not depending on f and Eq. (5.6) reduces to

$$\frac{\Delta_0}{z} - \left[\Delta_o + \frac{1}{1-f}\right] z \phi_\nu^2(z) + \frac{(1-f)^2}{2} H''(f) L_z[\phi_\nu^2(t)] = 0. \tag{5.7}$$

The transition point ($\Delta_0 = 0$) corresponds to a set of $c_n \equiv c_n^*$ for which the equation $H(f) = f/(1-f)$ is satisfied with real f. The decay of the density autocorrelation $\phi(t)$ in the vicinity of the transition becomes extremely slow, eventually freezing at a nonzero value f. This freezing signifies a dynamic transition of the fluid to a nonergodic state, and the limiting value f is known as the nonergodicity parameter. For the Leutheusser model [$H(f) = c_2 f^2$] this occurs for $f = 1/2$ when the coupling c_2 has a critical value of $c_2^* = 4$. For $H[\phi] = c_1\phi + c_2\phi^2$ we obtain the ϕ_{12} model (Götze, 1991). The critical values (c_1^*, c_2^*) for the ϕ_{12} model follow $c_*^1 = 2\sqrt{c_*^2} - c_2^*$, representing the critical line of the ergodic-nonergodic transition. For higher-order models there are critical surfaces.

b. The nonergodic phase $\Delta_0 \geqslant 0$

Let us now consider relaxation near the transition. For the high-frequency region Eq. (5.7) reduces to

$$z\phi_\nu^2(z) - \lambda_s L_z[\phi_\nu^2(t)] = 0, \tag{5.8}$$

where the term proportional to Δ_0 has been neglected in the limit $(|\Delta_0|)^{1/2} \ll |z\phi_\nu(z)|$. At the transition point $\lambda_s = \frac{1}{2}H''(f)/[H'(f)]^{3/2}$. Equation (5.8) corresponds to the power-law relaxation,

$$\phi(t) = f + A(t/\tau_\beta)^{-a}, \tag{5.9}$$

valid for the time window $t_0 \ll t \ll \tau_\beta$ and A a constant. The time $t_o = \Omega_o^{-1}$ represents a microscopic scale, and $\tau_\beta \equiv t_o|\Delta_0|^{-1/2a}$ diverges at the ideal transition point as $\Delta_0 \to 0$. The exponent a of power-law decay is given in terms of the exponent parameter λ_s by the equation $\Gamma^2(1-a)/\Gamma(1-2a) = \lambda_s$, where Γ stands for the gamma function (Abramowitz and Stegun, 1965). For $\Delta_o > 0$, Eq. (5.7) has the solution $\phi_\nu(z) \sim \Delta_0^{1/2}/z$ as $z \to 0$. The long-time limit f of $\phi(t)$ in the glass phase is therefore given by

$$f = f_0 + A_o(\Delta_0)^{1/2} + O(\Delta_0), \tag{5.10}$$

where f_0 is the value of f at the ideal transition point and A_o is a positive constant. The nonergodicity parameter of the transition f in the nonergodic state thus shows a square-root cusp behavior in the vicinity of the transition point.

c. The ergodic phase $\Delta_0 < 0$

Initially the power-law relaxation (5.9) occurs over shorter time scales, as indicated above in Sec. V.A.1.a. A possible solution of $\phi_\nu(z)$ in Eq. (5.7) is more singular than $1/z$ in the limit $z \to 0$. This corresponds to what is referred to as the *von-Schweidler relaxation law* (von-Schweidler, 1907),

$$\phi(t) = f - B_o(t/\tau_\alpha)^b. \tag{5.11}$$

The power-law exponent b is positive and satisfies the equation $\Gamma^2(1+b)/\Gamma(1+2b) = \lambda_s$. For even longer times (smaller z) the inequality $|z\phi_\nu(z)| \ll 1$ is violated. This t^b behavior is valid in the region $\tau_\beta \ll t \ll \tau_\alpha$, where $\tau_\alpha = |\Delta_0|^{-(1/2a+1/2b)}$ represents the scale beyond the von-Schweidler relaxation and is termed the α-relaxation regime. In this regime a full analytic solution of the mode-coupling equations is not known. Numerical solution of the equations is well fit by a stretched exponential form. Assuming $\phi(t) = fe^{-(t/\tau_\alpha)^\beta}$ to be a solution of Eq. (5.4), we obtain an approximate expression for the stretching exponent β in terms of the parameters c_n,

$$\sum_{n=1}^{M} c_n f n^{-1/\beta} = 1. \tag{5.12}$$

Thus, for example, with the Leutheusser model we obtain the stretching exponent $\beta_L = \ln 2/\ln[c_2 f]$. Since for the ideal transition $c_2^* = 4$ and $f = \frac{1}{2}$, we obtain $\beta = 1$, showing that the relaxation is exponential. For the ϕ_{12} model, $\beta_G = \ln 2/\ln[c_2 f/(1-c_1)]$ and varies accordingly along the transition line $c_1^* = 2\sqrt{c_2^*} - c_2^*$.

Let us summarize the sequence of relaxation behavior that follows from the self-consistent equations of the simplified mode-coupling theory. For $\Delta_o < 0$, there is a two-step relaxation process. First there are two power-law decays: critical behavior of the t^{-a} type followed by von-Schweidler relaxation with a positive power-law exponent. Over longer times, the α-relaxation regime is described by a function similar to that of a stretched exponential (this will be discussed further in the next section). For $\Delta_o = 0$ the power-law decay is extended to the longest time scale, while for $\Delta_o > 0$, after the initial power-law decay, the density correlation function freezes in a state of structural arrest. This is of course a prediction of the simple model. In an actual system there are ergodicity-restoring processes by which the dynamic transition is smeared. These will be discussed in Sec. VI.

2. Effects of structure on the dynamics

The schematic model outlined above demonstrates that the feedback mechanism central to mode-coupling theory is insensitive to the wave vector. The predicted transition here is essentially dynamic in the sense that the divergence of viscosity at the critical point is not accompanied by any sharp change in the thermodynamic

properties of the liquid. However, it is important to realize that mode-coupling theory for the glass transition is not just a self-consistent treatment of an integral equation with one degree of freedom. The actual impact of the feedback mechanism becomes clear when we consider the wave-vector-dependent model. Using the static structure factor as an input, we can link the predictions of the theory directly to thermodynamic properties like temperature or density. In the wave-vector-dependent model, even with the simplest form of quadratic coupling of density fluctuations, many different time scales (corresponding to different wave numbers) get coupled and produce stretched exponential behavior in relaxation. In the present section we consider the effects of structure on the dynamics predicted by mode-coupling theory. However, it should also be noted that for certain mean-field models with intrinsic (quenched) disorder equations similar to those of the schematic model provide a useful description of the dynamics (see Sec. X).

In the nonergodic phase $\phi(q,t)$ has a nondecaying part $f(q)$ in the long-time limit,

$$\phi(q,t) = f(q) + [1 - f(q)]\phi_\nu(q,t). \tag{5.13}$$

$\phi_\nu(q,t)$ goes to zero for large t. The $f(q)$'s, or nonergodicity parameters, are determined from a set of coupled nonlinear integral equations,

$$\frac{f_q}{1-f_q} = \frac{1}{\Omega_q^2}\tilde{m}^L(q,t\to\infty) \equiv \mathcal{H}_q[f_k], \tag{5.14}$$

where we have treated the integral over the wave vector **k** in the mode-coupling term as a sum over a discrete set of k values uniformly distributed over a grid of size say N_g and extending up to a suitable upper cutoff value. In discretized form we denote the $f(q)$ as f_q and $\phi(q,t)$ as $\phi_q(t)$ with q a discrete index. The functional $\mathcal{H}_q$ in the right-hand side of Eq. (5.14) is obtained from the long-time limit of the expression for $\tilde{m}^L(q,t)$ in Eq. (4.4) and is a functional of all the f_q's. Equation (5.14) now represents a set of M coupled integral equations which are numerically solved using iterative methods. The necessary input for this is the static structure factor $S(q)$ for the liquid. For low densities, only the trivial solution set with all f_q's equal to zero (corresponding to the ergodic liquid state) is obtained. The critical density at which all the f_q's simultaneously converge to a nonzero set of values marks a dynamic transition of the fluid to a nonergodic state. For example, we consider a system of hard spheres of diameter σ with the packing fraction $\varphi = \pi n\sigma^3/6$. The Percus-Yevick solution with the Verlet-Weiss correction (Barker and Henderson, 1976) for $S(k)$ of a hard-sphere system is used as input in Eq. (5.14). The fluid undergoes an ergodic-to-nonergodic transition at the critical value of the packing fraction $\varphi_c = 0.525$. The contributions to the mode-coupling integral (5.14) from k values above the upper cutoff value $50\sigma^{-1}$ have little effect on the transition point.

a. The cusp behavior of the nonergodicity parameter

In the close vicinity of this dynamic transition point, the order parameter of this transition, i.e., the f_q's show a cusp behavior similar to Eq. (5.10) in the schematic model. Understanding this behavior in the wave-vector-dependent model involves an asymptotic analysis of the integral equation (5.14) near the ideal transition point (Götze, 1985). The starting point of such an exercise is the stability matrix C_{qk} defined as

$$C_{qk} = \frac{\delta\mathcal{H}_q}{\delta f_k}(1-f_k)^2, \tag{5.15}$$

all elements of which are positive numbers by definition. Let e_k^c and $\hat{e}_k^c$, respectively, denote the right and left eigenvectors of the matrix C_{qk}^c at the transition point corresponding to the eigenvalue 1; $\Sigma_k\, C_{qk}^c e_k^c = e_q^c$ and $\Sigma_q\, \hat{e}_c^q C_{qk}^c = \hat{e}_k^c$. The f_q's are related to the corresponding f_q^c's, the nonergodicity parameters, at the dynamic transition point as

$$f_q = f_q^c + g_\lambda h_q \Delta_0^{1/2} + O(\epsilon), \tag{5.16}$$

where the amplitude is given by $g_\lambda = (1-\lambda)^{-1/2}$ and $h_q = (1-f_q^c)^2 e_q^c$. The separation parameter Δ_o is defined in terms of ϵ, $\Delta_o = C\epsilon$, where $C = \Sigma_q\, \hat{e}_c^q C_q^c$ and ϵ is the relative distance from the dynamic transition point in terms of a suitable control parameter. For example, for a hard-sphere system in which the packing fraction is the controlling thermodynamic variable, $\epsilon = (\varphi - \varphi_c)/\varphi_c$. Finally the parameter λ in Eq. (5.16) is obtained as

$$\lambda = \sum_{qkp} \hat{e}_q^c C_{q,kp}^c e_k^c e_p^c, \tag{5.17}$$

with $C_q^c = n[\partial H_q/\partial n]_{n=n_c}$ and $C_{q,kp}^c = 1/2[(1-f_k)^2(1-f_p)^2\delta^2 H_q/\delta f_k \delta f_p]_{n=n_c}$.

The square-root cusp behavior of the nonergodicity parameter is an asymptotic result. Results extracted from experimental data for the Debye-Waller factor are used to locate the existence of a possible mode-coupling transition point. Since the sharp dynamic transition of the supercooled liquid gets smeared in a real system, the square-root cusp is an idealization. The cusp can only be concluded indirectly. Furthermore, even if we confine consideration to the ideal model and ignore the cutoff mechanism, the cusp behavior still gets modified due to leading-order corrections to the asymptotic result (5.16):

$$f_q = f_q^c + g_\lambda h_q \Delta_o^{1/2}[1 + \Delta_o^{1/2}\tilde{K}_q]. \tag{5.18}$$

The amplitude functions $\tilde{K}_q$ have been computed by Franosch *et al.* (1997b) for the simple form of the memory function (4.4). The leading asymptotes (5.16) which include contributions up to $O(\Delta_o^{1/2})$ describe $f_q - f_q^c$ within 10% accuracy for ϵ values extending up to 0.003, 0.08, and 0.002, respectively, for wave numbers $q\sigma = 7.0$, 10.6, and 17.4 in a hard-sphere fluid. The larger value for the range of validity ϵ at $q = 10.6$ is mainly due to accidental cancellation of higher-order terms (Franosch *et al.*, 1997b). With a hard-sphere structure factor,

the numerical solutions of the integral equations (5.14) for f_q's in the nonergodic phase agree well with an empirical fit $\epsilon^{\alpha(q)}$ involving a wave-number-dependent effective exponent α (Das, 1993).

b. Scaling in power-law relaxations

The decay of the density correlation function $\phi_q(t)$ has distinct relaxation regimes similar to those occurring in the case of the schematic model described in the previous section. First, $\phi_q(t)$ decays to a plateau value f_q algebraically,

$$\phi_q(t) = f_q^c + h_q(\tau_\beta/t)^a. \tag{5.19}$$

As in the schematic case, Eq. (5.19) is valid in the time window $t_o \ll t \ll \tau_\beta$. The time scale τ_β diverges algebraically with the separation parameter Δ_o such that $\tau_\beta = t_o|\Delta_0|^{-1/2a}$. Above the critical density, in the nonergodic glassy phase $\phi_q(t)$ decays by a power law t^{-a} to the corresponding value of the nonergodicity parameter f_q. For densities less than the critical value, the initial power-law relaxation crosses over to the von-Schweidler relaxation,

$$\phi_q(t) = f_q^c - h_q(t/\tau_\alpha)^b. \tag{5.20}$$

This occurs in the time window $\tau_\beta \ll t \ll \tau_\alpha$, the same as in the schematic case [Eq. (5.11)]. Both the exponents a and b of the power-law relaxations follow from the same transcendental equation as in the corresponding schematic case. The parameter λ_s in the schematic case now correspond to the exponent parameter λ and is computed using the formula presented in Eq. (5.17). For hard-sphere systems with one-loop vertex contributions, $\lambda = 0.74$ (Fuchs, Hofacker, and Latz, 1992).

The power-law decays in different time windows are sometimes expressed in the form of a single scaling function,

$$h_q^{-1}[\phi_q(t) - f_q^c] = \sqrt{\Delta_o}\, g_\pm(\hat{t}), \tag{5.21}$$

where $g_\pm(\hat{t})$ refers to the master functions in terms of the reduced time $\hat{t} = t/\tau_\beta$, above and below the dynamic transition point. The left-hand side of Eq. (5.21) scaled with a factor of $\sqrt{\Delta_o}$ will follow one master curve independent of wave number q. The power-law relaxations described above then follow from the asymptotic behavior of the scaling functions. For short times when $t \ll \tau_\beta$, to leading order $g_\pm(\hat{t} \ll 1) = \hat{t}^{-a}$. In the other limit of $t \gg \tau_\beta$, the scaling functions are different above and below the transition point. In the nonergodic state g_+ approaches the value $g_\lambda = (1-\lambda)^{-1/2}$ for $\hat{t} \gg 1$. In this case, Eq. (5.21) reduces to the cusp behavior of the nonergodicity parameter described by Eq. (5.16). A crossover time $\hat{\tau}_+$ is sometimes defined when the monotonically decreasing function reaches within, say, 0.1% of its asymptotic value, i.e., $g_+(\hat{\tau}_+) = 1.001 g_\lambda$. On the other hand, for the liquid side, g_- for large $\hat{t}$ approaches the von-Schweidler law, $g_-(\hat{t} \gg 1) = -B\hat{t}^b$, where B is a constant. In this case a corresponding crossover time $\hat{\tau}_-$ can be defined where $g_-(\hat{\tau}_-) = 0$. The characteristic power-law relaxation of the mode-coupling theory is termed as the β-relaxation and the scaling behavior in the corresponding region as β-scaling. We will use this terminology in the subsequent sections.

c. The factorization property

Both the exponents a and b in the time regimes corresponding to the power-law relaxations are independent of temperature or density. From Eq. (5.21) it is clear that the space and time dependences of the quantity $\phi(q,t) - f(q)$ become separable. This rather remarkable prediction of the mode-coupling theory has been termed the *factorization property*. This is an asymptotic result, which holds in the close vicinity of the dynamic transition point. Higher-order corrections can be presented in the form of a series with factorized terms (Franosch *et al.*, 1997b) in powers of $(\tau_\beta/t)^b$,

$$\phi_q(t) - f_q^c = h_q\left(\frac{\tau_\beta}{t}\right)^a \left[1 + K_q^{(1)}(a)\left(\frac{\tau_\beta}{t}\right)^a\right], \tag{5.22}$$

and a similar expansion in powers of $(t/\tau_\alpha)^b$ is possible for the von-Schweidler relaxation,

$$\phi_q(t) - f_q^c = -h_q\left(\frac{t}{\tau_\alpha}\right)^b \left[1 - K_q^{(1)}(-b)\left(\frac{t}{\tau_\alpha}\right)^b\right]. \tag{5.23}$$

The q-dependent amplitudes $K_q^{(1)}(x)$ (Franosch *et al.*, 1997b) are referred to as "corrections to scaling." One will need to keep adding higher-order terms as the distance from the transition increases.

The wave-vector independence implied in the factorization property is also affected by other properties. For example, the microscopic time scale t_o in the q-dependent model now assumes special significance (Das, 1993). It quantifies the matching of the short-time decays for *all* the q values to the transients which are obviously dependent on the wave number (the microscopic frequency for wave number q is $\Omega_q^2 = q^2[\beta m S(q)]^{-1}$). The time window between the crossover from the transient to the power-law behavior given by Eq. (5.22) is now strongly dependent on wave number. Furthermore, for q values at which the amplitude of the correction term becomes small, the range of validity of the leading term is naturally over longer times. Thus the range of validity of the leading-order solution and hence that of the so-called factorization property is strongly dependent on q.

With the next-to-asymptotic-order terms in Eq. (5.21) taken into account, the new scaling functions consist of corresponding correction terms,

$$h_q^{-1}[\phi_q(t) - f_q^c] = \sqrt{\Delta_o}[g_\pm(\hat{t}) + \sqrt{\Delta_o}\{g_\pm^{(1)}(q,\hat{t})\}], \tag{5.24}$$

where $\hat{t} = t/\tau_\beta$ is the rescaled time. The leading-order correction terms $g_\pm^{(1)}$ for the master functions are presented by Franosch *et al.* (1997b). The corrections are dependent on wave number q and hence, as we move away from the dynamic transition point, the q independence of the right-hand side of Eq. (5.24) becomes invalid. In short, the closer we get to the dynamic transition point,

the more the time window expands over which the correlation function $\phi(q,t)$ remains near the plateau f_q^c. Hence the range of validity of the factorization property also grows. The corrections to the scaling described here are for the simple mode-coupling model in which all aspects of the ergodicity-restoring mechanism have been ignored. In the presence of physically relevant processes that remove the sharp dynamic transition, it is not *a priori* clear whether the system will ever get close enough to the transition point to clearly display the above behaviors.

d. Alpha-relaxation scaling

In the region asymptotically close to the dynamic transition at φ_c with the time scale τ_α tending to ∞, the α relaxation in the mode-coupling theory is described in terms of a temperature-independent master function $\phi_q(t) \equiv \hat{\Phi}_q(t/\tau_\alpha)$. All the relaxation curves at different temperatures will merge into a single curve with a temperature-dependent relaxation time τ_α. This property is known as the *time/temperature superposition principle*. Alpha relaxation is defined in the limit that the control parameter φ asymptotically approaches the critical value $\varphi \to \varphi_c$, with $z \to 0$, $\tau_\alpha \to \infty$, so that $\hat{z} = z\tau_\alpha$ remains finite. The mode-coupling prediction for α relaxation is obtained through numerical solution of the model equations. The leading-order result, i.e., the master function Φ, was computed by numerically solving the equation (Fuchs, Hofacker, and Latz, 1992)

$$\hat{\Phi}_q(\hat{z}) = \frac{\hat{m}_q(\hat{z})}{1 + \hat{z}\hat{m}_q(\hat{z})}. \tag{5.25}$$

Equation (5.25) is obtained from Eqs. (4.2)–(4.4) by taking the scaling limit $z \to 0$, $\tau_\alpha \to \infty$, so that $\hat{z} = z\tau_\alpha$. $\tau_\alpha \hat{m}_q(\hat{z}) = -im^L(q,z)/\Omega_q^2$, and $\tau_\alpha \hat{\Phi}_q(\hat{z}) = \phi(q,z)$. The mode-coupling integrals in $\hat{m}$ are evaluated at the transition point $\varphi = \varphi_c$. The microscopic and power-law relaxations are eliminated here so the $\hat{t} = 0$ value of the scaling function $\hat{\Phi}$ is equal to f_q. Therefore Eq. (5.14) for locating the dynamic transition now corresponds to the $\hat{t} \to 0$ limit of Eq. (5.25). The scaling function $\Phi_q(\hat{t})$ is obtained very accurately by numerically solving (Fuchs *et al.*, 1991) Eq. (5.25) in the time-space domain as

$$\hat{\Phi}_q(\hat{t}) = \hat{m}_q(\hat{t}) - \frac{d}{d\hat{t}} \int_o^{\hat{t}} ds \hat{m}_q(\hat{t} - s)\hat{\Phi}_q(s). \tag{5.26}$$

For the input static structure factor $\hat{\Phi}_q(\hat{t})$ the Percus-Yevick solution is used. An asymmetrically stretched shape of the spectrum in the frequency space is obtained due to the overlap of the von-Schweidler relaxation. The stretched exponential form is a good fit for the master function at all wave numbers, with better quality of agreement at large q. The stretching exponent β is wave-number dependent and β_q shows a minimum at the first peak of the static structure factor. The corresponding relaxation times $\tau_\alpha(q)$ also shows a strong peak at this wave vector.

Similar to the scaling function for the initial power-law regimes, the relaxation behavior described by the master function Φ is an asymptotic result valid in the close vicinity of the transition point. The time/temperature superposition is a prediction of the simple mode-coupling theory only near the dynamic transition point. As we move away from the transition the temperature-independent master function requires correction terms very much in the same way as for the power-law regime,

$$\phi_q(t) = \hat{\Phi}_q(\hat{t}) + \Delta_o(1 - f_q^c)^2 \hat{\Phi}_q^{(1)}(\hat{t}) + O(\Delta_o^2). \tag{5.27}$$

The temperature independence of the α-relaxation master function is lost with the inclusion of the correction term. In contrast to the case of power-law relaxations, the leading-order correction to the α master function in Eq. (5.27) is of $O(\Delta_o)$. The corresponding correction to the power-law scaling function is of $O(\Delta_o^{1/2})$. Indeed, the numerical solutions for $\phi_q(t)$ from the simple mode-coupling model show a marked departure from time/temperature superposition unless one is in the close vicinity of the dynamic transition point. The solutions of the mode-coupling equations away from the transition follow power-law or stretched exponential forms with effective exponents that are dependent on both temperature and wave number.

e. Viscoelastic behavior

The viscoelastic behavior of dense liquids is understood in mode-coupling theory using the liquid structure as an input and without resorting to empirical models. The dynamic response of the fluid to shear is studied through an analysis of the transverse current correlation function $\phi_T(q,z)$, expressed in the form (3.18) generalizing the corresponding transport coefficient $m_o^T(q)$ in terms of the generalized shear viscosity $m^T(q,z)$,

$$m^T(q,z) = m_o^T + \int_o^\infty dt e^{izt} \tilde{m}^T(q,t). \tag{5.28}$$

The one-loop contribution to $\tilde{m}^T$ from the coupling of density fluctuations is obtained as

$$\tilde{m}^T(q,z) = \frac{n}{2m\beta} \int \frac{d\mathbf{k}}{(2\pi)^3} (1 - u^2)[V_T(\mathbf{k}_1, \mathbf{k})]^2 \times S(k_1)S(k)\phi(k_1,t)\phi(k,t), \tag{5.29}$$

where $u = \hat{\mathbf{q}} \cdot \hat{\mathbf{k}}$ and $\mathbf{k}_1 = \mathbf{q} - \mathbf{k}$. The vertex function $V_T(\mathbf{q} - \mathbf{k}, \mathbf{k}) = k[c(k) - c(k_1)]$. The memory function or the generalized shear viscosity $\tilde{m}^T$ develop correlations over long time scales as the result of the slow dynamics of the density correlation function. We shall describe below two consequences of this.

(A) The transverse autocorrelation function ϕ_T obtained from the coupled equations (5.28) and (5.29) shows that a critical value q_o exists such

that with $q > q_o$ the relaxation of ϕ_T is a damped oscillatory mode. This indicates that the system sustains shear waves up to this wave number. Below q_o the decay of $\phi_T(q,t)$ is exponential. In the simple mode-coupling model with a dynamic transition, q_o approaches zero as $\varphi \to \varphi_c$. This corresponds to a maximum wavelength $L_o = 2\pi/q_o$ for the propagating shear waves (Kirkpatrick, 1984) in the liquid. For a hard-sphere system, as the critical packing fraction of the dynamic transition $\varphi_c = 0.525$ is approached, L_o tends to diverge (Ahluwalia and Das, 1998), implying complete freezing at all length scales. This divergence of L_o approaching the ideal transition point is prompted by the divergence of the shear viscosity. In the complete analysis with the extended mode-coupling theory (described in the next section) the sharp transition is smeared and hence L_o does not diverge (Das, 2000). Similar behavior has been observed (Mountain, 1997) in molecular-dynamics simulations of fragile liquids for which the mode-coupling models generally apply.

(B) Anomalous stretching is seen in the shear modulus. The elastic response of the supercooled liquid is defined over a time scale in terms of the corresponding frequency-dependent modulus $G(\omega) = i\omega\eta(\omega)$, where $\eta(\omega)$ is the frequency transform of the time-dependent shear viscosity. $G(\omega)$ for a typical glass-former, di-n-butylphthalate (DBP), was measured by Menon *et al.* (1994) and was fitted to the Cole-Davidson (Davidson and Cole, 1951) form,

$$G_{CD}(\omega) = G_\infty \left(1 - \frac{1}{(1 + i\omega\tau)^{\beta_{CD}}} \right), \tag{5.30}$$

where β_{CD} is the stretching exponent. The experimental data show that β_{CD} increases with decrease in temperature. This anomalous inverse temperature dependence of the stretching can be understood via the simple mode-coupling model (Srivastava *et al.*, 2002) as a consequence of the characteristic two-step relaxation process, that is, power laws crossing over to a stretched exponential behavior. The effective power-law exponents as well as the stretching exponents computed from mode-coupling theory are temperature dependent when the liquid is away from the dynamic transition point. The stretching exponent of the α-relaxation part shows a normal behavior, i.e., an increase (towards 1) with increase of the temperature. However the low-frequency wing of the power-law relaxation overlaps with that of the stretched exponential form to produce the anomalous effect. To have such an overlap, it is therefore required that the time scales of the two processes not be widely separated. The observation of this anomalous effect indicates that the system does not get too close to the transition.

The frequency-dependent shear viscosity controls the elastic behavior of the supercooled liquid in terms of the dynamic shear modulus. In a similar way the specific heat (which also relates to the equilibrium state) develops frequency dependence (Birge and Nagel, 1985; Nielsen and Dyre, 1996), which is understood in terms of the frequency dependence of the longitudinal viscosity of the liquid (Zwanzig, 1988). Such frequency dependences can follow from the simple model described above (Harbola and Das, 2001) or from more involved treatments (Marchetti, 1986; Oxtoby, 1986).

The self-consistent mode-coupling equations (4.2)–(4.4) have a rich mathematical structure characterized by a class of bifurcation singularity (Arnol'd, 1992). The discussion above refers to the lowest-order (fold bifurcation) singularity, which is generally linked to structural relaxation. Higher-order singularities were analyzed (Götze and Haussmann, 1988) obtaining a different relaxation behavior. Götze and Sperl (2002) have recently studied those singularities to predict relaxations expressed in polynomials of $\ln(t)$. The interaction potential between the liquid particles influences its dynamics through the effect on the static correlations, used as input parameters in the mode-coupling theory. When mode-coupling equations were studied with structure factors corresponding to sticky hard spheres (Fabbian *et al.*, 1999), square-well system (Dawson *et al.*, 2001) they exhibited signatures of higher-order singularity (cusp bifurcation). Logarithmic dependences on relaxation are reported to be seen in experiments on colloids of micellar particles (Mallamace *et al.*, 2000) as well as in molecular-dynamics simulation (Puertas *et al.*, 2002). If the short-range attractive interaction or the stickiness of the particles dominates the dynamics, the glassy behavior can occur at much lower densities than close packing. This has been referred to as attractive glass and is linked to the re-entrant glass transition seen in experiments on colloids with short-range attraction (Eckert and Bartsch, 2002; Pham *et al.*, 2002), copolymer micellar system (Chen, Chen, and Mallamace, 2003). The mode-coupling model has also been used to study how the short-range attractive interaction between the liquid particles affects its mechanical properties (Zaccarelli *et al.*, 2001a) and the nature of the tagged particel dynamics (Kaur and Das, 2003b).

3. Tagged-particle dynamics

We shall consider here the theoretical model for the slow single-particle dynamics in the context of mode-coupling theory. The slow relaxation of the density correlation which result from the feedback mechanism influences the single-particle dynamics. The density of a tagged particle is formally denoted by $\rho_s(\mathbf{r},t) = m\delta[\mathbf{r} - \mathbf{r}_\alpha(t)]$. The corresponding density correlation or van Hove correlation function,

$$G_s(|\mathbf{r} - \mathbf{r}'|, t - t') = \langle \rho_s(\mathbf{r},t)\rho_s(\mathbf{r}',t') \rangle, \tag{5.31}$$

represents the time-dependent spatial distribution of the tagged particle. $\int d\mathbf{r} G_s(r,t) = 1$ ensures particle conserva-

tion. In the thermodynamic limit the average $\langle \rho_s \rangle$ is zero and hence $\delta\rho_s \equiv \rho_s$. The Fourier-Laplace transform van Hove correlation function $\phi_s(q,z)$ is obtained in the form of a two-step continued fraction,

$$\phi_s(q,z) = \left[z - \frac{q^2 v_o^2}{z + i\Gamma_o^s} \right]^{-1}, \tag{5.32}$$

similar to Eq. (3.17) for the total density correlation, with v_o being the average speed of the fluid particle. In the long-time limit (small z) ϕ_s develops a diffusive pole $\phi_s(q,z) = 1/(z + iq^2 D_B)$ with the bare self-diffusion coefficient $D_B = v_o^2/\Gamma_o^s$.

The tagged-particle density ρ_s satisfies the continuity equation, $\partial_t \rho_s + \nabla \cdot \mathbf{g_s} = 0$. The equation of motion for the current $\mathbf{g}_s$ is obtained as

$$\frac{\partial g_s^i}{\partial t} + \Gamma_o^s g_s^i + v_o^2 \nabla_i \delta\rho_s = \zeta_s^i, \tag{5.33}$$

similar to the corresponding equations (4.12) and (4.13) for ρ and $\mathbf{g}$, respectively. The noise ζ_s^i in the equation for $\mathbf{g_s}$ is related to the friction coefficient Γ_o^s through the fluctuation-dissipation relation $\langle \zeta_s^i(\mathbf{r},t)\zeta_s^j(\mathbf{r}',t')\rangle = \Gamma_0^s \delta_{ij}\delta(\mathbf{r} - \mathbf{r}')\delta(t-t')$. Equation (5.33) for the tagged-particle density is only approximate, because the momentum $\hat{\mathbf{g}}_s$ of the tagged particle in the sea of identical particles is not a conserved quantity nor is it like that of a Brownian particle of heavy mass. There is no basis for assuming a separation of time scales between the "noise" and "regular" parts in this equation. Γ_o^s is a constant in the small-q limit. For a hard-sphere system Γ_o^s computed from the Enskog model gives $\Gamma_o^s = 2/(3t_E)$. Therefore Eq. (5.32) obtained in the form of a two-step continued fraction, using the equations of motion for ρ_s and $\mathbf{g}_s$, can only be considered approximate, as well.

The nonlinear terms in the Langevin equation for $\mathbf{g}_s$ are computed following an approach like that for the total momentum density $\mathbf{g}$. The mode-coupling correction to the bare friction coefficient Γ_o^s is obtained (Kirkpatrick and Nieuwoudt, 1986a, 1986b) from the corresponding nonlinear term $\rho_s(\delta F_U/\delta\rho_s)$ as in Eq. (4.13). Using the standard form of the expansion (4.16) for the free energy F_U one obtains the relevant vertex function for the coupling of $\delta\rho_s$ and $\delta\rho$ as $V_s(\mathbf{q}-\mathbf{k},\mathbf{k}) = (\hat{\mathbf{q}}\cdot\mathbf{k})c(k)$. The Γ_o^s in Eq. (5.32) is now renormalized to $\Gamma_s^{\mathbf{r}}(q,z) = \Gamma_o^s + \tilde{\Gamma}_s(q,z)$ with a mode-coupling contribution from the density fluctuations,

$$\tilde{\Gamma}_s(q,t) = \frac{n}{\beta m}\int \frac{d\vec{k}}{(2\pi)^3}[V_s(\mathbf{q}-\mathbf{k},\mathbf{k})]^2 \times S(k)\phi_s(\mathbf{q}-\mathbf{k},t)\phi(k,t) \equiv \tilde{m}_L^s(q,t). \tag{5.34}$$

The renormalized expression (5.34) for Γ_o^s can also be obtained (Götze, 1991) by following a procedure similar to that described in Appendix A.1. This involves taking projections on the space of coupled slow modes $\mathcal{C}_s(\mathbf{k}p\cdots) = \delta\rho(\mathbf{k})\delta\rho_s(\mathbf{p})\cdots$. The same model for tagged-particle correlation was studied to conclude that the self-diffusion coefficient goes to zero (Bengtzelius *et al.*, 1984) at the dynamic transition point.

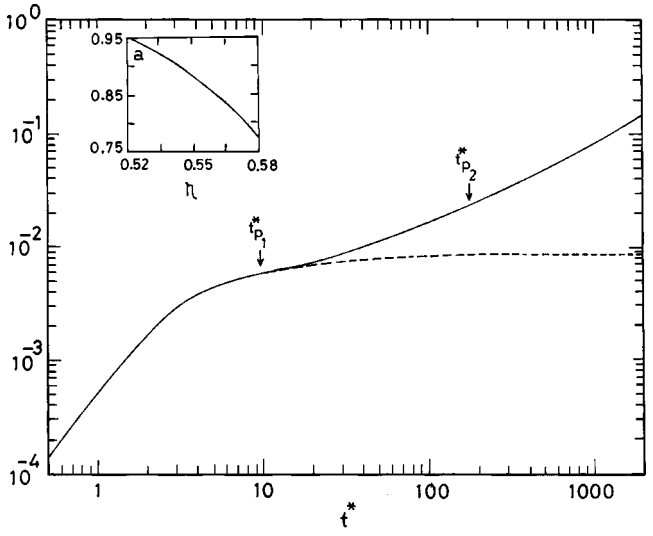

FIG. 3. Mean square displacement $\langle r^2(t)\rangle$ vs t at packing fraction $\eta \equiv \varphi = 0.565$: solid line, extended mode-coupling theory; dashed line, simple mode-coupling theory. The inset shows the power-law exponent a defined by a power-law behavior of $\langle r^2(t)\rangle$ (see text) with packing fraction η. Length is expressed in units of hard-sphere diameter σ and t in the corresponding Enskog time t_E for hard spheres (see text). The arrows indicate the times where the non-Gaussian parameter $\alpha_2(t)$ (Rahman, 1964) shows peaks. From Kaur and Das, 2002.

The model presented above for the tagged-particle dynamics is somewhat phenomenological in nature and unlike the case of the collective density. Nevertheless, the above form of mode coupling has been very widely investigated. The form (5.34) of the memory function provides a mechanism for producing the cage effect in dense fluids. The self-correlation $\phi_s(q)$ in Eq. (5.32), driven by the memory function (5.34), freezes to f_q^s at the dynamic transition point described by Eqs. (4.2)–(4.4). The corresponding equation for the nonergodicity parameter f_q^s is

$$\frac{f_q^s}{1-f_q^s} = \frac{1}{\Omega_{sq}^2}\tilde{m}_s^L(q,t\to\infty) \equiv \mathcal{H}_q^s[f_k], \tag{5.35}$$

with $\Omega_{sq}^2 = q^2 v_o^2$. In the close vicinity of the transition, on the liquid side, $\phi_s(q,t)$ follows a sequence of relaxation similar to that of the density correlation functions, as discussed earlier in Sec. V.A.2. Away from the transition, corrections similar to those discussed for the density correlation function in Sec. V.A.2 apply (Fuchs *et al.*, 1998). At the dynamic transition point, the self-diffusion coefficient approaches zero and the corresponding mean-square displacement $\langle r^2(t)\rangle$ also freezes in time, signifying complete localization of the particle (see Fig. 3, dashed line). The renormalization of the self-diffusion coefficient due to coupling of ρ_s to the total momentum density $\mathbf{g}$ (Bodeaux and Mazur, 1973), on the other hand, follows directly from the equations conforming to the conservation laws. Such contributions have been ignored

above, since they do not give rise to the feedback mechanism.

B. Extensions to more complex systems

The feedback mechanism due to coupling of density fluctuations producing slow dynamics has been applied in a number of other systems with higher complexity. We consider two specific examples here.

1. Mode-coupling theory for binary mixtures

The feedback mechanism central to mode-coupling theory is formulated for binary systems (Bosse and Thakur, 1987; Krieger and Bosse, 1987; Barrat and Latz, 1990; Harbola and Das, 2002) in the same manner as for the one-component case described above. The choice of slow variables for the binary system is important in determining the form of mode coupling that follows. From the underlying conservation laws, the slow variables for a binary fluid are the two partial densities $\rho_s(\mathbf{x})$, $s=1,2$ and total momentum density $\mathbf{g}(\mathbf{x})$,

$$\rho_s(\mathbf{x}) = m_s \sum_{\alpha=1}^{N_s} \delta[\mathbf{x} - \mathbf{x}_s^{\alpha}(t)], \tag{5.36}$$

$$\mathbf{g}(\mathbf{x}) = \sum_s \sum_{\alpha=1}^{N_s} \mathbf{p}_s^{\alpha} \delta[\mathbf{x} - \mathbf{x}_s^{\alpha}(t)], \tag{5.37}$$

where $\mathbf{x}_s^{\alpha}(t)$ is the position and $\mathbf{p}_s^{\alpha}$ the momentum of the αth particle in the sth species. N_s is the number of particles of the sth species, and the total number of particles is given by $N=N_1+N_2$. The momentum densities $\mathbf{g}_s$ for individual species can be represented similarly to Eq. (5.37). $\mathbf{g}=\mathbf{g}_1+\mathbf{g}_2$ is a microscopically conserved property, but not $\mathbf{g}_1$ or $\mathbf{g}_2$. An essential input in constructing the Langevin equations is the free-energy functional, which is expressed in terms of $\mathbf{g}$ and ρ_s's. $F=F_k+F_U$, where the kinetic part F_k is same as given by Eq. (4.11) (Harbola and Das, 2002) with the total density $\rho=\rho_1+\rho_2$. This form is essential for generating the Galilean-invariant form of the generalized Navier-Stokes equation. The potential part F_U has contributions similar to that of the one-component system, i.e., an ideal-gas part F_{id} and an interaction part F_{int}. The F_{id} is taken as a generalization of the one-component result (4.15), while F_{int} is obtained (Sinha and Marchetti, 1992) in terms of the equilibrium two-particle direct correlation function $c_{ss'}(\mathbf{x})$ between species s and s' (Hansen and McDonald, 1986). Thus $F_U=F_{id}+F_{int}$ is

$$F_u(\rho) = \frac{1}{m_s}\int d\mathbf{x}\rho_s(\mathbf{x})\left[\ln\frac{\rho_s(\mathbf{x})}{\rho_{os}} - 1\right] - \frac{1}{2m_s m_{s'}}\int d\mathbf{x}d\mathbf{x}' c_{ss'}(\mathbf{x}-\mathbf{x}')\delta\rho_s(\mathbf{x})\delta\rho_{s'}(\mathbf{x}'), \tag{5.38}$$

where ρ_{os} is the average density of the sth species in the mixture.

For binary mixtures the 2×2 matrix $\mathbf{C}(q,t)$ of correlations of density fluctuations between the s and s' species is defined as

$$C_{ss'}(\mathbf{x}-\mathbf{x}',t-t') = \frac{1}{N}\langle \delta\rho_s(x,t)\delta\rho_{s'}(x',t')\rangle. \tag{5.39}$$

The mode-coupling theory for a binary mixture is formulated in two different forms. In an approach that will be referred to as model A, the individual momentum densities $\mathbf{g}_1$ and $\mathbf{g}_2$ of the two species, together with the corresponding mass densities ρ_1, ρ_2, are treated as slow variables. The generalized Langevin equations corresponding to the $\mathbf{g}_s$, $s=1,2$ are obtained as

$$\frac{\partial g_{is}}{\partial t} + \nabla_j \frac{g_{is}g_{js}}{\rho_s} + \rho_s \nabla_i \frac{\delta F_u}{\delta \rho_s} + \sum_{s'} Ł_{ij}^{ss'} \frac{\delta F}{\delta g_{js'}} = \tilde{f}_{is}, \tag{5.40}$$

with the individual densities satisfying $\partial_t\rho_s + \nabla\cdot\mathbf{g}_s = 0$. The equations for the ρ_s's now only have reversible parts computed from the corresponding Poisson brackets. The self-diffusion and interdiffusion of the two species are ignored. Since $\mathbf{g}_s=\mathbf{g}(\rho_s/\rho)$, F_k reduces to the form $F_k = \int d\mathbf{x}[g_1^2/2\rho_1 + g_2^2/2\rho_2]$. The thermal noise $\tilde{\mathbf{f}}_s$ in the equation for the momentum density $\mathbf{g}_s$ follows the fluctuation-dissipation relation,

$$\langle \tilde{f}_{is}(\mathbf{x},t)\tilde{f}_{js'}(\mathbf{x}',t')\rangle = 2k_B T L_{ij}^{ss'}\delta(\mathbf{x}-\mathbf{x}')\delta(t-t'), \tag{5.41}$$

where $L_{ij}^{ss'}$, for s, $s'=1,2$ are the elements of the bare transport coefficient matrix. Renormalization of the elements of the bare matrix $L_{ij}^{ss'}$, as a result of the nonlinearities in the equations for $\mathbf{g}_1$ and $\mathbf{g}_2$, are computed within the self-consistent mode-coupling approximations of dominant density fluctuations. To one-loop order the contribution is

$$\tilde{M}_{ss'}(q,t) = \frac{n}{2n_s n_{s'}}\int \frac{d^3k}{(2\pi)^3} V_{s\mu\sigma}(q,k)V_{s'\mu'\sigma'}(q,k) \times C_{\mu\mu'}(k,t)C_{\sigma\sigma'}(k_1,t), \tag{5.42}$$

where $V_{s\mu\sigma}(q,k) = [n/(m_\mu m_\sigma)][\hat{q}\cdot k\,\delta_{s\sigma}c_{s\mu}(k) + \hat{q}\cdot k_1\,\delta_{s\mu}c_{s\sigma}(k_1)]$ with the notation $\mathbf{k}_1=\mathbf{q}-\mathbf{k}$ and $n=n_1+n_2$ for the total number density. The long-time limit of the matrix $C_{ss'}(q,t)$ leads to the nonergodicity parameters and is denoted by the matrix $F(q)$. A set of nonlinear integral equations, similar to Eq. (5.14) in the one-component case, is obtained for the $F(q)$'s (Harbola and Das, 2002). These equations involve the long-time limit of $\tilde{M}_{ss'}(q,t)$. The same mode-coupling model was earlier obtained by an analysis of the memory function (Krieger and Bosse, 1987; Barrat and Latz, 1990; Fuchs and Latz, 1993) using the projection operator technique.

In a somewhat different approach, which we shall refer to as model B, the mode-coupling theory for a binary system is formulated with the set of slow variables consisting of ρ_s, $s=1,2$ and the total momentum density $\mathbf{g}$ (Harbola and Das, 2002). The generalized Langevin equations for the slow variables are obtained as

$$\frac{\partial \rho_s}{\partial t} + \nabla \cdot \left[\frac{\rho_s}{\rho} \mathbf{g} \right] + \gamma_{ss'} \frac{\delta F_u}{\delta \rho_{s'}} = \theta_s, \quad s = 1,2, \tag{5.43}$$

$$\frac{\partial g_i}{\partial t} + \nabla_j \frac{g_i g_j}{\rho} + \rho_s \nabla_i \frac{\delta F_u}{\delta \rho_s} + L_{ij} \frac{\delta F}{\delta g_j} = f_i, \tag{5.44}$$

where the repeated indices are summed over. The bare transport matrix L_{ij} is related to the noise by the usual fluctuation-dissipation relation. For an isotropic liquid, L_{ij} is expressed in terms of a longitudinal and shear viscosity, as described in Sec. III in the one-component case. It is instructive to write the partial density equations (5.43) in the form of balance equations, $\partial_t \rho_s + \nabla \cdot \tilde{\mathbf{g}}_s = 0$, where the current associated with ρ_s is

$$\tilde{\mathbf{g}}_s = \left[\frac{\rho_s}{\rho} \mathbf{g} \right] + \gamma_{ss'} \nabla \frac{\delta F_u}{\delta \rho_{s'}} + \alpha_s, \tag{5.45}$$

with $\nabla \cdot \alpha_s = -\theta_s$. The momentum density $\tilde{\mathbf{g}}_s$'s individually are not conserved quantities, but their sum is. The dissipative and the random parts of the currents $\tilde{\mathbf{g}}_s$'s maintain a detailed balance to ensure the continuity equation (4.12) for the total density ρ. Equation (5.43) includes the interdiffusion in the dynamics that was ignored in model A. This is crucial in considering the phenomenon of jamming or the glass transition in binary systems. The corresponding mode-coupling theory is formulated in terms of the renormalized longitudinal viscosity Γ^{mc}, which has the following one-loop expression:

$$\Gamma^{mc}(q,t) = \frac{1}{2\rho_0 q^2} \int \frac{d\mathbf{k}}{(2\pi)^3} V_{ss'}(q,k) V_{ll'}(q,k_1) \times C_{l's'}(k,t) C_{ls}(k_1,t), \tag{5.46}$$

where $\mathbf{k}_1 = \mathbf{q} - \mathbf{k}$ and the vertex functions $V_{ss'}$ is obtained in terms of direct correlation functions $c_{ss'}$. Unlike model A, here the renormalization corresponds to the longitudinal part of the memory function. A set of nonlinear integral equations [similar to Eq. (5.14)] involving Γ was obtained by Harbola and Das (2002).

Using partial static structure factors for a binary hard-sphere system, Lebowitz (1964) and Ashcroft and Langreth (1967) obtained the dynamic transition point for the mixture in both of the above described models as in the one-component case [see the discussions with Eq. (5.14) above]. There are several difference between the two cases.

(i) The dynamic transition occurs in model A (Thakur and Bosse, 1991a, 1991b) generally at much lower packing fraction values than in model B (Harbola and Das, 2002). This result means that model B is in better qualitative agreement with the results of computer simulations (see Sec. X.A). Model A has been extensively applied (Sciortino and Kob, 2001; Foffi, Götze, *et al.*, 2003; Götze and Voigtmann, 2003) by treating the transition point of the theoretical model (Kob *et al.*, 2002) as an adjustable parameter.

(ii) In model A, the dependence of the mass ratio ($\alpha_m = m_2/m_1$) of the constituent particles on the dynamic transition point drops out. The model-B equations, on the other hand, predict that the transition point will be influenced by α_m as well as by the size ratio (α) and the relative abundance of the two species (Harbola and Das, 2003b). However, this mass ratio dependence of the transition is substantial only in extreme cases of asymmetry. Recent results of computer simulations (Zaccarelli *et al.*, 2004) demonstrate the mass ratio dependence of the self-diffusivities in the binary system.

(iii) In both cases the mode-coupling equations for the total density correlation function reduce to those for a one-component system (Bengtzelius *et al.*, 1984) if individual components in the mixture become identical, i.e., if $\alpha_m \to 1$ and $\alpha \to 1$. If, in addition, $N_1 = 1$ and $N_2 = N - 1$, then model A obtains the equations for the tagged-particle correlation ψ_s, described in Sec. V.A.3. This is simply a manifestation of the fact that model A begins with the same phenomenological approach of writing the equation of motion (5.33) for tagged-particle momentum in Eq. (5.40). In Model B the approach is different. Here the renormalization of the self-diffusion coefficient has contributions only from convective-type nonlinearities in the equations of motion, obtained with a Gaussian free energy (5.38). In model B the mechanism for freezing ψ_s can only arise from a non-Gaussian driving free-energy functional F_u. It is important to note here that in the one-component model the dynamic transition is not linked to freezing of the ϕ_s, but to freezing of the total density correlation function ϕ. ϕ_s is actually slaved to ϕ through Eqs. (5.32) and (5.34).

2. The molecular liquid

The basic idea of the nonlinear feedback mechanism from density fluctuations producing slow dynamics has also been applied to molecular liquids in which there are orientational degrees of freedom in addition to the translational degrees of freedom. A general approach to understanding the orientational dynamics in a molecular liquid is to study the Smoluchowski dynamics. The theories (Bagchi and Chandra, 1990) that consider the dynamics at the linear level predict exponential relaxations and are generally applicable to the normal-liquid state. Numerical studies show the evidence of nonexponential relaxation with orientational degrees of freedom (Gallo *et al.*, 1996). In a more advanced theory valid at moderate densities (Madden and Kivelson, 1984), the correlation functions are obtained as a three-step continued fraction representation. However, the memory kernel is treated here in the Markov approximation. The role of cooperative dynamics in the molecular liquids at high density has been studied using the mode-coupling ap-

proximations to lowest order (for a recent review see Bagchi and Bhattacharyya, 2001). The self-consistent mode-coupling model for a molecular liquid has been considered by several authors. Kawasaki (1997) has included orientational degrees of freedom in addition to that of translation in a generalized hydrodynamic approach. A mode-coupling theory for a liquid of linear molecules (Schilling and Scheidsteger, 1997) and one for single linear molecules in a simple liquid (Franosch *et al.*, 1997a) have been worked out by taking into account the role of the dominant density fluctuations.

An arbitrary molecular liquid is described in terms of the microscopic one-particle density

$$n(\mathbf{x},\Omega,t)=\sum_i \delta[\mathbf{x}-\mathbf{x}_i(t)]\delta(\Omega,\Omega_i(t)), \tag{5.47}$$

where $\delta(\Omega,\Omega_i(t))$ denotes the invariant delta function (Gray and Gubbins, 1984) with the index i referring to the phase-space index ($i=1,\ldots,N$). The variable Ω in general will correspond to the three Euler angles corresponding to the orientational degrees of freedom. The tensorial densities corresponding to Eq. (5.47) are defined as

$$\begin{aligned} n_{lmn}(\mathbf{q},t) &= i^l\sqrt{(2l+1)}\int d\mathbf{x}\int d\Omega n(\mathbf{x},\Omega,t)e^{i\mathbf{q}\cdot\mathbf{x}} \\ &\quad\times D^l_{mn}(\Omega)^* \\ &= i^l\sqrt{(2l+1)}\sum_i e^{i\mathbf{q}\cdot\mathbf{x}_i(t)}D^l_{mn}[\Omega_i(t)]^*, \end{aligned} \tag{5.48}$$

where $D^l_{mn}[\Omega]$ are Wigner rotation matrices with $l=0,1,2\ldots$, $-l\leq m\leq l$, and $-l\leq n\leq l$. A linear molecule is a special case, which represents a system with five degrees of freedom (three translational and two rotational). In this case the moment of inertia along the symmetry axis is zero. The density correlation functions are obtained in a matrix form,

$$S_{\kappa\kappa'}(\mathbf{q},t)=\frac{1}{N}\langle n_\kappa(\mathbf{q},t)^* n_{\kappa'}(\mathbf{q},0)\rangle, \tag{5.49}$$

where $\kappa\equiv lmn$. For light-scattering cross sections from the molecular liquid, the main contributions comes from $l=l'=0$, while for dielectric spectra the $l=1$ is of more relevance.

The starting point of the mode-coupling model is the choice of a suitable set of slow variables. The separation of the translational and rotational degrees of freedom require the choice of a reference point, e.g., the center of mass of the molecule. The model equations for the dynamics must remain independent of any specific choice of reference point. In addition to the density variables $n_\kappa(\mathbf{q},t)$, the set of slow variables for the molecular system includes the corresponding currents $\mathbf{j}^\alpha_\kappa$ related through the continuity equations, $\dot{n}_\kappa(\mathbf{q},t)=[iq^{\alpha\mu}_{\kappa\kappa'}(\mathbf{q})]^* j^{\alpha\mu}_{\kappa'}$, where the superscripts $\alpha=T$ and R represent translational and rotational degrees of freedom, respectively, while μ corresponds to the vector indices in three dimensions. The symbol $q^{\alpha\mu}_{\kappa\kappa'}$ used in the continuity equation is equal to $q_\mu\delta_{\kappa\kappa'}$ for $\alpha=T$, and it is related to the angular momentum operators L_μ (Schilling, 2002) for $\alpha=R$. The corresponding current densities $\mathbf{j}^\alpha_\kappa$ are given by

$$j^{\alpha\mu}_\kappa(\mathbf{q},t)=i^l\sqrt{(2l+1)}\sum_i v^{\alpha\mu}_i(t)e^{i\mathbf{q}\cdot\mathbf{x}_i(t)}D^l_{mn}[\Omega_i(t)]^*, \tag{5.50}$$

where $v^{\alpha\mu}_i(t)=\dot{x}^\mu_i(t)$ is the translational velocity corresponding to $\alpha=T$ and $v^{\alpha\mu}_i(t)=\omega^\mu_i(t)$ is the angular velocity corresponding to $\alpha=R$. The theory constructed with the set of variables $\{n_\kappa, j^{T\mu}_\kappa, j^{R\mu}_\kappa\}$ keeps the long-time dynamics independent of the mass m and the moments of inertia I_i ($i=x,y,z$) of the molecules. In an equivalent approach to site representation (Chong and Hirata, 1998) the dynamics are formulated using the partial density $n_i(\mathbf{x},t)$, $i=1,2,\ldots,M$ for the atomic sites in each individual molecule. The corresponding density correlators are given by $S_{ij}(\mathbf{q},t)=(1/N)\langle n_i(\mathbf{q},t)^* n_j(\mathbf{q},0)\rangle$. A comparison between the tensorial and site-site descriptions for a single dumbbell molecule in a hard-sphere liquid has been made by Chong *et al.* (2001). A mode-coupling theory for a system of symmetric dumbbells of fused hard spheres was worked out by Chong and Götze (2002a, 2002b).

a. The memory function

The equations of motion for the density correlation functions of a molecular liquid have been obtained for an arbitrary shaped molecule. For simplicity we discuss here only the corresponding results for the linear molecule, $\kappa=lm0$. In the following we denote the matrix of correlation functions $S_{\kappa\kappa'}$ by $\mathbf{S}$. The time evolution of $\mathbf{S}$ is obtained in terms of the memory function,

$$\frac{\partial}{\partial t}\mathbf{S}(\mathbf{q},t)+\int_0^t ds\mathbf{K}(\mathbf{q},t-s)\mathbf{S}^{-1}(\mathbf{q})\mathbf{S}(\mathbf{q},s)=0. \tag{5.51}$$

The matrix $\mathbf{K}$ is defined as $\mathbf{K}(\mathbf{q},t)=\tilde{\mathbf{Q}}^\nu\mathbf{F}^{\nu\nu'}(\mathbf{q},t)\tilde{\mathbf{Q}}^{\nu'*}$ (repeated indices are summed over) where $\tilde{\mathbf{Q}}^{\kappa\kappa'}_\nu\equiv q^{\alpha\mu}_{\kappa\kappa'}(\mathbf{q})$ and the compact notation $\nu\equiv\{\alpha\mu\}$ is used. The static correlation matrix $\mathbf{S}(\mathbf{q})$ is expressed through the Ornstein-Zernike relation, $\mathbf{S}(\mathbf{q})=[1-n/(8\pi^2)\mathbf{c}(\mathbf{q})]^{-1}$, in terms of the direct correlation function matrix $\mathbf{c}$. $\mathbf{1}$ stands for the identity matrix. The corresponding equation of motion for the matrix $\mathbf{F}^{\nu\nu'}$ is

$$\frac{\partial}{\partial t}\mathbf{F}^{\nu\nu'}+\int_0^t ds\mathbf{M}^{\nu\nu''}(\mathbf{q},t-s)\mathbf{F}^{\nu''\nu'}(\mathbf{q},s)=0. \tag{5.52}$$

Equations (5.51) and (5.52) together are essential for obtaining the crucial two-step continued fraction form (3.17) for the density correlation functions. It is convenient to express the kernel $\mathbf{M}^{\nu\nu'}(\mathbf{q},t)=\mathbf{J}(\mathbf{q})^{\nu\nu''}\mathbf{m}^{\nu''\nu'}(\mathbf{q},t)$ in terms of the memory function matrix $\mathbf{m}$ and to denote by $\mathbf{J}^{\nu\nu'}$ the static correlation matrix (Schilling, 2002). $\mathbf{m}$ consists of a bare part, due to the uncorrelated short-time dynamics, and a slow part due to correlated mo-

tion. The slow part is obtained (Schilling, 2002) using the standard approximations of the self-consistent mode-coupling theory, in terms of the coupling of density correlation functions,

$$m^{\nu\nu'}_{\kappa\kappa'}(\mathbf{q},t) = \frac{1}{2N}\sum_{\mathbf{q}_1\mathbf{q}_2}\sum_{\kappa_1\kappa_1'}\sum_{\kappa_2\kappa_2'} V^{\nu\nu'}[\mathbf{q}\kappa\kappa'|\mathbf{q}_1\kappa_1\kappa_1';\mathbf{q}_2\kappa_2 \times \kappa_2' S_{\kappa_1\kappa_1'}(\mathbf{q}_1,t) S_{\kappa_2\kappa_2'}(\mathbf{q}_2,t). \quad (5.53)$$

The vertices $V^{\nu\nu'}[\mathbf{q}\kappa\kappa'|\mathbf{q}_1\kappa_1\kappa_1';\mathbf{q}_2\kappa_2\kappa_2']$ are expressed (Schilling, 2002) in terms of direct correlation functions $\mathbf{c}(\mathbf{q})$. Although much more involved in their structure, the above set of equations (5.51)–(5.53) are similar to what has been described earlier for atomic systems and constitute the usual two-step expressions for the density correlators essential for the feedback mechanism producing slow dynamics. However, unlike the case for atomic liquids, the vertices for the molecular liquids are not all positive. The set of slow variables discussed here for linear molecules were also considered for an arbitrary molecule by Fabbian, Latz, *et al.* (1999).

The mode-coupling equations described above maintain their form under a change of reference point (Schilling, 2002). To maintain covariance, angular velocity rather than angular momentum is (arbitrarily) chosen in the definition of the currents. The choice of slow variables plays an important role in maintaining the form of the equations. Keeping both longitudinal and transverse components of the rotational current density $\mathbf{j}^{R\mu}_{\kappa}$ is essential. For the translational current density, keeping only the longitudinal part $\mathbf{j}^{T\mu}_{\kappa}$ is sufficient to maintain covariance. Taking only the longitudinal components for both $\mathbf{j}^{R}_{\kappa}$ and $\mathbf{j}^{T}_{\kappa}$ (Franosch *et al.*, 1997; Schilling and Scheidsteger, 1997b) or the longitudinal component of $\mathbf{j}^{R}_{\kappa}$ (Latz and Letz, 2001) does not preserve covariance.

b. The glass transition scenario

As in the case of simple liquids, the ideal dynamic transition is characterized by the nonvanishing long-time limit of the density correlators:

$$f_{\kappa\kappa'}(\mathbf{q}) = \lim_{t\to\infty} S_{\kappa\kappa'}(\mathbf{q},t). \quad (5.54)$$

For l and/or $l' \neq 0$, the corresponding nonergodicity parameters describe the freezing of the orientational degrees of freedom. The $f_{\kappa\kappa'}(\mathbf{q})$'s have been obtained for a system of hard-sphere dipoles (Schilling and Scheidsteger, 1997) using static correlators in the mean spherical and Percus-Yevick approximations. The control parameters for the system are the packing fraction φ and temperature T ($\beta = 1/k_B T$). Note that the quantity $\beta\mu^2/d^3 \equiv 1/T^*$ represents the ratio of dipolar energy μ^2/d^3 to thermal energy. For molecules of arbitrary shape, all modes freeze simultaneously at the dynamic transition point (Fabbian *et al.*, 1999). The roles of translational and rotational coupling in dipolar hard spheres were studied by Theenhaus *et al.* (2001), who predicted a peak in the center-of-mass spectra (the density correlator at $l=0, m=0$) over intermediate frequencies, a decade below the high-frequency peak.

The theoretical predictions from molecular mode-coupling theory were tested through molecular-dynamics simulations performed on a liquid of linear molecules with a two-site Lennard-Jones interaction. The simulations examined structural relaxation for translational as well as rotational degrees of motion (Kämmerer *et al.*, 1997, 1998a, 1998b), both of which were fitted with correlators having a von-Schweidler exponent $b = 0.54$, corresponding to the exponent parameter $\lambda_s = 0.76$. The plateau value f^c_q, and the amplitude of the power-law terms in Eq. (5.20) were treated as adjustable parameters. The $l=1$ correlators corresponding to rotational variables did not show the von-Schweidler relaxation. The inconsistency in the $l=1$ case may possibly be linked to the observation (in molecular-dynamics simulations) that $l=1$ correlators are strongly influenced by the 180° flips of the molecular axis. Such "hopping processes" are not accounted for in the present version of simple mode-coupling theory for a molecular liquid. Molecular-dynamics simulations for a model of water, on the other hand (Sciortino *et al.*, 1996, 1997, 1999), obtained a von-Schweidler exponent $b = 0.50$ with a T_c identified at 223 K. The dynamic transition point was computed from the integral equations of mode-coupling theory with input static correlation functions taken from the computer simulation data. However, this procedure theoretically predicted a dynamic transition point at a much higher temperature than directly observed in the simulation, hence overestimating the glass transition temperature as in the case of atomic liquids (Nauroth and Kob, 1997). Improvements of this situation, along lines similar to the case for a binary system (Harbola and Das, 2002), have so far not been undertaken for molecular systems.

For single-particle motion in molecular liquids, the rotational diffusion constant is obtained in a Green-Kubo form,

$$D^R_{\mu\mu'} = \int_0^\infty dt \langle \omega^\mu(t)\omega^{\mu'}(0)\rangle. \quad (5.55)$$

Here $\omega^\mu(t)$ corresponds to the μth component of the angular velocity of a tagged particle in its body-fixed frame. The translational and rotational diffusion coefficients (Hansen and McDonald, 1986), denoted by D_s and $D_R = \Sigma_\mu D^{\mu\mu}_R$, were evaluated in the simulations with the angular velocity ω^μ in the laboratory frame. $D_s(T)$ showed a behavior similar to the case of atomic liquid, falling by four orders of magnitude with a power law. D_R, on the other hand, deviated from power-law behavior much earlier, at a much higher temperature and followed an Arrhenius law. This is in disagreement with the simple molecular mode-coupling theory described above. For translational motion D_s goes to zero for a particle caught in a cage and mean-square displacement is bound. If the molecule is caught in an orientational cage similar to a cone around the z axis (say), the tagged

correlator $S^{(s)}_{lm0,l'm'0}$ freezes. This does not, however, imply a vanishing rotational diffusion coefficient, since the azimuthal angle around the z axis can still grow with time.

We have discussed above some applications of the idea of the self-consistent mode-coupling model to situations in which new sets of conservation laws modify the basic model. A number of related studies have been carried out in recent years, applying the feedback mechanism to different types of complex liquids. For example, nonlinear fluctuating hydrodynamic equations related to mode-coupling theory were formulated for liquid crystals by De *et al.* (1993), and for a sheared fluid by Miyazaki and Reichman (2002). The role of dominant density fluctuations was studied recently for polymer melts (Chong and Fuchs, 2002) using the site representation. Mode-couping equations for the site-averaged density correlator as well as for a tagged polymer correlator were obtained in a form formally identical to their respective counterparts for one-component simple liquids. These equations for the polymer melt predict a sharp dynamic transition, which becomes independent of molecular weight. A theory for nonlinear rheology in a dense colloidal suspension with imposed flow $\mathbf{v}(\mathbf{x}) = \kappa\mathbf{x}$ ($\kappa_{ij} = \gamma_s \delta_{ix}\delta_{iy}$ for shear rate γ_s) was developed by Fuchs and Cates (2002), who started from a Smoluchowski equation and computed the time correlation of fluctuations around the steady state. The approach of the system to the steady state under shear was studied considering the dynamics in terms of coupling of the dominant density fluctuations in a manner similar to standard mode-coupling theory. Similarly a theory for colloidal gelation was developed by Bergenholtz *et al.* (2000). The feedback mechanism was applied to a dense star polymer (Foffi, Sciortino, *et al.*, 2003) to study the dynamic transition line in the phase space of the packing fraction φ and functionality f (the number of polymeric arms to the star). The main input in these models came from the proper structure factor for the corresponding soft matter.

VI. ABSENCE OF A SHARP TRANSITION

So far we have considered the simple form of mode-coupling theory in which the fluid undergoes, at a critical density, a dynamic transition to a nonergodic state. From a theoretical point of view, the occurrence of this sharp dynamic transition in a system having a finite number of participating degrees of freedom is somewhat unexpected. This criticism holds even for the wave-vector-dependent model: in the absence of intrinsic disorder, ergodicity should be restored at any finite temperature. It should be emphasized here that the dynamic transition in a self-consistent model is not an artifact of some approximate solution. In certain cases, e.g., for a nonlinear oscillator (Siggia, 1985), the nonlinear equations for the dynamics are linked to an effective potential energy that is non-Gaussian. The corresponding ergodic-to-nonergodic transition predicted from perturbative solutions of the dynamical model will be destroyed due to the nature of the equilibrium states. However, as is clear from the special form of the nonlinearities in the reversible part of the generalized Navier-Stokes equation (Das *et al.*, 1985b), the mode-coupling model discussed here can be obtained even with a completely Gaussian interaction free energy, for which there is no possibility of such disordering agents. The crucial question to be addressed is whether the mode-coupling model really keeps this simple form (with the prediction of an ideal transition) under proper consideration of the equations governing the dynamics of the dense fluid. Indeed, the model obtained from a full analysis (Das and Mazenko, 1986) of the nonlinearities in the dynamics of compressible liquids shows that ergodicity holds at all densities. The full model (sometimes called *extended mode-coupling theory*) also reduces to the simple model described in the previous section if certain corrections are ignored. The ergodic behavior holds even when the liquid dynamics are controlled by an effective Gaussian potential energy with a single minimum and *no* thermally activated hopping.

A. Role of current fluctuations

For a discussion of the ergodicity-restoring processes and final decay of the density correlation function, we start from Eq. (A20). This expression for the correlation function is obtained from an analysis (see Appendix A.2) of the the proper set of nonlinear equations for a compressible liquid, which are discusssed in Sec. IV.B.2. The simplified model described above in Sec. V.A.2 follows from Eq. (A20) when one ignores the quantity $\gamma(q,z)$ in the denominator. The final decay of the correlation function is qualitatively changed when this term is included in the analysis. The dynamic transition discussed in the previous section is suppressed (Das and Mazenko, 1986) as a consequence of the coupling of currents and density fluctuations. Subsequent work has also demonstrated that similar ergodicity-restoring processes control the final relaxation of the supercooled liquid from different approaches (Götze and Sjögren, 1987; Sjögren, 1990; Schmitz *et al.*, 1993).

We begin the discussion of the cutoff mechanism with the model presented in Eq. (A20), which we put into the following form:

$$\phi(q,z) = \left[z + i\delta(q,z) - \frac{\Omega_q^2}{z + iq^2\Gamma^R} \right]^{-1}, \tag{6.1}$$

where we have used the definition

$$\delta(q,z) = \gamma(q,z)\left[\frac{iq^2\Gamma^R}{z + iq^2\Gamma^R} \right]. \tag{6.2}$$

In the asymptotic limit, for long enough times, or correspondingly for small enough z, when the longitudinal viscosity is large due to the feedback effect from the coupling of density fluctuations, we have $z \ll q^2\Gamma^R(q,z)$. The density autocorrelation function $\phi(q,z)$ given by Eq. (6.1) reduces to the form

$$\phi(q,z) = \frac{1}{z + i(c_o^2[\Gamma^R]^{-1} + \tilde{\gamma}q^2)}. \quad (6.3)$$

We have used above the leading-order result in q, $\gamma \sim q^2\tilde{\gamma}$. If the term involving $\tilde{\gamma}$ in the denominator is ignored, the longest time scale of relaxation for the density correlation function will be given by $[\Gamma^R]^{-1}$. A dynamic transition occurs in this model with $\phi(q,z) \sim 1/z$ corresponding to the situation in which Γ^R tends to diverge beyond a critical density. The enhancement of Γ^R occurs due to feedback effects from slowly decaying density fluctuations. For example, we have seen in Sec. V such a situation in a hard-sphere system at a packing fraction $\varphi_c = 0.525$. If, on the other hand, the nonlinear feedback mechanism from the coupling of density fluctuations is not strong enough at any density to drive Γ^R to diverge, there will be no dynamic transition, even in the absence of the cutoff function γ. Yet due to the presence of this term, the $1/z$ pole in ϕ is avoided, even if Γ^R grows arbitrarily large due to feedback effects. In this case, $\tilde{\gamma}q^2$ determines the pole of the density correlation function. However, this is not a new hydrodynamic mode in the system and there is no extra conservation law involved. The lowest-order contribution to $\tilde{\gamma}$ is at the one-loop level in the perturbation theory outlined in the Appendix. Since Γ^R remains finite, the leading-order relaxation behavior is controlled self-consistently by $[\Gamma^R]^{-1}$, as was pointed out by Latz and Schmitz (1996).

The asymptotic behavior of the density correlation function strongly depends on how small the cutoff function γ is. The smaller γ is, the longer the time scale over which the feedback mechanism is effective in enhancing the transport coefficient. For small enough γ, the time scale of final decay is much longer than the two-step relaxation of simple mode-coupling theory described in Sec. VIII. On the other hand, if γ does not become small enough self-consistently, many of the relaxation scenarios predicted in the simple mode-coupling theory will be screened out, since the system does not get close enough to the dynamic transition point. Indeed, in most of the mode-coupling models studied so far, it is simply assumed that the cutoff mechanism is weak so that the ideal transition model is applicable. The cutoff function, if considered, is treated as an adjustable parameter in seeking agreement with results from simulations or experiments.

So far we have discussed the cutoff function in a qualitative manner, while treating it from a nonperturbative approach. To determine the final relaxation behavior and how much slowing down can occur a quantitative approach is needed that will evaluate the relevant self-energies at the lowest or one-loop order.

The asymptotic behavior of the density correlation functions $\phi(q,t)$ is obtained from the solution of Eq. (A20) retaining the cutoff function $\gamma(q,z)$ given by Eq. (A22). Both these equations are combined in time space in the form of a coupled set of integro-differential equations (Das, 1987, 1990). In order to focus on the role of the cutoff mechanism, we consider here these equations for different q values in a schematic form (Das and Mazenko, 1986), ignoring all wave-vector dependence,

$$\ddot{\phi}(t) + \nu_o\dot{\phi}(t) + \phi(t) + \int_0^t ds\Bigg[H[t-s]\dot{\phi}(s) + \gamma(t-s) \times\Bigg\{\Gamma_o\phi(s) + \int_0^s ds' H[s-s']\phi(s')\Bigg\}\Bigg] = 0, \quad (6.4)$$

where Γ_o is related to the bare transport coefficient and time is rescaled with a microscopic frequency scale ν_o defined at a fixed q. The memory function $H[t] \equiv H[\phi(t)]$ is generally written in a schematic form as a polynomial of the density correlation function ϕ, e.g., the form $H[\phi(t)] = c_2\phi^2(t)$ corresponds to the Leutheusser (1984) model. The cutoff function γ for the wave-vector-independent case is obtained from Eq. (A22), which reduces to the simple form (ignoring couplings to the transverse part) $\gamma(t) = \gamma_o\dot{\phi}^2(t)$, where γ_o is a constant. Note that if the cutoff function γ is ignored in Eq. (6.4), then the idealized mode-coupling model described by Eq. (5.4) is obtained. The numerical solution of Eq. (6.4) with γ retained and the memory function H corresponding to the Leutheusser model has been studied by Das and Mazenko (1986). For smaller values of the density-dependent parameter $1 < c_2 < 4$, the longitudinal viscosity shows an initial enhancement, appearing to diverge at $c_2^* = 4.0$, with a power law having an exponent close to 2. For higher densities, $c_2 > 4$, the sharp transition is smoothed. The viscosity shows an enhancement by about three orders of magnitude. The ϕ_{12} model, i.e., $H[\phi(t)] = c_1\phi(t) + c_2\phi^2(t)$, was considered by Kim (1992). In this case the ideal model showed stretched exponential relaxation with a line of transitions in the c_1-c_2 plane (see Sec. V). The enhancement of the viscosity was similar to that seen in the earlier work with the extension of the Leutheusser model by Das and Mazenko (1986). Indeed, very slow relaxation can only result if the cutoff function γ also becomes very small in a self-consistent manner. In general with extended model calculations a qualitative change in the dynamics is observed around the ideal transition point, but no sharp transition occurs to a phase characterized by diverging viscosity. A similar behavior in experimental data was reported by Taborek *et al.* (1986) from a study of a large number of fragile liquids.

Following the analysis of Das and Mazenko, the ergodicity-restoring mechanism was considered by Das (1987, 1990) in a more realistic model for a liquid with a static structure factor having a proper wave-vector dependence. The extended mode-coupling model was studied at different densities or temperatures using the corresponding static structure factors for the liquid as an input. The wave-vector-dependent generalization of Eq. (6.4) constituted a set of coupled nonlinear integro-differential equations (Das, 1990). For a numerical solution, the wave numbers were taken to be distributed over a uniformly spaced grid extending up to an upper cutoff Λ. The cutoff function $\gamma(q,t)$ at large wave vector

q was approximated by the form (A22) obtained by Das and Mazenko (1986). When the static structure factor for a one-component Lennard-Jones liquid was used as an input in the model, the numerical solution of the mode-coupling equations showed reasonable agreement with the molecular-dynamics simulation data of Ullo and Yip (1985, 1989) at the corresponding temperatures and densities. Figure 3 shows the mean-square displacement of a tagged particle obtained by solving the model equations (Kaur and Das, 2002, 2003a) with a hard-sphere structure factor (Barker and Henderson, 1976) as input. In the extended mode-coupling result the corresponding cutoff function is adjusted up to an overall factor so that the self-diffusion constant D_s agrees with the results of computer simulations (Woodcock and Angell, 1981). In the intermediate regime ($\approx 500t_E - 1500t_E$) the variation $\langle r^2(t)\rangle \sim t^a$ is obtained. The exponent $\bar{a}$ is shown in the inset (denoted as a) in Fig. 3. Generally wave-vector-dependent models with structure factors corresponding to simple interaction potentials obtain an enhancement of the viscosity by three to four orders of magnitude, indicating a qualitative change in the dynamics around an intermediate transition point $T_c > T_g$. The viscosity follows a power-law divergence as T_c is approached, but with further lowering of the temperature the transition is suppressed.

In 1993 Schmitz *et al.* considered an extended mode-coupling model in which the dynamic transition was also smeared. These authors used the fluctuating nonlinear hydrodynamic approach in terms of two fluctuating variables $\mathbf{g}$ and ρ and without any nonlinear constraint like Eq. (4.14). The appearance of the $1/\rho$ nonlinearity in the equations of motion was avoided in this formulation by simplifying Eq. (4.11) for the kinetic-energy term F_k by using only the lowest-order term in the density fluctuations, i.e., $F_K = \int d\mathbf{x} g^2(\mathbf{x})/2\rho_o$. As a result there were two changes in the equations of motion:

(a) The convective nonlinearity of the standard form $\nabla_j[g_i g_j/\rho]$, which is essential for Galilean invariance, disappeared from the equation for the momentum density $\mathbf{g}$.

(b) The equations of motion retained the Poisson bracket between slow variables unchanged and the detailed balance condition $Q_{ij} = -Q_{ji}$ uncompromised. As a result the continuity equation now contained extra density-momentum nonlinearities. These additional bilinearities were imposed by requiring that the detailed balance prevent the structural arrest predicted by mode-coupling theories with only density-density nonlinearities in the pressure term. Interestingly, the form of the cutoff function in this model, responsible for the removal of the sharp transition, is identical at one-loop order to the same quantity in the analysis of Das and Mazenko (Das, 1996).

The nonlinear constraint (4.14) between the fluctuating fields was introduced to remove the $1/\rho$ nonlinearities in the equations of motion and is crucial in producing the cutoff mechanism. However, the smearing of the transition is not linked to a particular form of the nonlinear constraint $\mathbf{g} = \rho\mathbf{V}$ (compare this to, say, $\mathbf{V} = \mathbf{g}/\rho$). The difference between these forms is linked to a Jacobian for the change of variables in the delta function that is used as a constraint,

$$1 = \int D\mathbf{v}(\mathbf{x})\,\delta\left[\frac{\mathbf{g}}{\rho} - \mathbf{v}\right] = J[\rho]\int D\mathbf{v}(\mathbf{x})\,\delta[\mathbf{g} - \rho\mathbf{v}]. \quad (6.5)$$

This issue was analyzed by Mazenko and Yeo (1994) by formulating the model in terms of only two variables, ρ and $\mathbf{g}$, so that no constraint was needed. The $1/\rho$ nonlineraity appearing in both the viscous term and the convective term in the generalized Navier-Stokes equation were treated as a series in $\delta\rho/\rho_o$. The renormalized theory at one-loop order was shown to be identical to the previous formulation by Das and Mazenko (1986). The origin of the ergodicity-restoring mechanism obtained in the Das and Mazenko analysis discussed above lies in the $1/\rho$ nonlinearities in the equations of motion. The fluid dynamics described by the Langevin equation are not affected by a chemical-potential-like term linear in ρ in the interaction part F_u of the free energy. This follows directly from the form $\rho\nabla_i(\delta F_u/\delta\rho)$ of the nonlinear terms depending on F_u. Thus while the form the Jacobian does not affect the dynamics its possible influence on the renormalization can be absorbed in the definition of the chemical potential (Yeo and Mazenko, 1994).

B. Ergodicity-restoring and "hopping" processes

Subsequent to the work of Das and Mazenko (1986), Götze and Sjögren (1987) studied, from a kinetic theory approach, the role of ergodicity-restoring processes in the self-consistent mode-coupling theory. These authors also concluded that the dynamic transition of the simple model is absent and the density correlation function decays to zero beyond the critical point. The kernel and cutoff parameter reported here were of similar structure (involving the time derivative of the density correlation function and the transverse part of the current-current correlation function) to those found in the previous work of Das and Mazenko (1986). However, the wave-vector-dependent kernels appearing in the cutoff functions in the two works were different (Sjögren, 1990).

A lower cutoff time t_o in the time integrals involving the memory functions has often been used in mode-coupling theory. The memory effects are taken into account from t_o onwards (Sjögren, 1990). The rationale behind introducing the cutoff time is to account for the fact that the short-time dynamics or contributions from uncorrelated collisions are already taken into account in the theory through the bare transport coefficients. Similar short-time cutoffs have been used earlier in mode-coupling theory calculations for the shear viscosity (de Schepper *et al.*, 1986) near the freezing point. Sjögren (1990) analyzed the equations of the self-consistent model further to identify the overall scale δ_o (say) from

the ergodicity-restoring mechanism. It is claimed δ_o, which controls the α-relaxation process, decreases with the decrease of temperature with an Arrhenius dependence. In order to have such a behavior following from the mode-coupling theory it is necessary that (a) in the time window for the von-Schweidler relaxation ($\sim t^b$) the density correlation function have the form

$$\phi(q,t) \equiv \Phi(q,t\delta_o) = f(q) - \frac{h_q}{\sqrt{\lambda - \pi/4}}(t\delta_o)^{1/2} + \cdots, \tag{6.6}$$

with exponent $b=\frac{1}{2}$, and (b) the lower cutoff time t_o extend to the time scale of the von-Schweidler relaxation. The $t^{1/2}$ behavior required in (a) corresponds to the exponent parameter λ (introduced in the previous section) being greater than $\pi/4$. In this regard it is interesting to note that in dielectric spectroscopy experiments on CRN ($[Ca(NO_3)_2]_{0.4}[RBNO_3]_{0.6}$) $\lambda=0.91$ is obtained from fitting of the susceptibility minimum (see Sec. VII; Lunkenheimer, Pimenov, and Loidl, 1997). Here a $\nu^{-1/2}$ decay for the low-frequency wing was reported to be consistent with experimental data.

Numerical solutions of the mode-coupling equations, however, do not show such $t^{1/2}$ behavior (Kim, 1992) for the density correlation function δ_o in simple models nor does δ_o show an activated behavior. In principle, the parameter λ defined in Eq. (5.17) can be obtained from the static structure factor of the liquid, to test the inequality $\lambda \geqslant \pi/4$. In most cases λ is taken as a parameter for fitting experimental data. In the wave-vector-dependent one-loop model for a hard-sphere system, Fuchs, Hofacker, and Latz (1992) reported $\lambda=0.74$. It therefore seems untenable that the activated behavior of the cutoff parameter could follow from this special type of von-Schweidler relaxation. Subsequent to the above work, Liu and Oppenheim (1997) reexamined the formulation of the ergodicity-restoring mechanisms using the projection operator formalism. These authors concluded that introduction of an initial cutoff time t_o in the cutoff function amounted to neglecting a class of processes that might be of comparable or even greater importance than the terms kept. The cutoff function γ has a major contribution (Kim, 1992) from the short-time part and therefore γ is relatively small with the cutoff time t_o included. Even if the initial cutoff time is not introduced, there is still considerable slowing down (Das, 1987, 1990), though is not nearly as pronounced as is seen in real systems near the glass transition. If the magnitude of the cutoff function does not decrease dramatically on supercooling, much of the relaxation behavior predicted by simple mode-coupling theory (the ideal transition model) may be masked and the meaning of the mode-coupling temperature T_c becomes questionable.

In some work the ergodicity-restoring mechanisms have been interpreted as the "hopping process" in the supercooled liquid, drawing a similarity between the dynamics of supercooled liquids with the transport process in strongly disordered semiconductors (Götze and Sjögren, 1995). The impurities in the disordered semiconductor produce a static random potential (Belitz and Schirmacher, 1983), and the tagged-particle motion in such a system is characterized by phonon-assisted hopping. The metastable liquid, however, does not contain any quenched disorder. Nonlinear interaction of the density fluctuations signifies the cage effect for the single-particle motion. At higher densities the persistence of the cages grows in time until at a critical density this causes a dynamic transition of the liquid to a nonergodic glassy phase. A phenomenological model for the glass transition was formulated earlier using similar ideas of the movement of free volumes in the liquid (Grest and Cohen, 1981). The trapping diffusion model (Odagaki and Hiwatari, 1990; Odagaki, 1995) for glassy dynamics is also based on similar physical pictures of the amorphous state. This process of trapping of a particle in the cage formed by its neighbors can be interpreted as being produced by a static random potential, and the interaction between currents and density fluctuations, which smooth off the ideal transition, can be thought of as relaxation via jumps over the almost static potential barriers. Thus calling this "hopping" is clearly a matter of interpretation and could be misleading. The existing extended mode-coupling models, which are obtained from the equations of fluctuating hydrodynamics, assume expansions around a single fluid-type minimum of the free energy. No activated process of hopping is involved between states of different free-energy minima in reaching the cutoff mechanism. We shall discuss the process of hopping in supercooled liquid dynamics in a different context in Sec. IX.

In Sec. VI a somewhat simplified treatment of the dynamics, referred to as the dynamic density functional theory, is given in terms of density fluctuations only. This formulation obtains the ideal dynamic transition of the self-consistent MCT in the form of a lifetime renormalization. Kawasaki (1994) has suggested a possible link to the ergodicity-restoring processes in this theory through the operator D [see Eq. (4.20)], which gives the time evolution of the probability distribution function $P[\rho,t]$. If the momentum variable $\mathbf{g}$ is averaged out of the stochastic description involving the set $\{\rho,\mathbf{g}\}$, the Laplace transform of $\mathcal{D}$ is obtained in terms of the kinetic operator $\hat{\gamma}_D$ as

$$\mathcal{D}[\rho,z] = \int d\mathbf{r} \int d\mathbf{r}' \frac{\delta}{\delta\rho(\mathbf{r})}\hat{\gamma}_D[\mathbf{r},\mathbf{r}',z,\rho] \times\left[\frac{\delta}{\delta\rho(\mathbf{r})} + \beta\frac{\delta F_U[\rho]}{\delta\rho(\mathbf{r})}\right]. \tag{6.7}$$

The functional integral over $\mathbf{g}$ is now absorbed in the formal expression of the operator $\hat{\gamma}_D$. Though it would be somewhat premature to conclude at this stage, the kernel $\hat{\gamma}_D$ seems to act as a counterpart to the cutoff function of the extended mode-coupling theory. This comment follows from the following observation of Kawasaki (1994): An equilibrium average of the kinetic operator $\hat{\gamma}_D$ obtained by requiring it to operate on the cor-

responding distribution function $P_E[\rho] \sim \exp[-\beta F_U]$) has the spatial Fourier transform

$$\tilde{\gamma}_D(q,z) = \int d(\mathbf{r}-\mathbf{r}') e^{i\mathbf{q}\cdot(\mathbf{r}-\mathbf{r}')} \langle \hat{\gamma}[\mathbf{r},\mathbf{r}',z,\rho] \rangle. \tag{6.8}$$

The quantity $\tilde{\gamma}_D$ has a form very similar to the cutoff function γ obtained in the full hydrodynamic description given in Eq. (A22). However, at this stage it is not clear how the equations of the full mode-coupling theory, including the ergodicity-restoring mechanism for the density autocorrelation function, might follow from the present formalism of dynamic density functional theory. Even the feasibility of such a scheme is unclear, since the ergodicity-restoring processes are understood to be an outcome of the coupling of density fluctuations and currents in the dense fluid. The drastic approximations made on eliminating the momentum variable (see Sec. IV.C and the Appendix) might be the reason for the absence of this ergodicity-restoring process at the one-loop level.

VII. EVIDENCE FROM EXPERIMENTS

The predictions of the mode-coupling theory have been very widely tested with different types of experimental investigations. The experimental techniques used in such studies include neutron- and light-scattering methods, dielectric spectroscopy, and measurements of the mechanical response of the supercooled liquid to external perturbations. In making comparisons with theory, it is generally assumed that other variables, for example, the dielectric moment, couple to the density, both with correlations obeying the same type of relaxation law. Analysis of the experimental data can be broadly divided into a few categories,

(a) the location of the dynamic transition, i.e., identifying T_c through data analysis,

(b) the power-law relaxation over intermediate time scales, the β scaling as well as the factorization property of time and space correlations, and

(c) the subsequent relaxation or α relaxation relating to the issue of the time/temperature superposition principle.

These analyses of experimental data, barring a few exceptions, are mainly done with respect to the predictions of the idealized model, in which a sharp transition of the supercooled liquid to a nonergodic glassy state occurs. For experimental scattering data often the schematic theoretical model (see Sec. V.A.1) without wave-vector dependence is chosen. In most cases the data analysis is done by treating the relevant quantities (like the nonergodicity parameter f, or the exponent parameter λ) as fit parameters instead of computing them from first principles using the wave-vector dependence of the static structure factor for the liquid. The data from scattering experiments with colloids have been fitted more extensively with the wave-number-dependent model using hard-sphere structure factors. It is generally assumed that the role of the ergodicity-restoring mechanisms is minimal, at least over the time scale of the specific effect being studied. However, in reality a system is never in a nonergodic state over all time scales. Hence much of the analysis has involved looking for signatures of this so-called transition through interpretation of the data, within convenient time or temperature ranges. Claims of agreement with theory, therefore, in some cases have not been without criticism, as we shall see below. Our treatment of the subject here is meant only to broadly survey the various types of tests being performed with their assumptions or limitations, and it is by no means exhaustive. For a more detailed discussion the reader is referred to the specialized treatments of the topic by Götze and Sjögren (1992) and more recently Götze (1999).

A. The complex relaxation scenario

1. Signature of the dynamic transition

The nonergodicity parameters f_q and f_q^s, respectively, corresponding to the long-time limit of the density and tagged-particle correlation have been studied by a number of workers (Frick *et al.*, 1990; Li *et al.*, 1993). Theoretically the nonergodicity parameterr is the weight of the delta-function $\pi f_q \delta(\omega)$ contribution to the dynamic structure factor at densities beyond the dynamic transition point. In reality, however, the nonergodicity parameter is determined from the area under the α peak having finite width. If the correlation function is obtained in time, the nonergodicity parameter is approximated by the plateau value of the density correlation function or the tagged-particle correlation function, respectively, for f_q and f_q^s. By projecting the temperature dependence of the nonergodicity parameter onto a cusplike behavior [see Eq. (5.16)], one is able to identify the mode-coupling transition temperature T_c. The elastic modulus measured in the stimulated scattering of light from different wave vectors q (Yang and Nelson, 1996) is converted to obtain the nonergodicity parameter at $q=0$ relating to density fluctuations for macroscopic wavelengths. In Fig. 4, the effective Debye-Waller factor vs temperature T is shown for CKN $[0.4Ca(NO_3)_20.6KNOB_3]$ at $q=0$. The estimated critical temperature is $T_c=378\pm2$ K. The cusp behavior was similarly analyzed to identify T_c in other materials like orthoterphenyl (OTP) (Tölle *et al.*, 1997), CKN (Kartini *et al.*, 1996; Pimenov *et al.*, 1996), salol (Toulouse *et al.*, 1993; Yang and Nelson, 1995), and propylene carbonate (Yang *et al.*, 1996). In Table I, for a few commonly studied materials the mode-coupling temperature T_c as well as the corresponding T_g are listed. It should be noted here that the cusp behavior of the nonergodicity parameter is an asymptotic result and is only valid in the close vicinity of the transition point [see Eq. (5.18) and the related discussion]. The relative change of the nonergodicity parameter in the range where the cusp behavior dominates is not very large, and hence the identification

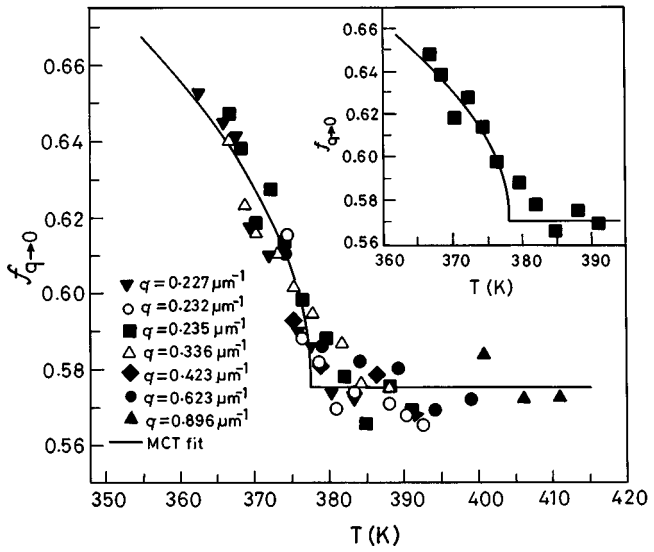

FIG. 4. The effective Debye-Waller factor for CKN vs temperature T at $q=0$. Different data points defined in legend. The $q=0$ value is obtained from the corresponding results at different q values measured with impulsive light-scattering spectroscopy. The curves are fits to the square-root cusp. From Yang and Nelson, 1996.

of T_c tracing a cusplike behavior (see inset of Fig. 4) in the nonergodicity parameter is somewhat arbitrary. More recently it has been reported (Mezei and Russina, 1999) from model-independent studies that the experimental data for CKN do not confirm the presence of any special transition temperature T_c.

2. Power-law relaxations

The mode-coupling predictions of the initial power-law decay as well as the von-Schweidler decay have been tested with data obtained from many different systems by various experimental techniques. In most cases the data were tested against the schematic model, treating the exponent parameter λ_s as freely adjustable.

a. The critical decay

The decay $(t/\tau_\beta)^{-a}$ given by Eq. (5.9), sometimes called the critical power law, has been observed in several systems beyond the microscopic time scales. For example, data for the molten salt $0.4Ca(NO_3)_20.6RbNO_3$ (CRN) from the dielectric loss function shows such decay with an exponent $a=0.20$ over three decades in time

TABLE I. List of T_c and the corresponding T_g in degrees Kelvin for some commonly studied glass-forming materials.

Material	T_m	T_c	T_g	T_c/T_g
CKN	483	378	333	1.1
PC	218	190	160	1.2
OTP	329	290	243	1.2
Salol	315	263	218	1.2

(Lunkenheimer, Pimenov, and Loidl, 1997). The nonergodicity parameter f, the amplitude of the power law h, and the time τ_β are treated here as fit parameters. This critical power-law-type relaxation is expected only over a limited time or frequency window where the correction terms indicated in Eq. (5.22) can be neglected. Numerical solution of the mode-coupling equations for a one-component Lennard-Jones system (Smolej and Hahn, 1993) indicates that the critical decay is observed for a relative distance from the dynamic transition (in terms of density) $\epsilon\approx 4.2\times 10^{-4}$ only. Thus demonstration of this critical decay t^{-a} is more of an exception than the rule (Götze, 1999).

b. von-Schweidler relaxation

Like the critical decay, identification of this second power-law regime is also problematic due to several factors. When the time t is not long enough, the correlation function is above the critical plateau value, merging the von-Schweidler relaxation (5.11) with the critical decay (5.9). On the other hand, higher-order corrections dominate at long times. Even the choice of the plateau is, in many cases, a bit arbitrary. To identify the power-law behaviors, the data analysis is sometimes done in terms of the frequency-dependent susceptibility function instead of a direct fit of the time correlation function. The susceptibility function is defined in terms of the Laplace-transformed quantity $\chi(z)=\phi(t=0)+z\phi(z)$. The corresponding Fourier-transformed function is given by the imaginary part χ''. The two power-law decays of t^{-a} and t^b in the time correlation function give rise to corresponding frequency dependence in χ'' of the form ω^a and ω^{-b}, respectively. As a result of these two opposite trends χ'' reaches a minimum at an intermediate frequency $\omega=\omega_{\min}$. In the region of this minimum the susceptibility function is interpolated with the schematic form

$$\chi''(\omega)=\frac{\chi''_{\min}}{a+b}\left[b\left(\frac{\omega}{\omega_{\min}}\right)^a+a\left(\frac{\omega_{\min}}{\omega}\right)^b\right]. \tag{7.1}$$

The frequency corresponding to the susceptibility minimum $\omega_{\min}$ is inversely proportional to the β-relaxation time scale τ_β, i.e., to $\Delta_o^{1/2a}$. Therefore the plot of $(\omega_{\min})^{2a}$ vs the corresponding temperature T of the liquid is expected to follow a straight line, extrapolating to meet the temperature axis at the dynamic transition point T_c. In Salol, for example, the von-Schweidler exponent is measured from the light-scattering data as $b=0.64\pm 0.08$ (Li *et al.*, 1992b), while Kerr-effect studies for the dynamic susceptibility χ'' give $b=0.66\pm 0.06$ (Torre *et al.*, 1998). The critical decay is observed only in the close vicinity of the transition, while the range of validity of the von-Schweidler relaxation is not known *a priori*, thus making the observation of Li *et al.* rather subtle.

Let us now consider the signature of β-scaling behavior in mode-coupling theory (outlined in Sec. V.A.2) in the experimental data for $\chi(\omega)$. Corresponding to the

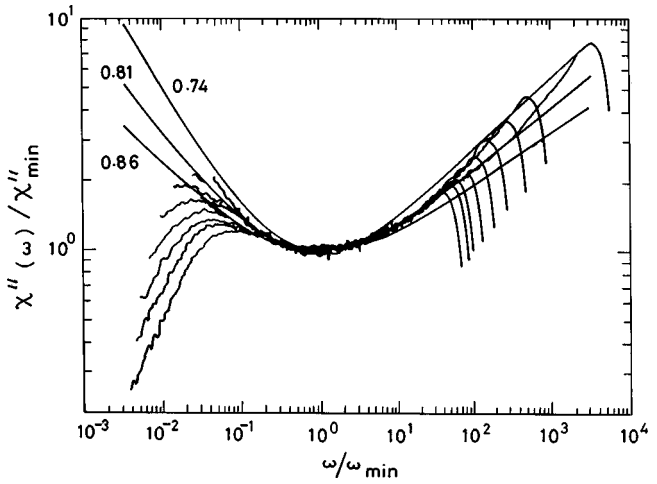

FIG. 5. Susceptibility χ'' vs $\omega/\omega_{\min}$ for CKN on a log-log plot. Different curves correspond to temperatures (top to bottom): 468, 453, 443, 433, 423, 413, 403, 393, and 383 K. Solid curves present the master function for different values of the exponent parameter λ (see text). From Li *et al.*, 1992a.

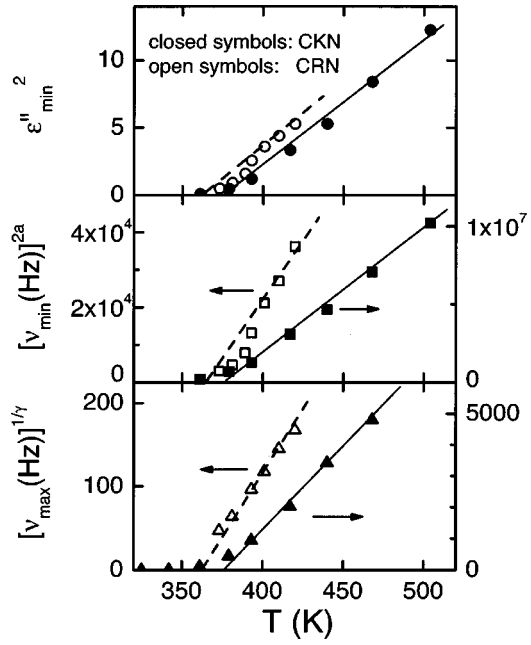

FIG. 6. Critical temperatures in two supercooled liquids, CKN (solid symbols) and CRN (open symbols), plotted in three ways: top panel, vs the height; center panel, vs the position of the dielectric loss minimum; bottom panel, vs the α-peak position. Representations along the vertical axes have been chosen so as to produce straight lines according to the predictions of mode-coupling theory. The solid lines are consistent with a critical temperature of $T_c=375$ K for CKN, and the dashed lines with $T_c=365$ K for CRN. From Lunkenheimer, Pimenov, and Loidl, 1997.

scaling function $g_\pm$ defined in Eq. (5.21), a susceptibility function is defined as $\hat{\chi}_\pm(\hat{\omega})=\hat{\omega}\hat{g}''_\pm(\hat{\omega})$ with $\hat{g}''_\pm(\hat{\omega})$ being the Fourier-cosine transform of $\hat{g}_\pm(\hat{t})$ in terms of the rescaled frequency $\hat{\omega}=\omega\tau_\beta$. It then follows from Eq. (5.21) that the generalized susceptibility is $\chi''(\omega)=C_\Delta\hat{\chi}_\pm(\hat{\omega})$ with $C_\Delta\sim\sqrt{\Delta_o}$. For experimental comparison it is generally assumed that the scaling relation also holds for variables other than density, due to their couplings with the latter. The β-relaxation scaling is tested by plotting χ'' with $\log(\omega)$. In such plots different curves for the susceptibilities corresponding to different values of Δ_o should be related by translations on the frequency axis. This was done for the typical glass-forming system CKN $[0.4Ca(NO_3)_20.6KNOB_3]$ for temperatures ($T>T_c$) by Li *et al.* (1992a). The scaling function $\hat{\chi}_-$ was chosen in the convenient form (7.1) given above, so that the minima lay at $\hat{\omega}=1$. The results for the susceptibilities for a number of temperatures ranging from 468 to 383 K were fitted with the scaling function corresponding to $\lambda=0.81$ (which obtained power-law exponents $a=0.27$ and $b=0.46$, respectively). This is shown in Fig. 5. The light-scattering data at $T=393$ K fit well to the master function over more than three orders of magnitude of frequency. Two other curves representing the master functions for $\lambda=0.86$ and 0.74 are also shown to indicate the range of tolerance for optimal fit. In comparison, the susceptibility curves from the dielectric loss spectra (Lunkenheimer, Pimenov, and Loidl, 1997) of CKN exhibited the minimum for $T\leqslant 417$ K with the master function corresponding to a somewhat lower value of $\lambda=0.76$. For Salol, depolarized light spectroscopy gives the scaling function with $\lambda=0.70\pm0.05$, implying $a=0.33$ and $b=0.64$ (Li *et al.*, 1992b). The minima located from neutron scattering (Toulouse *et al.*, 1996) on the same material agrees with these light-scattering results near T_c. For propylene carbonate, light scattering obtains $\lambda=0.78\pm0.05$, implying $a=0.33$ and $b=0.64$ (Du *et al.*, 1994). In general, the range of validity of the scaling behavior over time or frequency increases as the temperature T of the system approaches T_c from above. For OTP the scaling function g_- corresponding to $\lambda=0.77$ fits the data from incoherent and coherent neutron-scattering data (Wuttke *et al.*, 1993) over a dynamical window extending over two decades.

We have noted in Sec. V.A.1 that the frequency corresponding to the minimum of the susceptibility function is $\omega_{\min}\sim\tau_\beta^{-1}\propto|\Delta_o|^{1/2a}$. Similarly, the position of the α-relaxation peak of the susceptibility function at ω_α also corresponds to the time scale τ_α and hence $\omega_\alpha\sim\tau_\alpha^{-1}\propto|\Delta_o|^\gamma$ where $\gamma=1/2a+1/2b$. Furthermore, the intensity $\chi''_{\min}$ is proportional to $\sqrt{\Delta_o}$. Therefore plots of ω_β^{2a}, $\omega_\alpha^{1/\gamma}$, or $(\chi''_{\min})^2$ with temperature T should follow a straight line and meet the T axis on extrapolation at $T=T_c$ ($\Delta_o=0$) (Götze and Sjögren, 1992). When this approach was applied to CKN dielectric loss spectra (Lunkenheimer, Pimenov, and Loidl, 1997), it provided an estimate of T_c from the high-temperature side. The exponents a and γ were used as fit parameters. Figure 6 shows this estimate of T_c for CKN as well as CRN done by plotting the temperature dependence of, respectively, from the top panel, the height, position of dielectric loss minimum, and the α-peak position of the CKN (filled symbols) and CRN (open symbols). The best fit results,

$a=0.30$ and $\gamma=2.6$, were obtained for CKN (corresponding to the exponent parameter $\lambda=0.76$). The transition temperature T_c for CKN obtained by extrapolating the dielectric loss data is close to 375 K. This is comparable to the corresponding result $T_c=378\pm2$ K obtained by studying the location of the square-root cusp in the nonergodicity parameter from the low-temperature side. Similar fits with $\omega_{\min}$ extracted from light-scattering data (Li *et al.*, 1992a) for CKN obtained $a=0.28$ and $\gamma=2.9$, corresponding to $\lambda=0.81$, roughly in agreement with the above dielectric spectroscopy results. For CRN these exponent values are, respectively, $a=0.20$ and $\gamma=4.3$ (corresponding to $\lambda=0.91$) and the estimate for T_c lies between 360 and 375 K. Schneider *et al.* (1999) have made measurements using dielectric spectroscopy over more than 18 decades of frequency on propylene carbonate in the normal as well as the supercooled state. Their analysis, done with the minimum of the dielectric susceptibility data as well as the α-relaxation time scales, obtained $T_c=187$ K. The minimum in the dielectric susceptibility function was described with the scaling form (7.1) corresponding to $a=0.29$ and $b=0.50$, consistent with the exponent parameter value $\lambda=0.78$. This result of $T_c=187$ K is in agreement with previous light-scattering studies by Du *et al.* (1994) and solvation dynamics experiments (176 K) by Ma *et al.* (1996). On the other hand, neutron-scattering studies by Börjesson *et al.* (1990) obtained a much higher T_c (180–200 K). Subsequent reexamination of propylene carbonate by Wuttke *et al.* (2000) with neutron-scattering measurements improved this result. From the susceptibility minimum analysis, these authors obtained $T_c\approx182$ K, corresponding to $\lambda=0.72$.

The experimental data we have considered so far correspond to the fragile glass formers (according to the Angell classification; see the Introduction). Torell *et al.* (1995) have argued that even for strong glass formers like B_2O_3, the relaxation can be described in terms of the mode-coupling predictions of the two-step relaxation process. The ratio of the crossover temperature T_c to the corresponding T_g is higher for a strong glass former ($T_c\approx1.6T_g$) than for a fragile system ($T_c\approx1.2T_g$). The temperature T_c identified from the behavior of the nonergodicity parameter of B_2O_3 using light-scattering (Brodin *et al.*, 1996) and neutron-scattering data (Engberg *et al.*, 1998) was $T_c\approx850$ K ($T_g\approx523$ K for B_2O_3).

For temperatures below T_c, inclusion of ergodicity-restoring mechanisms becomes more important. Schematic forms of extended mode-coupling models that include in the theoretical description an additional parameter δ have been considered in this respect. The data from depolarized light-scattering experiments on CKN, Salol (Cummins *et al.*, 1993), and OTP (Cummins *et al.*, 1997) were fitted in the β-relaxation regime with this extra fitting parameter. In the extended model, the sharp divergence of the time scales was eliminated. Signatures of the cutoff mechanism in the dielectric data are apparent in Fig. 6, in which as $T\to T_c$ from above, there is clear deviation from straight-line behavior, showing that the dynamic transition is finally suppressed. More recently Götze and Voigtmann (2000) have studied the susceptibility spectra of propylene carbonate using a schematic model involving, in addition to the usual density correlator, a second schematic correlator (Sjögren, 1986). The critical temperature extracted is $T_c\approx180$ K and $\lambda=0.75$ giving $a=0.30$ and $b=0.56$. In this model the cutoff parameters for both of the correlators are included. The same model was further applied by Brodin *et al.* (2002) for analyzing the Brillouin-scattering spectra of propylene carbonate. The glass-forming material α-picoline was studied by Adichtchev *et al.* (2002), who showed that the nonergodicity parameter follows the predicted cusp when the excess contribution due to the α process (for $T<T_c$) is taken into consideration.

It is worth mentioning that the above procedure of identifying a mode-coupling transition temperature T_c (Li *et al.*, 1992a, 1992b; Götze and Sjögren, 1992) has been criticized by a number of authors. Zeng *et al.* (1994) argued that instead of treating the location of $\omega_{\min}$ as adjustable, one could take a and b to be independent in the data-fitting procedure. However, in that case, the resulting power-law exponents a and b do not satisfy the transcendental equations predicted from mode-coupling theory [see related discussion with Eqs. (5.9) and (5.11)]. Nagel and co-workers also argued (Dixon *et al.*, 1994) that the decrease of $\omega_{\min}$ (the susceptibility minimum between the microscopic peak and the α peak) with temperature is a simple consequence of the fact that the α peak shifts to lower frequency with lowering of temperature, while the microscopic peak does not. It was also pointed out that the data on dielectric relaxation in Salol did not show any crossover behavior around a critical temperature 256 K. Kim and Mazenko (1992) gave an interesting explanation of the signature of T_c in the dynamic data of Nagel and co-workers. We discuss this below with reference to the Nagel plot.

A characteristic feature of supercooled liquids is the observation of extra intensity in neutron scattering (Frick and Richter, 1993; Kanaya *et al.*, 1994; Kartini *et al.*, 1996) and Raman scattering (Fischer, 1993; Sokolov *et al.*, 1994) at low frequencies, showing a peak that is distinct from the quasielastic peak. This is called the boson peak, and it is particularly prominent for the strong glass formers. From the fluctuating hydrodynamic approach such an intermediate peak has been obtained (Das, 1999) in a study of the coupling of the translational and vibrational modes in an amorphous solid (Kojima and Novikov, 1996). Two correlator schematic models were also studied earlier by Alba-Simionesco and Krauzman (1995) and Götze and Sjögren (1996) to obtain the extra peak over intermediate time scales. The coupling of vibrational modes in the supercooled liquids, with structural relaxation producing an anomalous oscillation peak, has been recently studied by Götze and Mayr (2000).

3. The α-relaxation regime

The relaxation of the correlation function beyond the corresponding plateau f_q^c of the so-called nonergodicity parameter and subsequent to the von-Schweidler decay is generally referred to as *α relaxation*. In the close vicinity of the dynamic transition point the α relaxation is described to leading order in terms of a temperature-independent master function (discussed in Sec. VII.A.2). This also implies time/temperature superposition. However, as the distance from the transition increases, correction terms of $O(\Delta_o)$ to this master function become significant [see Eq. (5.27)]. Furthermore, the effects of ergodicity-restoring mechanisms described in the extended mode-coupling theory will also influence the predictions for final relaxation in the theoretical model.

a. The temperature dependence of the α peak

The time scale τ_α of the α relaxation (see Sec. VII.A.1) increases as $|\Delta_o|^{-\gamma}$ with $\gamma=1/2a+1/2b$. The temperature dependence of the peak frequency is therefore of the form $\omega_\alpha \sim (T-T_c)^\gamma$. This is shown in the lowest panel of Fig. 6, in which $\omega_\alpha^{1/\gamma}$ is plotted with temperature. The values used of $a=0.28$ and $\gamma=2.9$ are kept the same as those obtained in fitting ω_β and $\chi_{\min}$ described above. In comparison, similar fits with τ_β and τ_α extracted from light-scattering data (Li *et al.*, 1992a) for CKN obtain $a=0.28$ and $\gamma=2.9$ with the corresponding $\lambda=0.81$. Schönhals *et al.* (1993) did an extensive study of the α relaxation in propylene carbonate. The result for the transition temperature $T_c=186.6$ K is comparable to the corresponding transition temperature $T_c=180$ K from neutron-scattering results (Börjesson *et al.*, 1990; Elmroth *et al.*, 1992). The temperature dependence of the α peak frequency ν_p ($\sim\omega_\alpha$) fits to a power law proposed by mode-coupling theory, $\nu_p \sim (T-T_c)^\gamma$ with exponent $\gamma=2.45$. However the data reportedly also fit an Arrhenius behavior. Beyond a temperature T_A, the power-law behavior crosses over to a Vogel-Fulcher-Tamann form, as shown in Fig. 7. The mode-coupling T_c (186.6 K) lies in between the temperatures T_o and T_A, which are, respectively, equal to 130 and 216.6 K for propylene carbonate. Subsequent measurements of the dielectric susceptibility over even wider frequency ranges by Schneider *et al.* (1999) fit the α-relaxation time scale, with $\gamma=2.72$ and $T_c=187$ K conforming to the above findings of Schönhals *et al.* An interesting aspect of the mode-coupling theory predictions is that for $T>T_c$, the relaxation times measured with different experimental methods should have a common temperature dependence. Schneider *et al.* (1999) report that the relaxation time measured in light scattering experiments (Du *et al.*, 1994) is smaller than that obtained from dielectric measurements by a temperature-independent factor of 3.

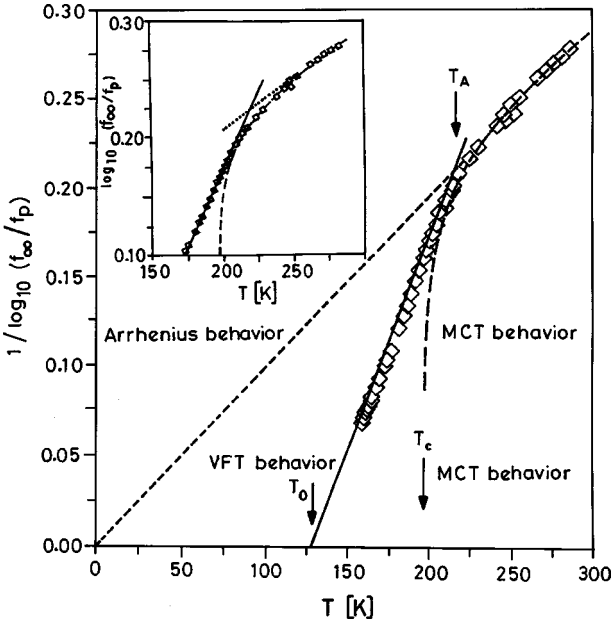

FIG. 7. The behavior of the peak frequency $1/\log_{10}(\nu_\infty/\nu_p)$ vs temperature T for propylene carbonate with $\log_{10}\nu_\infty=13.11$. The Vogel-Fulcher-Tamann (VFT) temperature T_o, the mode-coupling (MCT) T_c, and the crossover temperature T_A are indicated by arrows. The crossover behavior is shown more clearly in the inset. From Schönhals *et al.*, 1993.

b. The scaling in the α regime

Time/temperature superposition for the α relaxation is a leading-order asymptotic behavior in the simple mode-coupling theory. There have been claims and counterclaims on the validity of this assertion in a number of experiments. For depolarized light-scattering spectroscopy of OTP (Cummins *et al.*, 1997), the α peak was fitted with a Kohlrausch form. A temperature-independent stretching exponent $\beta=0.78$ was found to fit the data provided the higher-frequency wing was interpreted as an overlap from β relaxation or von-Schweidler-type decay. The corresponding von-Schweidler exponent $b=0.6$ was obtained from an analysis of the β process (Cummins *et al.*, 1997). Similarly, a temperature-independent β for $T>T_c$ was obtained (a) from light-scattering spectroscopy data for CKN (Li *et al.*, 1992a), glycerol (Wuttke *et al.*, 1994), and propylene carbonate (Du *et al.*, 1994); (b) from dielectric loss data for CKN (Pimenov *et al.*, 1996), glycerol (Lunkenheimer *et al.*, 1996), and propylene carbonate (Lunkenheimer, Pimenov, Dressel, *et al.*, 1997). Arguments in favor of the temperature independence of β are based on the reasoning that the observed temperature dependence of β, if any, is due to the overlapping from the power-law relaxation.

Some authors have argued, on the other hand, that a clear temperature dependence of the stretching exponent for α relaxation is seen in the data. By measuring the dielectric susceptibility in low-molecular-weight glass-forming liquid propylene carbonate, over 15 decades, Schönhals *et al.* (1993) obtained a temperature-

dependent stretching exponent β—a result that contradicted the earlier light-scattering results (Elmroth *et al.*, 1992) of a temperature-independent β. In dielectric experiments covering over more than 18 decades of frequency, Schneider *et al.* also found a temperature-dependent stretching exponent. However, these authors comment that the data fit reasonably to the Cole-Davidson form, with temperature-independent $\beta_{CD}=0.8$, as well. The stretching exponent β depends on the wave number (Fuchs, Hofacker, and Latz, 1992). Coherent neutron-scattering data on OTP (Tölle *et al.*, 1998) shows a wave-vector-dependent stretching exponent $\beta=0.64$ and 0.56 for $q=1.45$ A^{-1} and 1.20 A^{-1}, respectively. Theoretically even within the simple mode-coupling theory, away from the transition, temperature-dependent corrections add to the master function. The role of the ergodicity-restoring processes can further affect the simple result of time/temperature superposition.

B. The Nagel plot and mode-coupling theory

The primary relaxation of a supercooled liquid shows characteristic non-Debye (nonexponential) behavior and has been fitted with different types of empirical formulas such as Cole-Cole $\chi(\omega)\propto 1/[1+(i\omega\tau)^{1-a}]$ (Cole and Cole, 1941), Davidson-Cole, $\chi(\omega)\propto 1/[1+(i\omega\tau)]^a$ (Davidson and Cole, 1951), or the stretched-exponential $\chi(\omega)\propto\{\text{Fourier transform of}(d/dt)[-\exp(t/\tau)^\beta]\}$ (Williams and Watts, 1970). An interesting development regarding scaling in glassy dynamics was the discovery of a scaling plot initially proposed by Nagel and co-workers (Dixon, Menon, and Nagel, 1994). We discuss briefly this scaling and its possible links with mode-coupling theory.

Dixon *et al.* (1990) proposed a new scaling function with which the primary relaxation data from dielectric measurements for all sample liquids, over the entire 13 decades of frequency ($10^{-4}<\omega/2\pi<10^8$ Hz) collapse on a single curve. The new scaling function consists of only two parameters, namely, the peak frequency ω_p and the width of the relaxation curves w relative to the Debye width $w_d=2\log_{10}(2+\sqrt{3})=1.14$. This universal curve, which we refer to as the "Nagel plot," corresponds to defining the abscissa and ordinate, respectively, as

$$X=w^{-1}(1+w^{-1})\log_{10}(\omega/\omega_p),$$
$$Y=w^{-1}\log_{10}[(\chi_o''(\omega)/\chi_o)/(\omega/\omega_p)] \tag{7.2}$$

with χ_o being the static susceptibility. The new scaling behavior, which holds over a wide range of temperatures studied, evolves smoothly into a Debye or exponential relaxation function at high temperature. Dixon *et al.* include the data which (in the high-temperature range) fit to a stretched exponential form with temperature-dependent relaxation time τ_α and stretching exponents β, and therefore violate time/temperature superposition.

The relation of the scaling function to the mode-coupling theory follows from the analysis of the susceptibility function $\chi(\omega)$, which is related to the normalized density correlation function $\phi(\omega)$ through $\omega\phi(\omega)\sim\chi''(\omega)$. The characteristic relaxation predicted by mode-coupling theory involves power-law decays over intermediate times crossing over to a stretched exponential relaxation in the primary or α-relaxation regime. It has been argued (Kim and Mazenko, 1992) that the high-frequency tail of the Nagel plot is a consequence of von-Schweidler-type power-law relaxation. At low frequencies the Nagel plot agrees reasonably well with the stretched exponential relaxation but shows considerable variation at high frequency. In order for mode-coupling theory to have the universal slope of the Nagel plot of X and Y as defined in Eq. (7.2), the two exponents b and β must satisfy the linear relation $(1+b)/(1+\beta)=c$, where c is a system-independent constant (Kim and Mazenko, 1992). The experimental data conform to $c=\frac{3}{4}$. Since $b>0$, the above relation leads to the constraint $\beta>\frac{1}{3}$ and likewise, since $\beta\leqslant 1$, leads to $b\leqslant\frac{1}{2}$. However, the linear relation between β and b proposed above does not follow from a proper theoretical model (Kim and Mazenko, 1992). Thus the universal relaxation function of the Nagel plot cannot be quantitatively linked to the mode-coupling model apart from a qualitative similarity through an *ad hoc* schematic model in which the wave-vector dependence is ignored. Furthermore, the linear constraint is obtained by keeping only the leading-order power-law behavior and will be modified if higher-order corrections, discussed with Eq. (5.23), are included.

Fuchs, Hofacker, and Latz (1992) plotted the data for the α-relaxation master function $\hat{\Phi}_q(\hat{t})$ [see Eq. (5.25)] for different q in the form of the scaling function of Dixon *et al.* The numerical solutions of the master function for different wave vectors do not collapse on a single curve as happened with the macroscopic dielectric data. However, at the wave number corresponding to the diffraction peak, the agreement of the universal curve of the Nagel plot with the mode-coupling master curve is found to be better than that with the stretched exponential function or Cole-Davidson function. It is worth noting here that only the simple model with a sharp dynamic transition was considered by Fuchs, Hofacker, and Latz (1992) in comparing the Nagel plot with mode-coupling results for α relaxation. Finally, going back to the issue of locating a critical temperature in the dielectric relaxation data, indeed there is no obvious sign of a transition in the Nagel plot. However, Kim and Mazenko (1992) gave an interesting explanation regarding the signature of T_c from the dynamic data of Salol (Dixon *et al.*, 1990). The inverse of the square root of the peak frequency showed a clear crossover at an intermediate temperature. In Fig. 8 we show the data for Salol plotted in the universal scaling form of the Nagel plot and, in the inset, the corresponding crossover behavior of the peak frequency ν_p, as pointed out by Kim and Mazenko (1992). The crossover temperature is estimated to be 270 K, which is close to $T_c=267.7$ for Salol (Schönhals *et al.*, 1993).

The Nagel plot has been studied for simple liquids (Wu, 1991; Wu *et al.*, 1991; Menon *et al.*, 1992), for polymeric glass-forming liquids (Menon and Nagel, 1993),

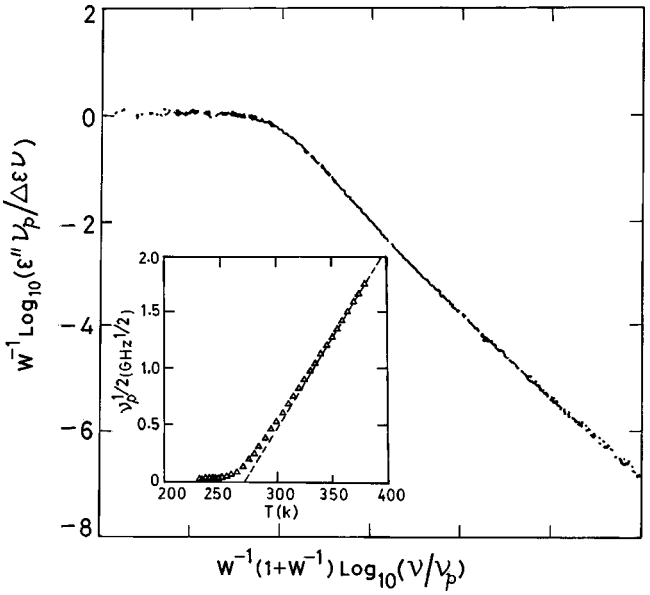

FIG. 8. Scaling plot for 13 decades of data for Salol. $(1/w)\log_{10}(\varepsilon''\nu_p/\nu\Delta\varepsilon)$ is plotted against $(1/w)(1/w+1)\log_{10}(\nu/\nu_p)$ where $\Delta\varepsilon=\varepsilon(0)-\varepsilon(\infty)$ is the measured static susceptibility. From Dixon *et al.*, 1990. The inset: $\nu_p^{1/2}(\mathrm{GHz}^{1/2})$ vs temperature T. The dashed line is a linear fit to the last five points. The crossover temperature is estimated to be 270 K. Inset from Kim and Mazenko, 1992.

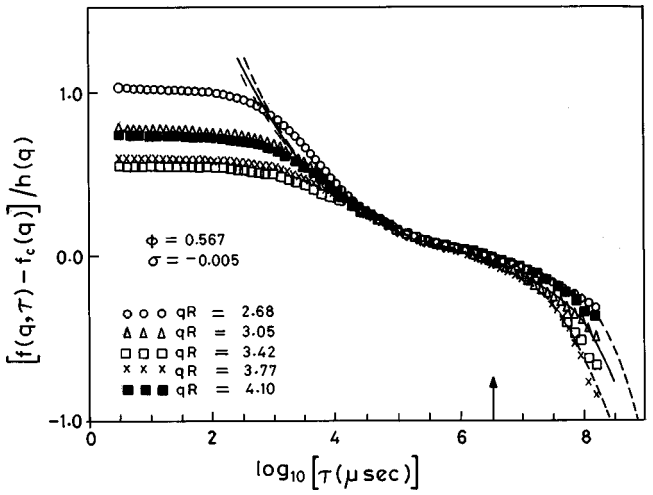

FIG. 9. The density correlator $\phi_q(t)\equiv f(q,\tau)$ in scaled form $[\phi_q(t)-f_q^c]/h_q$ vs time $t=\tau$: R, the hard-sphere radius, σ, the separation parameter; ϕ, the packing fraction; solid line, the mode-coupling master function $\sigma^{1/2}[g_-(\hat{t})]$ (see text) corresponding to exponent parameter $\lambda=0.758$; dashed lines, $\lambda=0.70$ and 0.80, respectively. The vertical arrow on the time axis corresponds to the β relaxation time scale τ_β. From van Megen and Underwood, 1994.

and even for crystalline systems with orientational disorder, cyclo-octanol (Leslie-Pelecky and Birge, 1994). There were some criticisms of Nagel scaling, especially for the low-frequency part of the spectrum (Schönhals *et al.*, 1991, 1993), for which the experimental data show some deviation from the universal curve. But for frequencies above the α-peak frequency, all the data for different systems fall on a universal curve. The stretching exponent β is temperature dependent, in disagreement with the leading-order results of mode-coupling theory. Some modifications of the Nagel plot have been proposed (Dendzik *et al.*, 1997), which were applied to dielectric spectroscopic data on propylene carbonate by Schneider *et al.* (1999). Based on the above universal scaling of dielectric loss data, Menon and Nagel (1995) have argued that the static susceptibility shows a divergence at low temperature. This essentially implies constant loss behavior for the high-frequency part of the spectrum at low temperature.

C. Glass transition in colloids

The predictions of the fully wave-vector-dependent mode-coupling model discussed in Sec. V.A were compared extensively with the data from dynamic light-scattering studies on colloidal systems (van Megen and Underwood, 1993a, 1993b, 1994). A colloid consists of suspended particles in a solvent liquid treated as an inert continuous background. Although colloids are very different from atomic systems, they share certain characteristic properties. The effective interactions between particles suspended in a colloid can be made strongly repulsive by using suitable techniques, and hence colloidal equilibrium phase behavior mimics that of a hard-sphere system. For example, the melting volume fraction $\varphi_m=0.542\pm0.003$ in a colloid is in agreement with that obtained from simulation of hard-sphere crystals (Hoover and Ree, 1968). The microscopic dynamics of colloid particles involve frequent collisions of solvent molecules. But the positions of these suspended particles change over a much slower time scale. This large difference in time scales allows use of the stochastic Langevin equations for the dynamics of colloid particles, in contrast to the deterministic Newtonian equations of motion in an atomic system. However, over long time scales the dynamics of the two types of systems are similar, showing essentially diffusive behavior. At high density for both systems diffusive motion becomes extremely slow, leading to effective freezing in an amorphous configuration. Colloidal suspensions thus have become a suitable choice for studying glassy dynamics.

The normalized density correlation function $\phi(q,t)$ computed in a light-scattering experiment on this system almost freezes to a constant value for a change of the packing fraction within 1% around $\varphi_c=0.574$ (van Megen and Underwood, 1993a, 1993b). This structural arrest (in the range $0.574<\varphi_c<0.581$) in colloids has been identified with the dynamic transition of the simple mode-coupling theory. From the relaxation data the β-scaling of mode-coupling theory is demonstrated in Fig. 9. This plot also tests the q independence of the left-hand side of Eq. (5.24) over a suitable range of time. The theoretical curve shown in Fig. 9 consists of the contribution from the β relaxation [given by Eq. (5.21)] as well as the α-relaxation master function Φ. Thus ex-

perimental data fit a β-scaling function obtained with the exponent parameter $\lambda=0.758$. Using the hard-sphere structure factor in Eq. (5.17), one obtains the corresponding value of the exponent parameter as $\lambda=0.77$.

The agreement between theory and experiment is thus remarkable in the β-relaxation regime. It is worth noting, though, the large number of parameters involved in the fitting:

(a) the nonergodicity parameter $f_c(q)$ and the amplitude function $h(q)$, which are kept constant for different φ at a fixed value of q,

(b) the separation parameter Δ_o (denoted by σ in the figure), which is kept the same for different q at a fixed φ, and

(c) the scale of the α-relaxation time τ_α in the corresponding contribution from the α master function to the dynamics.

Setting these parameters fixes the β-relaxation time τ_β as well. A number of consistency checks need to be made, to find the optimum choices for these parameters. The fitted values for $f_c(q)$ and its ratio to $h(q)$ have been found to agree reasonably well with the corresponding predictions of the hard-sphere model. The α-relaxation time scale τ_α is almost q independent, agreeing well with the predictions of mode-coupling theory. Finally, the values of Δ_o used as a fitting parameter roughly conform to $\Delta_o=c_o[(\varphi_c-\varphi)/\varphi_c]$ with the constant $c_o=1.27$ (Fuchs, Götze, *et al.*, 1992). The experimental data describe the scaling function for glass over about 2.5 decades for $t>10^5$ μs, which is also the range over which the factorization property is expected to hold.

The α-relaxation master function of mode-coupling theory (to leading order) has been reported to fit well to the experimental data (van Megen, 1995) even for $\varphi=0.494$ [for the separation parameter $\epsilon=(\varphi-\varphi_c)/\varphi_c=0.02$]. For the self-correlation function (van Megen *et al.*, 1998) the decay in the α-relaxation range fit well with the stretched exponential form, with a temperature-independent stretching exponent $\beta=0.95$. The-long time diffusion coefficient for the tagged particle shows a power-law divergence, $D_L\sim\varepsilon^{\gamma'}$, with $\varphi_c=0.57$. The exponent $\gamma'=2.7\pm0.1$ from the best fit to the experimental data matches well with the mode-coupling prediction of $\gamma=2.6$. The value $\gamma=2$ is predicted by an alternative theory (Tokuyama and Oppenheim, 1997) for the glass transition in colloids. Unlike the computer simulation results (see Sec. X.A), in the case of colloids the power-law exponent for the self-diffusion coefficient is reported to match well (van Megen *et al.*, 1998) with mode-coupling theory predictions. The comparisons described above are all based on the simple model predicting a dynamic transition. It has generally been argued that since the momentum exchange with colloid particles occurs on much shorter time scale, the cutoff mechanism is weak in these systems. However, the data, even at the highest density, do not rule out the presence of an ergodicity-restoring processes (Srivastava and Das, 2002) and call for comparison with the extended mode-coupling models.

VIII. PHENOMENOLOGICAL EXTENSIONS OF MODE-COUPLING THEORY

Several phenomenological models of supercooled liquids or glasses have been constructed by including in the hydrodynamic description extra slow modes in addition to the usual set of conserved densities considered so far. Such new modes, for example, refer to the description of (a) the orientational order in the supercooled state (Dattagupta and Turski, 1985, 1993; Kree *et al.*, 1987); (b) the amorphous structure of the glassy state (Sachdev, 1986); and (c) the frequency-dependent thermal response (Oxtoby, 1986). We shall discuss here two specific extensions of the self-consistent mode-coupling theory formulated by including new slow modes. These are, respectively, the description of a solidlike amorphous state and the structural relaxation in a dense liquid. The introduction of the new slow modes is not based on any new conservation law or long-range order, but is aimed towards capturing the observed phenomena in glassy relaxations.

A. Hydrodynamics of solids

A unified hydrodynamic approach to the description of systems that are less symmetric than an isotropic liquid, e.g., liquid crystals, crystals, and glasses, was first proposed by Martin *et al.* (1972). This was further developed by Cohen *et al.* to describe linear transport in a crystal (Fleming *et al.*, 1976) and in an amorphous solid (Cohen *et al.*, 1976). The extra slow modes take into account the broken symmetry of this state with elastic properties. For a crystal these are the displacement vectors for the different lattice sites, defined as $\mathbf{u}(\mathbf{x})$ in terms of the phase-space coordinates,

$$\hat{\rho}(\mathbf{x},t)\hat{u}_i(\mathbf{x},t)=m\sum_{\alpha=1}^{N}u_\alpha^i(t)\,\delta[\mathbf{x}-\mathbf{r}_\alpha(t)], \tag{8.1}$$

where $\mathbf{u}_\alpha(t)$ ($\alpha=1$ to N) denote the displacements of the individual particles from their respective mean positions $\mathbf{r}_\alpha^o$ so that $\mathbf{r}_\alpha(t)=\mathbf{r}_\alpha^o+\mathbf{u}_\alpha(t)$. In a crystal, the underlying lattice has a long-range order. For a supercooled liquid or glass, on the other hand, the local metastable positions of the atoms $\{r_\alpha^o\}$ define an amorphous structure which remains unaltered only up to certain time scales.

An essential ingredient in the construction of the nonlinear Langevin equations with an extended set of slow modes is the corresponding free-energy functional F ($=F_k+F_u$). The kinetic part, F_k, dependent on momentum density $\mathbf{g}$ is the same as Eq. (4.11) for the isotropic case. The interaction part of the effective Hamiltonian now contains an elastic part $F_{\rm el}$ written in terms of the strain tensor field $s_{ij}=\frac{1}{2}(\nabla_i u_j+\nabla_j u_i)-\frac{1}{2}\nabla_i u_m\nabla_j u_m$ and its trace $\bar{s}$. The equation for $\mathbf{g}$ is a balance equation with the stress-energy tensor σ_{ij} now including coupling to the

solidlike modes as well as a random part (Das and Schilling, 1994). The equation for the displacement field **u** is

$$\frac{\partial u_i}{\partial t} + \mathbf{v} \cdot \nabla u_i = v_i - \Gamma_v \frac{\delta F_u}{\delta u_i} + f_i^e, \tag{8.2}$$

where the correlation of the noise f_i^e is related to the bare transport coefficient Γ_v. Since **u** is not a conserved property, Eq. (8.2) is not a balance equation. In a perfect crystal without vacancies the density fluctuation is given by $\delta\rho = -\rho_o(\nabla \cdot \mathbf{u})$. The difference, therefore, gives the vacancy density (Cohen *et al.*, 1976; Zippelius *et al.*, 1980) in the imperfect crystal, $n_D(\mathbf{x},t) = \delta\rho(\mathbf{x},t) + \rho_o(\nabla \cdot \mathbf{u})$.

A phenomenological model for an amorphous solid (Das and Schilling, 1994; Das, 1999) was considered with the assumption that freezing occurred on the scale of local structure but overall translational invariance would hold over long length scales. An important component of the description of an amorphous state is the presence of free volumes (Cohen and Grest, 1979). The extended hydrodynamic description of Das and Schilling, including the diffusion of free volumes, was constructed treating the final relaxation process of the density fluctuations and the voids as similar. Kim (1992) considered the coupling of the displacement field **u** with density fluctuations to obtain the mode-coupling terms of the ϕ_{12} model (discussed in Sec. V.B) from a hydrodynamic approach. The transverse parts of the displacement field **u** in the case of an amorphous solid (Kim, 1992) give rise to transverse sound modes in experiments (Grimsditch *et al.*, 1989). The above theoretical description of the dynamics of an amorphous-solid-like state is, however, limited by the fact that the definition of the displacement field **u** requires reference to a rigid lattice. The concept of this underlying structure is only valid over initial time scales and finally ceases to hold for a supercooled liquid, which is ergodic over the longest time scale. A more appropriate theory would require a self-consistent treatment of the problem, connecting the elastic and viscous behaviors (Götze and Latz, 1989) of the metastable system.

In an alternative approach, Yeo and Mazenko (1994, 1995) avoided the issue of the underlying lattice for an amorphous state by simply defining a defect density $n_D(\mathbf{x},t)$ analogous to the order parameter of the disordered state. To obtain the equations for the dynamics of n_D it is sufficient to assume that it is a densitylike variable, i.e., it has the usual Poisson bracket relations of a scalar variable with the momentum density **g**. The driving free-energy functional F_u is expressed as a sum of three parts, $F_u = F_{\rm is} + F_D + F_C$, where the first term $F_{\rm is}$ is the isotropic part given by Eqs. (4.15) and (4.16), while the contribution from defects is $F_D \equiv \int d\mathbf{x} h[n_D(\mathbf{x})]$, so that $h[n(\mathbf{x})]$ corresponds to the defect potential. A key underlying assumption of this model is that the defect relaxation is very slow. This is realized by choosing an explicit double form for $h(n_D)$ in the defect potential-energy part F_D of the free-energy functional. The position of the extrema of the potential is denoted by $\bar{n}_D$ such that $h'(\bar{n}_D) = 0$. A very small diffusion coefficient Γ_v for the defect density results from choosing parameters to describe a shallow metastable well whose parameters are suitably chosen. A very small diffusion coefficient Γ_v for the defect density corresponds to the system rolling in a shallow metastable well characterized by suitably chosen parameters. The defect-mass density interaction part F_C is obtained as

$$F_C = B_D \int d\mathbf{x} \int d\mathbf{x}' \, \delta n_D(\mathbf{x}) c(|\mathbf{x} - \mathbf{x}'|) \delta\rho(\mathbf{x}'), \tag{8.3}$$

where the role of the defect density here is taken to be similar to the mass density variable (Yeo, 1995). The mass density and defect density coupling B_D is expressed in terms of the dimensionless quantity $x = B_D \rho_0 \bar{n}_D / (n k_B T)$. In the mode-coupling model described below the dynamics of the metastable liquid is considered in the limit of weak defect-density interaction ($B' \to 0$) and a shallow well for the defect density relaxation ($\tilde{\mu} \to 0$), such that $B' \sim \tilde{\mu}^2$. The density autocorrelation function follows a complex relaxation behavior due to couplings with long-lived defects. The present model really does not address the question of how the observed slowing down of the defect density occurs. Instead it is simply assumed that the system arranges itself to be near the critical surface associated with the mode-coupling theory.

The renormalization of the longitudinal viscosity (4.4) is now modified (Yeo, 1995) to

$$\tilde{m}^L(q,t) = \frac{1}{\beta m} \int \frac{d\mathbf{k}}{(2\pi)^3} [V^{(1)}(\mathbf{q},\mathbf{k}) \phi(k,t) + V^{(2)}(\mathbf{q},\mathbf{k}) \phi(k,t) \phi(|\mathbf{q} - \mathbf{k}|,t)], \tag{8.4}$$

where it is assumed that the defect correlation remains constant over the time scale considered. The mode-coupling vertices $V^{(1)}$ and $V^{(2)}$ with full wave-vector dependence are obtained in terms of the liquid structure factors. The Landau coefficients of the free energy in F_C and F_D become control parameters in the mode-coupling integrals. Two dimensionless parameters y and κ are defined for this purpose in terms of $\tilde{\mu}$ and $\tilde{\nu}$, respectively, as $y \equiv \tilde{\nu}/(n_o k_B T)$ and $\kappa \equiv (\tilde{\nu}^2 x)/\tilde{\mu}^2$, where n_o is the average particle number density.

The dynamic transition is identified from a self-consistent solution of the nonlinear integral equations similar to Eq. (5.14) for the nonergodicity parameters f_q with Eq. (8.4) as the corresponding memory function. A set of critical parameters $\{\kappa_c, y_c, \varphi_c\}$ above which all f_q''s converge to nonzero values, is identified. As a result, instead of the single transition point of the simple mode-coupling theory, a line of transitions is predicted in the present case. The metastability parameters of the free-energy surface relating to defect dynamics, as well as the exponents describing the observed sequence of time relaxations, are smooth functions of temperature or density without evidence of any special transition point. Yeo (1995) considered the static structure factor of the liquid in this model to be that of a hard-sphere system. The

exponent parameter and hence the power-law exponents were computed from an analysis of the stability matrix as described in Sec. V.B. The density dependence of the power-law exponents was computed for several choices of the metastability parameters κ and y. Corresponding to the line of transitions, the exponents become density dependent in a natural way. This is in sharp contrast with the constant critical exponents (similar to second-order phase transitions) of the simple mode-coupling models. The density correlation function $\phi(q,t)$ can also be obtained by numerically solving the mode-coupilng equations. The density-dependent exponents of power-law relaxations (Srivastava and Das, 2001) are similar to the results obtained by Yeo (1995) from the computation of the exponent parameters.

In the simple mode-coupling theory, for a hard-sphere system the critical packing fraction $\varphi_c=0.525$ for the dynamic transition is somewhat lower than what the experiments on colloids (see Sec. VII.C) suggest for an underlying structural arrest. The order parameters of this transition, i.e., the $f_c(q)$s at $\varphi=\varphi_c$, are fixed, to be determined by the structure factor for the liquid. However in the actual data fitting the $f_c(q)$'s often have to be treated as adjustable parameters (see Sec. VII.C). In the phenomenological model presented above, a line of transitions is obtained. The nonergodicity parameters $f_c(q)$ are not constrained to remain fixed and vary along the line of transitions in a natural way. It is worth noting here that the existence of a special transition temperature T_c ($>T_G$) has been questioned in a number of experimental studies of glassy dynamics (see Sec. VII). The approach taken here tries to circumvent this by taking into consideration the coupling of the mass density to another slow variable, the defect density mode, in a manner that keeps many of the qualitative features of the original mode-coupling theory. It also includes in a very natural way the essential feature of metastability in the glassy dynamics. The price paid in this formulation is that by introducing the defect density it is now basically a phenomenological approach, since no connection between the particle interaction potential and the parameters of the defect potential is carried forward. The better data-fitting ability is a result of introducing additional metastability parameters in the theory.

B. A model for structural relaxation

A model for structural relaxation in the supercooled liquids was proposed in terms of the dynamics of particle clusters (Liu and Oppenheim, 1997; Manno and Oppenheim, 1999) based on the following phenomenological picture: In a low-density liquid a single tagged particle is temporarily trapped by neighboring particles in a cage with a lifetime of a few collisions. With increased supercooling these cages become long lived and trapping of the particle is more effective.

A dynamical variable which describes the geometry of the center of mass within a prescribed volume of length scale L is defined as the new order parameter $\hat{o}(\mathbf{r},t)$,

$$\hat{o}(\mathbf{r},t)=\sum_{\alpha,\beta}{}'w(\mathbf{r}_{\alpha\beta})\delta[\mathbf{r}-\mathbf{r}_{\alpha}(t)], \tag{8.5}$$

where $\mathbf{r}_{\alpha\beta}(t)=\mathbf{r}_{\alpha}(t)-\mathbf{r}_{\beta}(t)$ and the prime indicates that the $\alpha=\beta$ term is omitted from the sum. Here o is introduced (in an *ad hoc* manner) to capture the process of decay of the cage formed around a single particle. The weight function $w(\mathbf{r})$ used in the definition (8.5) incorporates a cutoff length L to describe a cluster. A simple choice is $w(\mathbf{r})=f(\mathbf{r})U_L(r)$ where $f(\mathbf{r})$ is a smoothly varying function reflecting the cluster geometry and $U_L(r)\equiv\Theta(r-L)$ is the unit step function. A convenient form of the new order parameter is expressed in the Fourier-transformed form

$$o(\mathbf{q},t)=\delta n_w(q,t)-\frac{\langle n_w(q)n^*(\mathbf{q})\rangle}{\langle n(\mathbf{q})n^*(\mathbf{q})\rangle}n(\mathbf{q},t), \tag{8.6}$$

where $\delta n_w(q,t)$ is the fluctuation of

$$n_w(q,t)=\int\frac{d\mathbf{k}}{(2\pi)^3}w(\mathbf{k})n(\mathbf{q}-\mathbf{k},t)n(\mathbf{k},t) \tag{8.7}$$

from its average value and $w(\mathbf{k})$ is the Fourier transform of $w(\mathbf{r})$. The equations of motion for the above set of collective modes are obtained by defining the projection operator $\mathcal{P}$ with respect to the set $\{n(\mathbf{q},\mathbf{t}), g_l(\mathbf{q},\mathbf{t}),o(\mathbf{q},\mathbf{t})\}$. The matrix of equal-time correlations is diagonal with respect to this set.

The density autocorrelation function is obtained following standard procedures in the form (3.17),

$$\phi(q,z)=\left[z-\frac{1}{z+i\bar{m}^L(q,z)}\right]^{-1}, \tag{8.8}$$

where $\bar{m}^L(q,z)$ represents the effective longitudinal viscosity consisting of two parts, $\bar{m}^L(q,z)=m^L(q,z)+m_\delta(q,z)$. The first part $m^L(q,z)$ contains the bare (short-time) contribution as well as mode-coupling contributions. The second part m_δ is due to the structural relaxation of the cluster through the newly introduced local order parameter $o(\mathbf{r},t)$ and is

$$m_\delta(q,z)=\frac{\tilde{v}_o^2(q)\Re(q)^2}{z+i\delta_h(q,z)}, \tag{8.9}$$

where $\tilde{v}_o^2(k)$ is defined as $\tilde{v}_o^2(k)=[\beta mS_o(k)]^{-1}$ in terms of the equal-time correlation of the local order parameter $nS_o(k)=V^{-1}\langle o(\mathbf{k})o^*(\mathbf{k})\rangle\equiv\chi_{oo}$. The expression for m_δ describing the structural relaxation has two main components. Using the projection operator method, the amplitude function $\Re(q)$ is obtained from the reversible part of the dynamics formulated in the frequency matrix Ω in the memory function equation (3.8). Ignoring correlations beyond the two-particle level (Liu and Oppenheim, 1997) we obtain

$$\Re(q)=n\int\frac{d\mathbf{k}}{(2\pi)^3}w(\mathbf{k})V_L(\mathbf{q}-\mathbf{k},\mathbf{k}), \tag{8.10}$$

where the vertex function is as defined in Eq. (4.5) for the standard form of mode-coupling theory. Contributions from three-point direct correlation functions are

also ignored in Eq. (8.10) for simplification. The quantity δ_h appearing as a pole for m_δ represents the process of structural relaxation in the supercooled liquid. Using the relation (3.10) the so-called "hopping kernel" δ_h is expressed as $\delta_h(\mathbf{q},t)=\langle f_o(\mathbf{q},t)f_o(\mathbf{q})\rangle\chi_{oo}^{-1}$, in terms of the noise f_o in the equation of motion for o. Using the definition $f_o=(1-\mathcal{P})\dot{o}$ it is straightforward to obtain (Liu and Oppenheim, 1997)

$$\delta_h(q,z)=\frac{\chi_{oo}^{-1}}{V^2}\int_o^\infty dt e^{izt}\sum_k V_h(\mathbf{q}-\mathbf{k},\mathbf{k}) \times\langle\{e^{i(1-\mathcal{P})\mathcal{L}t}\mathcal{F}^*(\mathbf{q},\mathbf{k})\}\mathcal{F}(\mathbf{q},\mathbf{k})\rangle \tag{8.11}$$

with the vertex function V_h given by

$$V_h(\mathbf{q}-\mathbf{k},\mathbf{k})=w(\mathbf{k})w(\mathbf{q}-\mathbf{k})+w(\mathbf{k})w(\mathbf{k}),$$
$$\mathcal{F}(\mathbf{q},\mathbf{k})=(1-P)\frac{d}{dt}\{n(\mathbf{q}-\mathbf{k})n^*(\mathbf{k})\}. \tag{8.12}$$

This is of course a formal result, and for a realistic calculation a simplification of Eq. (8.12) using $\mathcal{P}$ can be employed. Manno and Oppenheim (1999) have argued that in the hydrodynamic limit $\delta_h(q,z)$ is proportional to $\tilde{\nu}^{-1}(k)$, where $\tilde{\nu}(q)$ is the zero-frequency viscosity at wave number q. This dependence of $\delta_h(q,z)$ on the viscosity remains valid even when the corresponding mode-coupling corrections are added to m^L (Manno and Oppenheim, 1999).

The present model describes the dynamics of a dense fluid with similar implications to those of the extended mode-coupling theories described in Sec. VI, in which the conserved hydrodynamic modes are the slow variables. In the extended mode-coupling models the renormalization of the transport properties due to bilinear coupling of density modes is obtained from a perturbative approach. The slow dynamics are a natural outcome of the nonlinear feedback mechanism and occur while the static structure factor remains finite through the transition. In the Liu-Oppenheim model, on the other hand, in addition to the usual set of conserved modes a particular subset of the bilinear modes of density fluctuations are included at the outset as an extra slow variable ($\hat{o}$). The long time scales developing in the supercooled state are linked to the slow structural relaxation process described by the newly defined local order parameter o. With increased supercooling δ_h becomes arbitrarily small. For $\delta_h=0$, the longitudinal viscosity would diverge and the density correlation function would develop a $1/z$-type pole. We note from Eq. (8.11) that the quantity δ_h, which is crucial for the final decay of ϕ, is associated with the decay of bilinear density-momentum modes similar to the cutoff function γ of the self-consistent model in Eq. (A22). Since the macroscopic viscosity for small q is very large on approaching the transition, δ_h (which is inversely dependent on the viscosity) becomes correspondingly small. The wave-number cutoff $2\pi/L$ in the definition of o is an input in the theory. This is similar to, though somewhat less *ad hoc*, than the case of the lower cutoff time t_o discussed in Sec. VI.B. As the glass transition approaches, δ_h is expected to become $\bar{m}^L$ and m_δ become very large. The above scenario for the slow dynamics of structural relaxation needs to be tested with more specific calculation for a model system.

IX. BEYOND MODE-COUPLING THEORY: NONPERTURBATIVE APPROACH

In the present form of the mode-coupling theory, the renormalization of the transport coefficients due to nonlinearities in the generalized hydrodynamic equations is considered only to the order of one-loop diagrams (see Appendix A.1), except in a few cases (Das *et al.*, 1985; Manno and Oppenheim, 1999) where a higher class of loop diagrams has been considered. In this section we shall discuss some recent work on the dynamics of dense fluids going beyond the low-order mode-coupling approach. We focus here on two different nonperturbative approaches to the study of the dynamics, (a) direct numerical integration for the stochastic equations for the nonlinear fluctuating hydrodynamics (Valls and Mazenko, 1991; Dasgupta and Valls, 1994) and (b) mapping the problem to a lattice gas model (Fuchizaki and Kawasaki, 2002).

A. Numerical solution of the Langevin equations

The Langevin equations can be numerically solved (Lust *et al.*, 1993) by treating them in a suitable dimensionless form,

$$\frac{\partial\rho}{\partial t}+\rho_o^{-1}\nabla\cdot[\rho\mathbf{g}]=0,$$
$$\frac{\partial g_i}{\partial t}=-\rho\nabla_i\frac{\delta F_u}{\delta\rho}-\sum_j\left[\nabla_j\frac{g_ig_j}{\rho_o}+\frac{g_j}{\rho_o}\nabla_ig_j\right] +\rho_o^{-1}\eta_o\nabla^2g_i+f_i. \tag{9.1}$$

In the above equations length is expressed in units of a lattice constant h of a chosen grid, while time is in units of $t_o=h/c_o$ with $c_o=\sqrt{1/(mn\kappa_o)}$ being the speed of sound, and κ_o the compressibility. The density ρ is thus rescaled with m/h^3 and the current density $\mathbf{g}$ with mc_o/h^3. The correlation of the noise f_i defines the bare transport coefficient,

$$\langle f_i(\mathbf{r},t)f_j(\mathbf{r}',t')\rangle=2K\lambda_o\eta_o\rho_o\delta_{ij}\nabla^2\delta(\mathbf{r}-\mathbf{r}')\delta(t-t'), \tag{9.2}$$

where η_o is the bare shear viscosity and the longitudinal viscosity is taken to be zero for simplicity. λ_o is a dimensionless parameter introduced to control the strength of equilibrium fluctuations. The fluctuating equations (9.1) are somewhat different from Eqs. (4.12) and (4.13). They are the same only at linear order. The continuity equation is now changed and the Galilean invariance of the equations is affected. Equations. (9.1) are obtained for a special choice $F_k=\int d\mathbf{x}[g^2/2\rho_o]$, which is different from

Eq. (4.11) in that the denominator contains ρ_o instead of ρ. With the new F_K, if the momentum variable $\mathbf{g}$ is integrated out from $F[\rho,\mathbf{g}]$, the free energy $F_u[\rho]$ is identical to the Ramakrishnan-Yussouff (1979) form (4.16) used in the density-functional models. On the other hand, retaining the form (4.11) for F_K in F gives rise to a term $\ln[\rho/\rho_o]$ on integrating the momentum variable (Yeo and Mazenko, 1995), and the resulting $F_u[\rho]$ is not of the Ramakrishnan-Yussouff form. The standard form (4.11) of F_K is obtained from a coarse graining of the microscopic partition function (Langer and Turski, 1973) and leads to the correct equations of nonlinear fluctuating hydrodynamics (Valls and Mazenko, 1992). The set of equations (9.1), on the other hand, are similar to the form used by Schmitz *et al.* (1993). They still have the basic coupling of density fluctuations included in the model.

Equations (9.1) are solved on a cubic lattice of grid size h. The size $N=15$ used for the lattice is adequate in the present case, since the direct correlation $c(r)$ is short ranged, corresponding to the strongly repulsive interaction potential. An incommensurate choice of $\sigma/h=4.6$ (σ is the hard-sphere diameter) is made to avoid crystallization at high density. This is also suitable for studying the dynamics over the relevant wave-vector range. The density autocorrelation function $C(\mathbf{x},\mathbf{x}',t,t_o)$ is computed by averaging the product of density fluctuations at time t_o and t_o+t over different runs of the dynamics. This procedure is repeated shifting t_o over a range t_R. After an initial time $t_o \sim t_K$ of the order 10 in units of Enskog time t_E for a hard-sphere system, the correlations of momentum fluctuations reach their equipartition value. For the density correlator $C(\mathbf{x},\mathbf{x}',t,t_o)$, independence of t_o implies abscence of transients while independence of t_R implies ergodicity. It is found that the time required to reach this stage of independence of the density correlator from t_o to t_R is much longer compared to t_K. In a deeply supercooled state the density fluctuations equilibrate over much longer time scales than the momentum fluctuations.

1. Nature of the relaxation

The stochastic equations of nonlinear hydrodynamics were analyzed (Dasgupta and Valls, 1994) mainly over two different density ranges.

The lower density range refers to the packing fraction $0.393 \geqslant \varphi \geqslant 0.487$. Angular averages of q-dependent quantities were obtained by averaging over $\mathbf{q}$ values in the first Brillouin zone. At low densities the normalized correlation function $\phi(q,t)$ fit the stretched exponential form $\exp[-(t/\tau_o(q))^{\beta}]$. The relaxation time $\tau_o(q)$ and stretching exponent β depended on both the packing fraction φ and the wave number q. $\tau_o(q)$ had a maximum at the peak of the structure factor, but the simple form $\tau_o(q) \propto \eta_o S(q)$ was not obeyed, indicating a q-dependent renormalization. The stretching parameter β remained close to 1 and decreased with the increase of density. The time $\tau_o(q)$ corresponding to the vector q at which the decay was slowest was denoted by τ_m and followed a Vogel-Fulcher-type dependence on density, $\tau_m(\rho^*) \sim \exp[B_o/(v-v_c)]$, where the specific volume was defined as $v \sim 1/\varphi$. The value $\varphi_c=0.644$ obtained from the fitting of the data was in good agreement with the corresponding computer simulation result (Woodcock and Angell, 1981) predicting $\varphi_c=0.634$. The Vogel-Fulcher form for τ_m was reported to be a better fit to the numerical results than a three-parameter power-law form. For wave vectors large compared to the first peak position of $S(q)$, even at packing fraction values as low as $\varphi \sim 0.393$, the stretched exponential fit was found unsatisfactory in comparison to a two-step relaxation process,

$$C(q,t) = (1-f)e^{-(t/\tau_1)^{\beta}} + fe^{-t/\tau_2}. \tag{9.3}$$

The stretched exponential is a special case of Eq. (9.3) [for $f=0$ or $\tau_1 \approx \tau_2$ and $\beta \approx 1$].

For higher densities with $\varphi \geqslant 0.470$, two-step relaxation becomes valid over a wider range of wave vectors, extending to values lower than that corresponding to the first peak. The parameter f is weakly dependent on density but has a q dependence that is correlated to that of the static structure factor. The time scales of the two relaxations τ_1 and τ_2 are widely separated at high density. For $\varphi=0.487$ at large wave numbers a quasiergodic behavior is seen, i.e., the time scale is $\tau_2(q) \to \infty$, which in practical terms means that τ_2 is larger than the longest time considered in the computation. This wave-vector dependence also conforms to the usual scenario in which glassy behavior sets in first over short length scales. For all densities and wave vectors the first part of the decay of $C(q,t)$ is better fitted by a stretched exponential form than by the power-law decay predicted by mode-coupling theory. This stretched exponential part of the two-step process was interpreted (Lust *et al.*, 1993) as a mixing of microscopic (phonon) dynamics with the β relaxation. For most wave vectors, the final decay crosses over to the second relaxation process linked to α-relaxation.

On the whole, the similarities in the nature of the relaxation seen from the numerical solutions with the corresponding predictions of mode-coupling theory is rather vague and only very qualitative. The reasons may be linked to the fact that, despite the very basic nature of the simple mode-coupling model, it is a theory that treats the effects of the nonlinearities only up to low order in a perturbation series in an *ad hoc* manner. In the above described numerical solution of the stochastic equations, while the uncontrolled perturbative approach is avoided, one is limited by a finite size and numerical instabilities to high densities.

2. Dynamics in the free-energy landscape

For packing fractions $\varphi \geqslant 0.487$, the above method of computing relaxation time $\tau(q)$ fails. At high density the fluid, instead of equilibrating after a brief transit time t_o, fails to reach a steady state over the time of computation. The time scales involved become too long. Further-

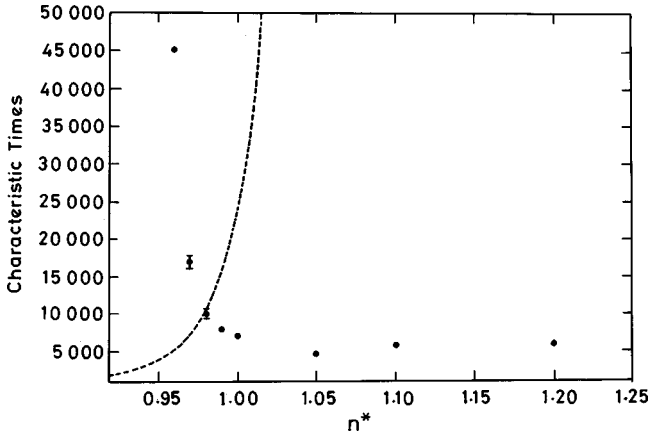

FIG. 10. Characteristic relaxation times τ' (filled circles) and τ (dashed line) vs average fluid density n^*. For definitions of τ' and $\tau \equiv \tau_m$ see the text. The times are expressed in units of t_o of the order of phonon time for the system, and density is expressed in units of σ^3 where σ is the hard-sphere diameter. From Dasgupta and Valls, 1994.

more, the large-scale fluctuations in the system lead to numerical instabilities. The dynamics of the fluid in this density range has been investigated (Dasgupta and Valls, 1994) by computing the corresponding mean-field free energy from the solution of the Langevin equations. The difference between the computed free energy and the corresponding homogeneous liquid-state free energy $\delta F = F[\rho] - F_l[\rho_o]$ is now monitored with time. Starting from an initial configuration, δF is monitored at each time step until after a time τ' (averaged over different independent runs) it becomes negative. For $\varphi \leqslant 0.487$, τ' is very large, decreasing with increase of density and finally becoming independent of density beyond $\varphi \approx 0.523$. This variation of τ' with density is shown in Fig. 10. The corresponding relaxation time τ_m (denoted by τ in the figure) is also shown by a dashed line to be sharply increasing with density. The evolution of the system beyond the time scale of τ' is analyzed by studying its dynamics in the free-energy landscape. This is done by using the final-state configurations obtained from a dynamical simulation (Dasgupta and Valls, 1994) as the input in a minimization routine and then searching for the minimum of the free energy as a functional of the density distribution lying closest in phase space to this initial configuration. Thus the minimization routine acts as a surrogate to fast dynamics in order to determine the final configuration of the system. For starting configurations corresponding to δF positive, the flow is invariably to the liquid-state minimum. With initial configurations from times beyond τ' the corresponding flow is towards a highly inhomogeneous distribution resembling more a crystalline state with defects.

The above study (Dasgupta and Valls, 1994) gives the following picture of the dynamics in the free-energy landscape: For low densities the system fluctuates around the liquid-state minimum. The dynamics are controlled at this stage by the coupling of density fluctuations and the physics of the system at this relatively low supercooling is as described by the mode-coupling theory. The self-diffusion coefficients corresponding to these densities extrapolate to zero at a point $\varphi = \varphi_c$, which is identified with the mode-coupling instability. However, with the increase of density a crossover occurs at $\varphi = \varphi_x$, less than φ_c. The free-energy landscape changes with density. For $\varphi > \varphi_x$ the system easily hops out of the liquidlike minimum and goes to a nearby minimum representing a highly inhomogeneous state. The corresponding time τ' the system spends near the uniform liquid-state minimum is now small. In a hard-sphere system this crossover occurs at $\varphi_x \approx 0.497$ (Dasgupta and Valls, 1994). The free-energy landscape study described above has been extended (Dasgupta and Valls, 1996, 1999) to higher densities, showing activated transitions between the glassy minima. The above scenario finds support in computer simulation results with hard-sphere systems. Molecular-dynamics simulations (Woodcock, 1981) show that such a system cannot be locally equilibrated in the supercooled liquid state if the packing fraction φ exceeds a critical value $\varphi_s = 0.565$. Dasgupta and Valls identify the crossover φ_x (defined above) with this φ_s. Hopping between adjacent minima in the free-energy landscape starts occurring at φ_x, before the system reaches the mode-coupling transition point φ_c, which is between 0.576 and 0.602. Therefore, according to this scenario, the issue of a crossover in the dynamics around φ_c does not arise, since it has already occurred at φ_x, which is generally lower than φ_c.

Finally it should be noted that, in general, the value of the crystallization transition φ_f as well as the crossover density φ_x concluded from the numerical studies of Dasgupta and Valls are somewhat lower than the corresponding values obtained in molecular-dynamics simulations. For example, from density-functional studies, Dasgupta (1992) obtains $\varphi_f = 0.435$, while in molecular-dynamics simulations the fcc crystal formation occurs at $\varphi_f = 0.494$. Similarly from molecular-dynamics simulations (Woodcock and Angell, 1981) it appears that the crossover will occur at $\varphi_x = 0.565$, while the corresponding value in the Langevin simulation is 0.497. It is, however, interesting to note that the ratio φ_x/φ_f in both cases is 1.14. The difference in the actual numbers may be a result of the discretization procedure and the finite-size systems used in the present numerical scheme (Dasgupta and Valls, 2003).

B. Mapping onto a lattice gas model

Going beyond the low-order perturbative approach of the mode-coupling models, the dynamics of the dense fluid were studied by Kawasaki and Fuchizaki (1998) by mapping the problem to a kinetic lattice gas model. Here density was considered as the only relevant variable. A discretized version of the Fokker-Planck equation (4.19) was considered in the form of a mesoscopic kinetic equation (Kawasaki, 1966a). In the lattice description the system was divided into an assembly of primitive cells with lattice constant h. The dynamics

were governed by the following master equation for the probability distribution $P_o[n,t]$:

$$\partial_t P_o[n,t] = \sum_{n'} [w_o(n|n')P_o(n',t) - w_o(n'|n)P_o(n,t)], \tag{9.4}$$

where $n \equiv \{n_i\}$ denotes a set of occupation numbers with $n_i=0$ or 1 depending on whether the ith lattice site is vacant or occupied. The transition probability from $\{n'\}$ to $\{n\}$ is denoted as $w_o(n|n')$ which satisfies the detailed balance condition. The energy of the configuration $\{n\}$ is given by

$$H_o[\{n_i\}] = -\frac{k_B T}{2}\sum_{i\neq j} c(|\mathbf{r}_i - \mathbf{r}_j|)n_i n_j, \tag{9.5}$$

where $\mathbf{r}_i$ denote the position vector of the ith site and $c(r)$ is the two-point direct correlation function.

Equations (9.4) and (9.5) for the kinetic Ising model were solved by the Monte Carlo method to obtain a time sequence of $n(t)$ (Kawasaki and Fuchizaki, 1998). A system of size $\tilde{L}=15$ was chosen consisting of $\tilde{L}^3$ lattice points with lattice constant h taken from the solution of the Percus-Yevick equation, and with the hard-sphere diameter as $\sigma=3.3h$. The incommensurability of σ/h prevented crystallization. The occupation number $n_i(t)$ in the lattice gas formulation was related to the local particle density $\rho(\mathbf{r},t)=\Sigma_\alpha \delta(\mathbf{r}-\mathbf{r}_\alpha)$ in the continuum (for convenience we take the particle mass $m=1$) by the relation

$$\langle n_i \rangle_\tau = \langle \rho(\mathbf{r}_i,t)\rangle_\tau, \tag{9.6}$$

with the time average $\langle\cdots\rangle_\tau$ taken over the typical relaxation time τ. The occupation numbers n_i's in this present context actually refer to entities that are different from a real fluid particle. In coarse-graining the system over a length Λ_o (say) much larger than h, but smaller than σ, the identity of an individual particle is lost. The master equation (9.4) on coarse graining (Fuchizaki and Kawasaki, 1999) reduces to the Fokker-Planck equation (4.19) for a density distribution $\{\rho_\alpha\}$, where the subscript α corresponds to the αth cell in the coarse-grained description.

Since the Percus-Yevick direct correlation function is generally negative, the equations for the dynamics are the same as those corresponding to a spin-one-half Ising Hamiltonian with antiferromagnetic interaction in an external magnetic field. The nonlinear feedback mechanism enters here through the spin-exchange dynamics, unlike single spin-flip Glauber dynamics (Glauber, 1963). This is signified by the terms $\rho(\rho_m-\rho)\cong\rho\rho_m$ in the kinetic equation (9.4). The solution of the master equation (9.4) at the initial stage of the dynamics (Fuchizaki and Kawasaki, 1998a) correctly captures the mode-coupling mechanism due to density fluctuations. For low densities corresponding to $\varphi\leqslant 0.490$ the density correlation function follows the stretched exponential form $\exp[-[t/\tau_1(q)]^{\beta_q}]$. With increasing packing fraction the stretched exponential relaxation first appears at larger wave numbers. This is similar to the observation made in the numerical solution of the Langevin equation. The relaxation time $\tau_1(q)$ for $q\sigma=6.5$ fits well to a power-law form $(\varphi_c-\varphi)^{-\gamma}$ with $\varphi_c\simeq 0.49$ and $\gamma=2.2$. The data can also be fitted with slightly better agreement (Fuchizaki and Kawasaki, 1998b) with the Vogel-Fulcher form with a $\varphi_c=0.61$. This form is similar to the Langevin work described earlier in this section.

We now focus on the results obtained for the late stage of the dynamics dominated by thermally activated transitions between different free-energy minima. For this a reference state is defined in terms of the state vector

$$|n^\alpha(t)\rangle = \sum_{i=1}^{\tilde{L}^3} n_i(t)|e_i\rangle, \tag{9.7}$$

where $n_i(t)$ is the occupation variable equal to 0 or 1 depending on whether the ith lattice site is empty or occupied at time t and $|e_i\rangle = |0\ldots\overset{i}{0}10\ldots0\rangle$ is the ith orthonormal basis (of size $\tilde{L}^3$) in the Fock space. The superscript α refers to a particular initial state. Now an average state vector is defined as

$$|\Psi^\alpha_{\rm ref}\rangle = \frac{1}{\mathcal{N}^\alpha}|\bar{n}^\alpha\rangle \equiv \frac{1}{\mathcal{N}^\alpha}\left|\frac{1}{\tau}\int_{\tilde{t}_o}^{\tilde{t}_o+\tau} dt' n^\alpha(t')\right\rangle, \tag{9.8}$$

where the origin $\tilde{t}_o$ of the observation is chosen to be sufficiently large to ensure equilibration. The duration τ is much longer than the microscopic time scale (phonon characteristic time) but shorter than the time scale of thermally activated jumps. $\mathcal{N}^\alpha$ is the norm of the state $|\bar{n}^\alpha\rangle$ so that $N^{1/2}\geqslant\mathcal{N}^\alpha\geqslant N/(\tilde{L})^{3/2}$, N being the number of particles in the fluid. The first equality holds when the system is completely frozen during the time interval over which the average is taken, while the second one holds when the occupied sites are uniformly distributed. The state of the system at some later time t is denoted by $|\phi^\alpha_t\rangle$ with the averaging process done as defined in Eq. (9.8). In order to study how the system evolves in the free-energy landscape, the time evolution of the overlap function,

$$q(t) = \langle \phi^\alpha_t|\Psi^\alpha_{\rm ref}\rangle, \tag{9.9}$$

is considered. The time scale over which correlation is studied extends from t up to $t+\tau_1$, τ_1 being the time scale for decay of the density fluctuations. The result is shown in Fig. 11 for three different packing fractions, $\varphi=0.312$, 0.440, and 0.491. For $\varphi=0.312$, $q(t)$ is almost time independent (close to unity), since $|\phi^\alpha_t\rangle$ is independent of t and is essentially the same as $|\Psi^\alpha_{\rm ref}\rangle$. This indicates that the system stays around a single global liquid-state minimum. As the system becomes denser, $\varphi=0.440$, beyond the equilibrium crystallization packing fraction of $\varphi=0.430$, the fluctuation amplitude of $q(t)$ increases but the system is still trapped in a single minimum within the time scale of the computation. For a packing fraction beyond $\varphi_x=0.49$ with the initial time scale $\tau_1\sim 1000$

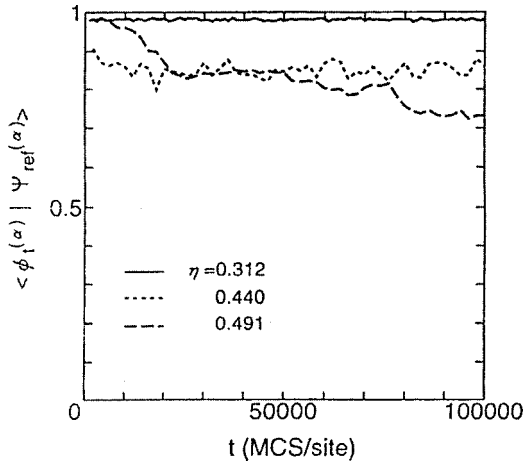

FIG. 11. Time evolution of $q(t)$ vs time t for three different packing fractions: solid line, $\eta \equiv \varphi = 0.312$; short-dashed line, 0.440; and long-dashed line, 0.491. Time is expressed in Monte Carlo steps per site. From Fuchizaki and Kawasaki, 1998b.

Monte Carlo steps (MCS) per site, the function $q(t)$ relaxes at two different levels: first at $t \sim 20\,000$ MCS and then at $t \sim 60\,000$ MCS. This is interpreted as the system's initially being trapped in a local free-energy minimum and eventually relaxing towards states with lower free energies through thermally activated hopping.

In short, both the above methods for studying the dynamics suggest that at low densities a hard-sphere system largely fluctuates around the liquid-state minimum. The relaxation time appears to diverge at very high density. Here, at the initial stage of supercooling, the dynamics are largely controlled by coupling of dominant density fluctuations and are well described in terms of the mode-coupling theory. As the density increases beyond a crossover value φ_x, the dynamics are controlled by thermally activated hopping in the free-energy landscape to configurations with inhomogeneous density distributions.

X. COMPUTER SIMULATION RESULTS

Computer simulation methods (Angell *et al.*, 1981; Allen and Tildesley, 1987; Barrat and Klein, 1991) have been extremely useful for studying the dynamics of supercooled liquids including nonequilibrium phenomena like aging. In traditional molecular-dynamics (MD) simulations, the classical equations of motion for a small number of particles (a few hundreds) are solved in the computer. The maximum time scale over which the particles are simulated in a typical MD simulation is not comparable to the time scales of glassy relaxation seen in real experiments. However, MD simulations easily obtain a variety of correlation functions not accessible to experimental techniques. Real-space correlation functions are as easily computed as their Fourier-transformed counterparts. The motion of a single particle in the fluid and its heterogeneous dynamics over different time scales are easily obtained in simulations (Sanyal and Sood, 1996, 1998; Kob *et al.*, 1997; Donati *et al.*, 1998, 1999). Monte Carlo methods are also used, in which a physical property of the fluid is obtained by generating a possible set of configurations used for ensemble averaging. The particles interacting through a known potential are assigned an arbitrary set of coordinates, which evolves through successive random displacements. Here the particle momenta do not enter in the computation and (unlike MD) no time scale is involved. A problem often faced in computer simulation of liquids in the supercooled state is that they crystallize too easily. Traditionally nucleation is avoided by studying binary mixtures of spherical particles of different diameters (Bernu *et al.*, 1985, 1987). As an alternative approach the dynamics of a monoatomic system (consisting of a small number of particles) has also been studied (Angelani *et al.*, 1998) with a master equation for the model system evolving in the potential-energy landscape. Crystallization is avoided in this approach by simply ignoring the corresponding minima from the landscape. We discuss here the results from simulation of the dense fluids that directly link to mode-coupling theory.

A. Comparison with mode-coupling theory

When earlier simulations of Lennard-Jones systems (Ullo and Yip, 1985) and hard-sphere fluids (Woodcock and Angell, 1981) were compared with the predictions of the wave-vector-dependent extended mode-coupling theory model, they showed reasonable agreement (Das, 1987, 1990). The predictions of mode-coupling theory were tested more extensively with MD simulation of a binary soft-sphere system by Roux *et al.* (1989, 1990). This work confirmed the factorization property and predicted deviations from the Stokes-Einstein relation in the vicinity of the transition. The extrapolated self-diffusion coefficient vanished for both components of the mixture with a power-law exponent roughly equal to 2 (Bernu *et al.*, 1987). Subsequently Kob and Anderson (1994, 1995a, 1995b) investigated a binary Lennard-Jones mixture (BMLJ) extensively, comparing it to various predictions of mode-coupling theory. The mixture consisted of 800 type-A and 200 type-B particles of the same mass m, interacting through the Lennard-Jones potential $u_{\alpha\beta}(r) = 4\epsilon_{\alpha\beta}[(\sigma_{\alpha\beta}/r)^{12} - (\sigma_{\alpha\beta}/r)^{6}]$ with $\alpha, \beta \in \{A, B\}$. The chosen parameters were $\epsilon_{AA} = 1.0, \sigma_{AA} = 1.0, \epsilon_{AB} = 1.5, \sigma_{AB} = 0.8, \epsilon_{BB} = 0.5$, and $\sigma_{BB} = 0.88$. Length was rescaled in units of σ_{AA}, temperature in units of ϵ_{AA}/k_B, and time in units of $(m\sigma_{AA}^2/48\epsilon_{AA})^{1/2}$. The temperature range studied was from $T = 5.0$ to a lowest value $T = 0.466$.

The BMLJ simulation data were analyzed by extrapolating the power-law fit on the self-diffusion coefficient at low temperatures, obtaining $T_c = 0.435$. The theoretical prediction for T_c was obtained by solving nonlinear integral equations similar to Eq. (5.14) for the two-component case. The input static structure factor for the binary mixture was taken from the simulation itself. Using the equations discussed in Sec. V.B.1. as model A, Nauroth and Kob (1997) obtained a transition tempera-

ture $T_c=0.922$. On the other hand, with the equations of model B with the same input structure factors showed that down to the lowest available temperature there was no nonzero solution for the nonergodicity parameter. A diffusion coefficient D_s could be computed with the model presented by Eq. (5.34) for the memory function and using the density correlation functions obtained from model B. This D_s extrapolated to zero at $T_c \approx 0.44$ (Harbola and Das, 2003a), showing better qualitative agreement between theory and simulations.

A generic feature of the tagged-particle correlation, signifying cage formation in a dense fluid, is the plateau it reaches over intermediate times prior to final relaxation. It ranges over almost three decades at $T=0.466$. This plateau has been identified as the value of the nonergodicity parameter and the corresponding time interval treated as the β-relaxation regime (Kob and Anderson, 1994). Over the time range $3 \geqslant t \geqslant 1868$ corresponding to the β-relaxation regime and close to the transition point, the simulation data agree with the factorization property of mode-coupling theory [see Eq. (5.22)]. The critical power-law relaxation (t^{-a}) is not seen in the simulation data. This could be explained by a strong influence of the microscopic dynamics on the early part of the power-law regime. In the later part of the β regime, von-Schweidler relaxation with a positive exponent is visible. Direct fitting of the correlation function data yields an exponent b' (say) that is wave-vector dependent, in contrast to the mode-coupling prediction. This is not surprising, given the fact that q independence is an asymptotic result and the time range over which such a behavior should hold depends on the specific q at which the corresponding correlation function is being considered. Kob and Anderson also computed a wave-vector-independent von-Schweidler exponent b (say) by optimally fitting the data with the β-scaling (q-independent) master curve predicted from mode-coupling theory. The tagged-particle correlation for the A particles close to the transition at the structure factor peak $q=q_{\max}=7.25$ showed the best fit with the master curve, corresponding to the exponent parameter value $\lambda=0.78$. In this way $b=0.51$ was obtained (Kob and Anderson, 1994). Alternatively, the susceptibility χ'' obtained from the frequency transform of the correlation function could be fitted with the master curve, corresponding to $\lambda=0.74$ and $b=0.49$.

Beyond the power-law behavior, on the scale of α relaxation, the correlation function data fit to a stretched exponential form with the stretching exponent β, which is different from the von-Schweidler exponent discussed above. At low temperature the relaxation time in the stretched exponential form $\tau_\alpha(T)$ followed a power-law increase, appearing to diverge (Kob and Anderson, 1995b) at the same temperature T_c at which the diffusion coefficient extrapolated to zero. The exponent of the divergence $\gamma=2.7$ approximately followed the mode-coupling prediction when b was chosen to have the value obtained with respect to β relaxation, i.e., $b=0.51$. An interesting consistency check may be made by plotting the location $\omega_{\min}$ of the minimum of χ'' with the position ω_α of the corresponding α peak. The leading-order analysis of mode-coupling theory (see Sec V.A.2) predicts $\omega_{\min} \sim \omega_\alpha^\mu$ with $\mu=b/(a+b)$. However, the simulation data do not agree with this relation. With $b=0.49$ (obtained above from frequency-transformed data) we expect $\mu=0.64$, while the plot of $\omega_{\min}$ with ω_α from simulation data gives $\mu=0.33$. One possible reason for these findings is that, since the critical decay is overshadowed by the microscopic relaxation, the location of the minimum and hence μ cannot be very accurate.

An interesting difference between the single-particle dynamics and the collective dynamics was found from an analysis of the computer simulation results (Kob and Anderson, 1994). The tagged-particle diffusion coefficient $D_s(T)$ showed a power-law behavior $D_s \sim (T - T_c)^{\gamma'}$. From the best fit, the temperature T_c as well as the exponent γ' were found to be the same for both types of species in the mixture. However, the exponent γ' did not match the exponent found from fitting the diverging behavior of the α-relaxation time scale around T_c. A similar behavior was reported by Schröder *et al.* (2000). This presumably indicates that the mechanism for slowing down of the density fluctuations is not the same as that for the self-diffusion (see also Kob, 2003).

Molecular-dynamics simulation studies of glassy dynamics have been carried out with particles following Newtonian dynamics and Brownian (stochastic) dynamics. Charge-stabilized colloids were studied with Brownian dynamics (Löwen *et al.*, 1991). Similarly binary mixtures of charged stabilized colloids have been studied by computer simulations (Sanyal and Sood, 1995) using Brownian dynamics. Löwen *et al.* (1991) initially concluded that the Newtonian and Brownian simulations led to qualitatively different results, e.g., the density correlation functions did not show any β relaxation in the Brownian case. Subsequently Gleim *et al.* (1998) extended the study of the BMLJ to much longer times and concluded that the long-time dynamics were in fact independent of the choice of the microscopic dynamics. They concluded that the dependence on microscopic dynamics is only in the early β-relaxation regime, whereas α-relaxation dynamics are independent of the microscopic picture. Gleim *et al.* (1998) claim that in the case of Brownian dynamics, over the initial stage the simulation data are in fact in better agreement with the β-relaxation predictions of mode-coupling theory. In the Newtonian case this early β part is strongly influenced by microscopic dynamics as was already indicated above. The mode-coupling theory for the above two cases were shown to be equivalent by Szamel and Lowen (1991).

B. Mode-coupling T_c: Landscape studies

In recent years simulation studies have been used in several innovative ways to obtain further insight into the physics of glassy systems. An important body of work has evolved from the study of the potential-energy sur-

face (PES) in multidimensional configuration space. For a system of N particles the PES is simply the total potential energy plotted in a $(3N+1)$-dimensional space against the $3N$ position coordinates (Goldstein, 1969). The PES is characterized by a large number of local minima, which are termed *inherent structures*. The set of points in the configuration space which correspond, via a steepest-descent trajectory, to the same local minimum on the PES constitute a *basin* associated with the minimum. The concept of basins was further developed by Stillinger and Weber (1982, 1984), and Stillinger (1995), who provided a recipe for apportioning the PES into disjoint basins. As the temperature is lowered, the system gets trapped in a very small number of basins of increasing depth (Jonsson and Anderson, 1988; Sastry *et al.*, 1998). The supercooled state has been widely studied (Bhattacharyya *et al.*, 1999; Kob *et al.*, 2000) by making a gradient descent starting at an initial equilibrium configuration reached through MD simulation of a sample system at a temperature T. This landscape scenario has been used to study thermodynamics of supercooled liquids in a number of works (Buchner and Heuer, 1999; Sciortino *et al.*, 1999; Coluzzi *et al.*, 2000). In an interesting study Schröder *et al.* (2000) looked at the successive configurations produced in a MD simulation of a BMLJ consisting of 251 A particles and 249 B particles. The configurations were mapped into a corresponding time series of local minima (inherent structures). The self-intermediate scattering functions for both the actual structure (representing the true dynamics) and the corresponding inherent structures (representing inherent dynamics) were compared. Beyond a crossover temperature $T_x \approx T_c$, the inherent dynamics were the same as the true dynamics from which the effects of vibrations had been removed. Beyond T_x the dynamics of the system in the configuration space consisted of its fast vibrational motion (intrabasin) in a local minimum and slow diffusive motion among different basins. A convenient method for the description of the dynamics in the configuration space is the study of *instantaneous normal modes* (Madan and Keyes, 1993; Keyes, 1997, 2000). The properties of the local curvature of the PES is studied by diagonalizing the Hessian matrix $\mathcal{H}$ for the potential energy V. The positive eigenvalues are associated with vibrations around the quasiequilibrium position while the negative eigenvalues are related (Sciortino and Tartaglia, 1997; Li and Keyes, 1999; Donati *et al.*, 2000) to the long-time diffusive processes. The number of diffusive eigenvalues decreases with T but does not vanish at a critical temperature identified with T_c. Such negative eigenvalues are also present in the corresponding case of a crystal at finite T (for which diffusivity is negligible). These presumably represent unstable nondiffusive modes in liquids and glasses present at all T (Bembenek and Laird, 1995; Gezelter *et al.*, 1997; Ribeiro and Madden, 1998). Recently trap models (Odagaki and Yoshimori, 2000; Odagaki *et al.*, 2000) have also been studied to understand the landscape dynamics (Denny *et al.*, 2003).

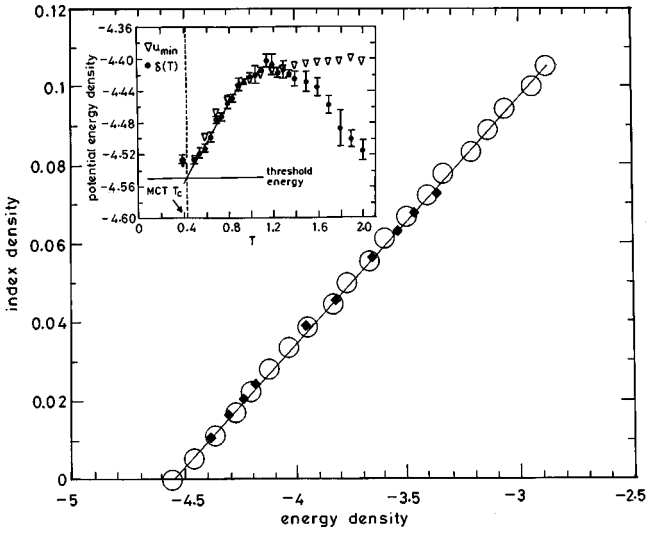

FIG. 12. Index density vs potential energy. Average over all data was obtained by sampling at $T^* \in [0.3, 2.0]$. The solid line is a linear fit meeting the energy axis at $u_{\rm th}$ (see text). Inset shows the average density of the local minima $u_{\rm min}$ as a function of the temperature of the initial MD trajectory. Circles represent δT, the average potential-energy density $\langle U/N \rangle(T)$ less the vibrational energy $3T/2$ in the harmonic approximation. The threshold energy $u_{\rm th} = -4.55$ is reached at $T^* = 0.44 \approx T_c$ (see text).

Our understanding of the dynamics of the representative point of the system on the PES grew clearer as the landscape was studied in terms of local minima as well as the saddles (Angelani *et al.*, 2000; Broderix *et al.*, 2000). The system was equilibrated at a given temperature using standard MD technique and the saddle of the PES $U(\mathbf{x})$ was located by looking for the absolute minima of $W(\mathbf{x}) = \nabla U \cdot \nabla U$. All the extrema were classified in terms of their potential energy u and the number of unstable directions $\mathcal{K}$ (number of negative eigenvalues of the Hessian matrix), called the *index density*. In Fig. 12 the index density $\mathcal{K}(u)$ vs the corresponding energy-density plot is shown. The data are obtained by (a) averaging the energy for all the extrema with a given index density (geometric average), and (b) at a given temperature T, averaging all the energies and the corresponding index densities (parametric average). The curve $\mathcal{K}(u)$ meets the energy axis at a threshold value $u_{\rm th}$, which marks the border between the saddle-dominated part of the PES and the minima-dominated part. Note that $u_{\rm th}$ is above the lowest-lying minima u_o found in the PES, indicating the existence of a finite energy-density interval over which minima predominate overwhelmingly over saddles. With increase of temperature, u_o increases and eventually at a critical temperature $T_{\rm th}$ crosses $u_{\rm th}$. This temperature therefore indicates a crossover from a nonactivated dynamics (above $T_{\rm th}$) to activated dynamics (below $T_{\rm th}$). The evidence from the landscape studies of model systems strongly suggests that $T_{\rm th}$ is close to the T_c of mode-coupling theory. For a BMLJ system at $\rho = 1.2$, a critical temperature $T_{\rm th}$

$=0.435$ was obtained by Angelani *et al.* (2000), and $T_{th}=0.44$ by Broderix *et al.* (2000). Compare this to the transition temperature $T_c=0.435$ obtained by extrapolating the power-law behavior of the diffusion coefficient by a simulation to zero (Kob and Anderson, 1994). The results from another typical fragile liquid, a soft-sphere mixture simulated using Monte Carlo methods, indicate a similar relation: $T_{\rm th}=0.242\pm0.012$ (Grigera *et al.*, 2002). T_c obtained by fitting to mode-coupling data is $T_c=0.226$ (Roux *et al.*, 1989).

The dynamics of the representative point for a simple Lennard-Jones system in configuration space has been studied (Angelani *et al.*, 2001) in a situation dominated by activated processes. At short times the system point visits the basins of saddles whose indexes and energies decrease with time, and at long times the system moves between basins of local minima with decreasing energy by crossing saddles of low order. The sharp increase in viscosity seen in a fragile system within a narrow temperature range T_g is linked with the large potential-energy barriers connecting the local glassy minima that develop near $T_{\rm th}$. Grigera *et al.* (2002) obtained for a soft-sphere system of 70 particles the barrier between lowest minima from the next saddle as $\Delta U(u_{\rm th})\approx 10k_BT_{\rm th}$. The relation of the relaxation dynamics of a BMLJ system to the nature of the PES topography has been studied recently by Doliwa and Heuer (2003). The findings of the landscape studies of the Lennard-Jones system are somewhat analogous to those obtained via studies of the hopping process in the free-energy landscape for hard-sphere systems, described earlier in Sec. IX.A.2. This is going beyond the domain of applicability of the present form of mode-coupling theory.

C. Generalized fluctuation-dissipation relation

The mode-coupling theory reviewed so far in this paper is concerned with fluctuations around the equilibrium state in which Eq. (2.9) between correlation or response functions or the fluctuation-dissipation theorem holds. However, the off-equilibrium dynamics and aging in structural glasses have been studied in recent years quite extensively through MD simulations. Mode-coupling theory for structural glasses in such a nonequilibrium situation has not been developed much. The conjecture of a similarity between structural glasses and spin glasses has been used to understand the findings of the simulation results for the structural glasses. Indeed, such findings further consolidate the underlying similarity between disordered systems with and without intrinsic disorder. For glassy dynamics the fluctuation-dissipation theorem is generalized in a parametric form by defining a quantity $X(t,t')$ (for $t>t'$) as

$$R(t,t')=\frac{X(t,t')}{T}\frac{\partial C(t,t')}{\partial t'}. \tag{10.1}$$

The crucial assertion here is that, taking similarity to the mean field spin-glass models, in the limit of long times $t_w,t\to\infty$, one can express $X(t,t_w)$ as a function of the correlation function $C(t,t_w)$ only, i.e., $X(t,t_w)\equiv x[C(t,t_w)]$. Equation (10.1) is expressed in terms of the integrated response function M, defined as

$$M(t,t_w)=\int_{t_w}^{t} dsR(t,s)=-\frac{1}{k_BT}\int_{C}^{1} x(c)dc, \tag{10.2}$$

where we have used $C(t,t)=1$. It is clear that a plot of $-k_BTM$ vs C will have the slope $-x(C)$. When the fluctuation-dissipation relation holds, $k_BTM(t-t_w)=C(t-t_w)-1$ and hence the slope $x=-1$. A more general form of $x(C)$ indicates violation of the fluctuation-dissipation relation, e.g., the one-step replica symmetry breaking in mean-field spin-glass models (Mézard *et al.*, 1987; Franz *et al.*, 1998) corresponds to a linear dependence on T. In the parametric representation in terms of $x(C)$, violation of the fluctuation-dissipation relation is presented in terms of correlation windows rather than time windows.

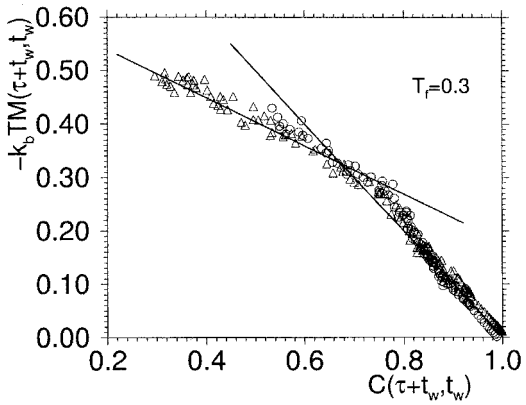

FIG. 13. Parametric plot of the integrated response function $M(t_w+\tau,t_w)$ and the correlation function $C(t_w+\tau,t_w)$ for wave vector $k=7.25$, at the quenched temperature (see text) $T_f=0.3$. ○, $t_w=1000$; △, $t_w=10\,000$. Time and wave vector are expressed in the Lennard-Jones units (see text). The straight lines have slopes −1.0 and −0.45. From Kob and Barrat, 1999.

The MD simulation data for a BMLJ system were studied in a parametric plot of $-k_BTM(t,t_w)$ vs $C(t,t_w)$ over different ranges of C by Kob and Barrat (1997, 1999). Their plot of the integrated response function and correlation function is shown in Fig. 13 for $T_f=0.3$, referring to the temperature to which the system is initially quenched. For short times (C close to 1) the data for different t_w collapse on a single curve of slope −1, showing that the fluctuation-dissipation relation holds. For smaller values of C the slope of this curve (Barrat and Kob, 1999; Kob and Barrat, 2000) is not unity, indicating violation. The corresponding values of the parameter $X\equiv m$ obtained by Kob and Barrat for three temperatures, $T_f=0.4,0.3$, and 0.1, were independent of wave vector and were compatible with a linear dependence of m on T_f. Similar behavior is seen in Monte Carlo simulations (Parisi, 1997) of the dynamics of a BMLJ. The fluctuation-dissipation violation parameter m is expressed as $T/T_{\rm eff}$ so that $T_{\rm eff}$ can be interpreted as the effective temperature associated with various time scales

of the system (Cugliandolo *et al.*, 1997). Over short times the fast degrees of freedom thermalize ($m=1$) and the fluctuation-dissipation relation holds. For longer times corresponding to the slow degrees of freedom $T<T_{\rm eff}$, that is, $m<1$.

Di Leonardo *et al.* (2000) studied the fluctuation-dissipation relation in a one-component Lennard-Jones system of 256 particles (Di Leonardo *et al.*, 2000) modified with a small many-body term in its potential energy to inhibit crystallization. They found that the fluctuation-dissipation violation parameter m was proportional to T at low temperatures, crossing over to $m=1$ at temperatures $T_{\rm eff}$ close to a characteristic temperature T_c'. From equilibrium MD studies it was shown that the potential energy for a liquid crosses over from $T^{5/3}$ behavior (liquidlike) to linear dependence (solidlike) at T_c'. The relation of $T_{\rm eff}$ to T_c or T_g is not very clear. For example, Kob and Barrat (2000) report a value $T_{\rm eff}\approx 0.7$ for the BMLJ ($T_c=0.435$). From a theoretical standpoint, the linear temperature dependence of m below T_g conforms to the predictions in the one-step replica symmetry-breaking scenario proposed for the spin glasses. The validity of the fluctuation-dissipation theorem in supercooled liquids has also been studied via a complimentary approach based on inherent structures in the PES (see Sec. X.B), identifying a new temperature $T_{\rm int}$.[1] In equilibrium $T_{\rm int}=T$, the temperature of the bath. From landscape studies of a typical fragile BMLJ system, it was shown that $T_{\rm int}$ is close to the corresponding $T_{\rm eff}$ (Sciortino and Tartaglia, 2001). Strong liquidlike silica (Scala *et al.*, 2003), however, showed the unexpected result $T_{\rm eff}<T$.

XI. MODE COUPLING AND SPIN-GLASS MODELS

In this section we shall discuss some models that are relevant for the mode-coupling approach to the structural glass problem but that were originally developed to understand other disordered systems. In particular, this refers to theories for disordered systems in which the dynamics are described in terms of correlation of spins and are referred to as spin glasses. The general analogy of a spin glass with a structural glass is rooted in the fact that both represent systems without any long-range order. Both structural and spin glasses differ from their corresponding paramagnetic states primarily in their time-dependent behavior. There are obvious differences as well. In a spin glass the disorder is "quenched," a situation in which the exchange-interaction coupling constants of the spins are random variables and are time independent on all experimental time scales. On the other hand, in the structural glasses the randomness is self-generated. However, a number of works (Bouchaud and Mézard, 1994; Marinari *et al.*, 1994a, 1994b; Chandra *et al.*, 1995, 1996; Cugliandolo *et al.*, 1995, 1996) have also shown the existence of spin-glass-like behavior in systems without any intrinsic disorder. The presence of frustration in such systems is crucial to produce the spin-glass state and not the quenched randomness. Systems with and without quenched disorder have similar behavior as long as a large number of uncorrelated metastable states exist. Another important difference comes from the nature of the transition. The supercooled metastable states are associated with a corresponding crystalline state with long-range order that is the most stable state having the lowest free energy. The existence of an ideal thermodynamic structural glass transition remains speculative. In a spin glass, on the other hand, a second-order phase transition (in zero magnetic field) characterized by diverging relaxation time and nonlinear magnetic susceptibility has been seen in experiments (Binder and Young, 1986; Mydosh, 1993).

There have also been interesting applications of spin-glass-type models (Kühn and Horstmann, 1997; Chamberlin, 1999) to capture the structural glass. It is important to stress that our discussion in the present context will be focused only on the mean-field spin-glass models, which are related to the feedback mechanism of mode-coupling theory and not aimed towards a general review of spin glasses. There exist excellent reviews and monographs on glassy systems with intrinsic disorder (Binder and Young, 1986; Mézard *et al.*, 1987; Fischer and Hertz, 1991; Young, 1997). For more recent work on structural glasses, applying the ideas developed earlier for spin glassses, see Franz and Parisi (1997), Mézard and Parisi (1999), and Coluzzi *et al.* (2000).

A. *p*-spin interaction spin-glass model

The similarties between structural and spin glasses were initially suggested by Kirkpatrick and Thirumalai (1987a, 1987b) on the basis of the p-spin ($p>2$) interaction Hamiltonian. Unlike Ising-type spin glasses, p-spin models lack reflection symmetry, somewhat reminiscent of the structural glasses. The similarity of the equations for the time evolution of the correlation and response functions in the p-spin models and structural glasses are a useful point of departure for a discussion here.

Let us consider the Hamiltonian of the mean-field p-spin spin-glass model in the following soft-spin version,

$$H=-\sum_{i_1<i_2<\cdots<i_p} J_{i_1\cdots i_p}\sigma_{i_1}\cdots\sigma_{i_p}-\sum_{i=1}^{N}[\tilde{H}(\sigma_i)+h_i\sigma_i], \tag{11.1}$$

where $\tilde{H}(\sigma)\equiv\Sigma_i(r_o/2)\sigma_i^2+\tilde{u}\sigma_i^4$ and $\{J_{i_1\cdots i_p}\}$ are independent random interactions whose probability distribution function has zero mean and variance $\overline{(J_{i_1\cdots i_p})^2}$

[1]The free energy of the liquid is obtained here as a sum of configurational and vibrational part, $f(u_{IS})=u_{\rm IS}-T_{\rm int}s_{\rm conf}+f_{\rm vib}(u_{\rm IS},T)$, where $u_{\rm IS}$ is the energy of the local minima corresponding to a basin of attraction in the PES, $s_{\rm conf}$ counts the number of minima with energy $u_{\rm IS}$, and $f_{\rm vib}$ is the average free energy of a basin of depth $u_{\rm IS}$. T denotes the temperature of the bath (attained by the fast degrees of freedom) and $T_{\rm int}$ is the Lagrange multiplier used to extremize f.

$=p!/2N^{p-1}$. The length of the soft spin σ_i is allowed to vary continuously from $-\infty$ to $+\infty$, and h_i is the external field. The constraint $\sigma_i^2=1$ corresponds to taking the coupling constants $\tilde{u}\to\infty$ and $r_o\to\infty$ with $\tilde{u}/r_o\to$const. The dynamics for $\sigma_i(t)$ are assumed to be given by the Langevin equation

$$\Gamma_o^{-1}\partial_t\sigma_i(t) = -\frac{\delta H}{\delta\sigma_i(t)} + \xi_i(t), \tag{11.2}$$

where Γ_o is a bare kinetic coefficient that sets the scale of the microscopic time and is related to the variance of the Gaussian random noise ξ as

$$\langle\xi_i(t)\xi_j(t')\rangle = 2\Gamma_o^{-1}\delta_{ij}\delta(t-t'). \tag{11.3}$$

The time correlation of the spins averaged over the quenched random interactions is calculated using the Martin-Siggia-Rose field theory outlined in the Appendix. The averaging can be suitably done since the Hamiltonian is linear in the random bond $J_{i_1\cdots i_p}$, which has a Gaussian distribution (de Dominicis, 1978; Ma and Rudnick, 1978; Kirkpatrick and Thirumalai, 1987b). Using the standard Martin-Siggia-Rose field-theoretic method and evaluating the integrations in the limit $N\to\infty$ through saddle-point methods yields the following equation of motion for the spin $\sigma_i(t)$ averaged over the quenched random interactions

$$\Gamma_o^{-1}\partial_t\sigma_i(t) + r_o\sigma_i + 4u\sigma_i^3(t) + \int_o^t \Sigma(t,\bar{t})\sigma_i(\bar{t})d\bar{t} = f_i(t) \tag{11.4}$$

with the renormalized noise f_i in the new Langevin equation being correlated as

$$\langle f_i(t)f_j(t')\rangle = \delta_{ij}\Xi(t-t'). \tag{11.5}$$

The kernels $\Sigma(t-t')$ and $\Xi(t-t')$ are obtained (Kirkpatrick and Thirumalai, 1987a) as

$$\begin{aligned}\Sigma(t-t') &= \mu(p-1)R(t-t')C^{p-2}(t-t'),\\ \Xi(t-t') &= 2\Gamma_o^{-1}\delta(t-t') + \mu C^{p-1}(t-t').\end{aligned} \tag{11.6}$$

The linear-response function R and the correlation function C are defined as

$$\begin{aligned}C(t,t') &= \frac{1}{N}\sum_{i=1}^{N}\langle\overline{\sigma_i(t)\sigma_i(t')}\rangle,\\ R(t,t') &= \frac{1}{N}\sum_{i=1}^{N}\left\langle\frac{\delta\bar{\sigma}_i(t)}{\delta\xi_i(t')}\right\rangle = \frac{1}{N}\sum_{i=1}^{N}\langle\overline{\sigma_i(t)i\hat{\sigma}_i(t')}\rangle,\end{aligned} \tag{11.7}$$

with the overbar indicating the average over the quenched randomness. The angular brackets in the expression above stand for the average over the noise ξ. For the equilibrium state, time translational invariance holds and the correlation function C is related to the response function R through the fluctuation-dissipation theorem (2.9). With $p=2$ this model would correspond to the equations obtained by Sompolinsky and Zippelius (1981, 1982).

The normalized correlation function $\phi(t)=C(t)/C(t=0)$ satisfies the dynamical equation

$$\bar{\nu}_o\dot{\phi}(t) + \phi(t) + \lambda_p\int_0^t ds\,\phi^{p-1}(t-s)\dot{\phi}(s) = 0, \tag{11.8}$$

where $\bar{\nu}_o=(\bar{r}_o\Gamma_o)^{-1}$ and $\lambda_p=\mu\bar{r}_o^{2-p}$, with the equal-time correlation being given by $C(t=0)=\bar{r}_o^{-1}$. For $p=3$ these equations are identical to the mode-coupling equations (apart from an inertial term involving second derivatives in time) of the structural glass problem [see Eq. (5.4)] corresponding to the Leutheusser model. This model shows a dynamic transition at a low enough temperature $T=T_c$, with the normalized density correlation $\phi(t)$ varying as $\phi(t)=(p-2)/(p-1)+At^{-a}$. The power-law exponent a satisfies (for $p>2$) the equation $\Gamma^2(1-a)=2\Gamma(1-2a)$ with the solution $a=0.395$ [see also the related discussion with Eq. (5.9)]. The renormalized kinetic coefficient is

$$\nu_R(\omega) = \nu_o + \lambda_p\int_o^\infty dt e^{i\omega t}\phi^{p-1}(t). \tag{11.9}$$

The zero-frequency limit of the transport coefficient satisfies $\nu_R(T\to T_c)\sim(T-T_c)^{-\gamma}$ with $\gamma=1.765$, similar to the behavior of viscosity in the structural glass case. This procedure (Kirkpatrick and Thirumalai, 1981a, 1987b) demonstrated that the self-consistent equations of mode-coupling theory can be obtained for mean-field spin-glass models with quenched disorder. A dynamic transition is predicted before the replica symmetry-breaking transition occurs (Mézard *et al.*, 1987). Subsequently Cugliandolo and Kurchan (1993) studied the related nonequilibrium problem and aging for a spherical p-spin model.

The above results can be generalized for a disordered spin system with the Hamiltonian

$$H_J = -\sum_{i_1<i_2<\cdots<i_p} J_{i_1\cdots i_p}\sigma_{i_1}\cdots\sigma_{i_p} \tag{11.10}$$

supplemented by a constraint that ensures the model is well behaved for all possible values of the random variable $J_{i_1\cdots i_p}$. This regularization, which was used in the soft-spin version [Eq. (11.1)] discussed above includes the function $\tilde{H}(\sigma)$ with a σ^4 term. Another choice for regularization would be to prevent σ_i from diverging in an unstable direction of the random coupling $J_{i_1\cdots i_p}$ by imposing the constraint

$$\frac{1}{N}\sum_{i=1}^{N}\sigma_i^2(t) = 1, \tag{11.11}$$

which also makes $C(t,t)=1$. Absence of the extra constraint (Bouchaud *et al.*, 1996, 1997) in some cases leads to spurious instabilities in the model at low temperatures. For the p-spin Hamiltonian this constraint gives rise to what is called the *spherical p-spin model* (Crisanti

and Sommers, 1992; Crisanti *et al.*, 1993), very widely investigated in recent times.

Kirkpatrick and Thirumalai (1987a) argued from the consideration of the statics of the p-spin models that at a temperature $T_s < T_d$ there is a thermodynamic transition. The static transition was identified with the one-step replica symmetry-breaking transition. In a recent letter Moore and Drossel (2002) have argued that the static transition at T_s does not survive in the finite-dimensional p-spin models. This observation gives rise to an important speculation. If the connection between the structural glasses and spin glasses is valid beyond the mean-field limit, this would indicate that there can be no genuine transition in structural glasses either.

B. Nonequilibrium dynamics: Spherical model

For a system out of equilibrium, the dynamic correlation $C(t,t_w)$ between fluctuations at two times depends on both times. The waiting-time (t_w) dependence of the correlation functions is generally termed the "aging" effect. Experimentally such nonequilibrium effects have been observed in spin glasses (Lundgren *et al.*, 1983; Norblad *et al.*, 1986; Vincent *et al.*, 1992) and also in structural glasses, e.g., polymeric systems showing strong slowing down as the waiting time after the quench is increased (Struik, 1978). Through MD simulations the phenomenon of aging has been studied in a number of works, as already discussed. In the present section we consider from a theoretical standpoint the out-of-equilibrium dynamics of the spherical p-spin model.

The time evolution of the p-spin spherical model is given by the dissipative Langevin equation

$$\frac{\partial \sigma_i(t)}{\partial t} = z(t)\sigma_i(t) - \frac{\delta H}{\delta \sigma_i(t)} + \xi_i(t), \tag{11.12}$$

where time has been rescaled with the bare transport coefficient. The term $z(t)$ in Eq. (11.12) follows from the regular (nonrandom) part of the Hamiltonian. Constructing the standard Martin-Siggia-Rose field theory outlined in Appendix A.1 we obtain the following equations of motion:

$$\frac{\partial R(t,t')}{\partial t} = -z(t)R(t,t')\delta(t-t') + \int_{t'}^{t} dt''\Sigma(t,t'')R(t'',t'),$$

$$\frac{\partial C(t,t')}{\partial t} = -z(t)C(t,t')\int_0^{t'} dt''\Xi(t,t'')R(t'',t') + \int_0^{t} dt''\Sigma(t,t'')C(t'',t'), \tag{11.13}$$

where the response function $R(t,t')$ and the correlation functions $C(t,t')$ are defined above in Eq. (11.7). For definiteness we shall take $t > t'$. The time-ordered property of the response function, that is, the fact that $R(t_1,t_2)$ is zero for $t_1 < t_2$ (due to causality), was used in obtaining Eqs. (11.13). For the p-spin Hamiltonian, the kernels Σ and Ξ are

$$\Sigma(t_1,t_2) = \mu(p-1)R(t_1,t_2)C^{p-2}(t_1,t_2),$$
$$\Xi(t_1,t_2) = 2\delta(t_1-t_2) + \mu C^{p-1}(t_1,t_2), \tag{11.14}$$

obtained by generalizing the result (11.6) for the soft-spin case without time translational invariance. The nonequilibrium dynamics for all times t and t' are thus given by the above first-order integro-differential equations, which admit unique solutions for finite times. At equal times the conditions maintained are $C(t,t)=1$, $R(t,t^-)=1$, and $\partial_t C(t,t^\pm) = \pm 1$. Similar equations for the nonequilibrium dynamics of a heteropolymer were subsequently studied by Pitard and Shakhnovich (2001).

The dynamics at low temperature can be broadly divided into two regimes (Cugliandolo and Kurchan, 1993) depending on the times t and t':

(i) The fluctuation-dissipation regime, for t,t' large such that $\tau/t \to 0$ where $\tau = t - t'$. Here the dynamics follows time translational invariance. In this regime the fluctuation-dissipation relation holds and the two equations (11.13) reduce to a single equation,

$$\left[\frac{d}{dt} + 1\right] C(\tau) + (\mu + p\beta\mathcal{E}_\infty)[1 - C(\tau)] + \mu\int_o^\tau d\bar{\tau} C^{p-1}(\tau - \bar{\tau})\frac{dC(\bar{\tau})}{d\bar{\tau}} = 0, \tag{11.15}$$

where $\mathcal{E}_\infty \equiv \mathcal{E}(t \to \infty)$. The transition temperature T_d is obtained by looking for a nonzero solution for the nonergodicity parameter q from

$$1 - p\beta\mathcal{E}_\infty + \mu(1 - q^{p-1}) = -\frac{1}{1-q} \tag{11.16}$$

(q is similar to the corresponding quantity f defined earlier in Sec. V.A.1 for the structural glass), where $q = \lim_{\tau\to\infty} C(\tau)$. The condition for the dynamic transition reduces to $(\beta_d^2/2)p(p-1)(1-q)^2 q^{p-2} = 1$ where $\beta_d = 1/T_d$.

(ii) The aging regime, for t and t' both going to infinity in a way such that $(t-t')/t' \sim O(1)$. Here t and t' are very widely separated, so that the time derivatives on the left-hand sides of both Eqs. (11.13) can be ignored. The following scaling ansatz for correlation and response functions are used:

$$C(t,t') = C\left[\frac{h(t)}{h(t')}\right], \quad R(t,t') = \frac{h'(t)}{h(t')}\mathcal{R}\left[\frac{h(t)}{h(t')}\right], \tag{11.17}$$

where $h(t)$ is a monotonically ascending function of time t and $h'(t)$ is the derivative with respect to time. The theory at this stage does not specify the function $h(t)$. A likely possibility is $h(t) \equiv t$ (Bouchaud and Dean, 1995). The power law $h(t) \equiv t^\gamma$, where γ is a constant, will correspond to the scaling behavior $C(t_w+\tau, t_w) \equiv \mathcal{C}(\tau/t_w)$ and is

termed *simple* aging. A numerical solution (Kim and Latz, 2001) of the p-spin equations (11.13) show this behavior in the asymptotic regime. A more general form $h(t)=\exp[t^{1-\kappa}/(1-\kappa)]$ has been used to fit experimental data on real spin-glass systems (Vincent *et al.*, 1997). The limit $\kappa=0$ corresponds to the absence of aging (time translational invariance holds), while $\kappa=1$ implies simple aging. The range $0<\kappa<1$ corresponds to what is termed sub-aging.

Numerical solutions of Eq. (11.13) for the quench to the final temperature $T=0.61$ below the dynamic transition point of $T_d=0.612$ show good agreement with the choice of the function $h(t)$, corresponding to $\kappa=0.82$ (Kim and Latz, 2001). The correlation function in the aging regime has the solution $C(\lambda)=\lambda^a$. The fluctuation-dissipation relation between correlation and response functions holds here in the modified form, $\mathcal{R}(\lambda)=x\mathcal{C}'(\lambda)$, which has the same form discussed in Eq. (10.1) for a constant fluctuation-dissipation violation parameter $X\equiv x$. Here $x=(p-2)(1-q)/q$ (Cugliandolo and Kurchan, 1993) for $q\neq 0$ below the dynamic transition point. In order to compute x for a given p one is required to solve for q from Eq. (11.16).

The dynamics of the system above and below T_d are qualitatively different from each other:

(a) For $T>T_d$, $\mathcal{E}_\infty+\beta/2=0$, and the nonergodicity parameter $q=0$. Equation (11.15) for the correlation function $C(\tau)$ becomes identical to Eq. (5.4) for a supercooled liquid, apart from the inertial term involving a second derivative. This is also the same as Eq. (11.8) for the soft p-spin model. In the high-temperature phase $x=1$, i.e., the fluctuation-dissipation relation is obeyed.

(b) For $T<T_d$, the nonzero value $q=q^*=(p-2)/(p-1)$ marks the location of the dynamic transition point at temperature $T_d=[p(p-2)^{p-2}/\{2(p-1)^{p-1}\}]^{1/2}$. For example, with $p=3$, $T_d\approx 0.612$ and $q^*=1/2$. For $q<q^*$ the fluctuation-disspation equation violation parameter $x<1$ and $(\mathcal{E}_\infty+\beta/2)>0$. Therefore, for $T<T_d$, the second term on the left-hand side of Eq. (11.15) with the factor $(\mu+p\beta\mathcal{E}_\infty)$ is present. This additional term in the spherical p-spin model makes the dynamics for $T<T_d$, even in the fluctuation-dissipation regime, somewhat different from the mode-coupling model of supercooled liquids. As a direct consequence near the transition point in the nonergodic phase the nonergodicity parameter shows a linear behavior (Kim and Latz, 2001) instead of the typical square-root cusp [see Eq. (5.10)] for a supercooled liquid. Note that for $T>T_d$ this extra term is absent.

The behavior of the correlation function $C(t,t_w)$ in the low-temperature phase $T<T_d$ is divided into the two broad regimes indicated above. First, there is the fluctuation-dissipation regime for waiting times $t_w\to\infty$ and $t-t_w=\tau\to\infty$, with τ still small compared to t_w. Here time translational invariance is valid and the correlation function is related to the response function through the fluctuation-dissipation relation. $C(\tau)=q+A\tau^{-a}$ with the exponent satisfying $\Gamma^2(1-a)/\Gamma(1-2a)=x/2$, where x is the fluctuation dissipation violation parameter $X\equiv x$ defined by Eq. (10.1). This transcendental equation for the exponent a is specific for temperatures below T_d. Above T_d the corresponding equation (with $x=1$) is the same as that in the Leutheusser model or the soft p-spin model. Next, we reach the aging regime, in which the correlation function has a final relaxation as long as the t_w is finite, i.e., $\lim_{\tau\to\infty}C(\tau+t_w,t_w)=0$, $\forall$ finite t_w. Below T_d the system of course remains perpetually out of equilibrium, and therefore for any finite waiting time t_w there exists a sufficiently large τ such that $C(\tau+t_w,t_w)$ tends to zero. This is termed *weak ergodicity breaking*.

Theoretical developments on the nonequilibrium dynamics of structural glasses using the mode-coupling approach are in the early stages. Preliminary steps include the study of the field-theoretic model without quenched disorder and with cubic nonlinearity (Franz and Hertz, 1995) and ideas for generalizing the dynamic density-functional model along lines similar to those for multicomponent fields (Kawasaki and Miyazima, 1997). More recently Latz (2000) has proposed a generalization of the projection operator method to construct an equation for the density correlation function in the nonequilibrium situation.

C. Generalization: Systems with intrinsic disorder

The parallels between mean-field dynamics with quenched impurities and the self-consistent mode-coupling model for a supercooled liquid can in fact be carried further (Bouchaud *et al.*, 1996; Cugliandolo, 2003). A similar analogy was pointed out earlier in reference to the direct interaction approximation (Kraichnan and Chen, 1989) in fluid turbulence (Kraichnan, 1961b; McComb, 1990) through a generalization of the Navier-Stokes equation containing quenched disorder. The equivalence of models with quenched impurities and without, in Navier-Stokes turbulence, was studied in the limit of large M, the number of components of the hydrodynamic field (Eyink, 1994; Bhattacharjee, 1996). Consider a generalized form of the Hamiltonian (11.10) with the intrinsic randomness

$$H_J^R[\sigma_i]=g\sum_{p\geq 2}^{\infty}V_p\sum_{i_1<\cdots<i_p}J_{i_1\cdots i_p}\sigma_{i_1}\cdots\sigma_{i_p} \tag{11.18}$$

with g and the V_p's being suitable coupling constants specific to the system. The interaction strengths $J_{i_1\cdots i_p}$, which are also symmetric with respect to change of indices, follow a Gaussian probability distribution of zero mean and variance $N^{-(p-1)}$. The crucial requirement of this equivalence, as indicated above, is that the H_J^R be linear in the $J_{i_1\cdots i_p}$'s. The dynamics of the spins follow the generalized Langevin equation (11.12). The formally exact set of equations (11.13) (in the large-N limit with t

finite) is obtained in the present context with the self-energies in Eq. (11.14) now generalized to

$$\Sigma(t,t') = F''[C(t,t')]R(t,t'),$$
$$\Xi(t,t') = 2\beta^{-1}\delta(t-t') + \mathcal{F}'[C(t,t')], \tag{11.19}$$

where the functional $\mathcal{F}$ of the correlation function C corresponding to the Hamiltonian H_J^R is $\mathcal{F}[C] = g^2\Sigma_{p=2}^{\infty}[V_p^2 C^p/p!]$. The correlation function C and the response function R are defined here in the same way as in Eq. (11.7). With respect to the structural glasses, this is similar to the model discussed with the generalized functional (5.3).

Finally the dynamics of a particle evolving in an N-dimensional space in a quenched random potential $U_R[\{\sigma\}]$ (the σ_i's now being treated as the coordinates of the particle in the large N-dimensional space) also follow equations similar to those of mode-coupling theory (Franz and Mézard, 1994a, 1994b; Cugliandolo and Le Doussal, 1996). This potential U_R is linked to the disordered multispin Hamiltonian (11.18) such that $U_R[\sigma] \equiv H_J^R[\sigma]$ with a zero mean and a variance

$$\overline{U_R[\{\sigma\}]U_R[\{\sigma'\}]} = N\mathcal{F}[Q_{\sigma\sigma'}], \tag{11.20}$$

where the overbar stands for the average over the quenched disorder and $Q_{\sigma\sigma'} = N^{-1}\Sigma_i\,\sigma_i\sigma_i'$. The explicit numerical integration of the model equations, similar to the model equations of the p-spin model, also support the asymptotic solutions sketched above. Another interesting result in this regard is that the dynamics of the spherical version of the ϕ^3 model (Amit and Roginsky, 1979) without quenched disorder are similar to those of the p-spin model for the case $p=3$ (Franz and Hertz, 1995).

D. Comparison with the structural glass problem

In spite of a similar mathematical structure of mode-coupling theory for structural and spin glasses, the nature of the nonlinearites in the fluctuating equations giving rise to these models is quite different. In the case of fluids the driving nonlinearities are generated from a trivial (Gaussian) Hamiltonian and are essentially of dynamic origin. This is a consequence of the special Poisson bracket structure of the relevant hydrodynamic variables contributing to the reversible part of the equations of motion (Das *et al.*, 1985a). In the p-spin models, however, the relevant nonlinearities come from the non-Gaussian part of the driving Hamiltonian and correspond to dissipative terms in the equation of motion. This difference has been further studied in a recent set of papers by Kawasaki and Kim (2001, 2002) through consideration of a toy model for an N-component fluid consisting of N density variables and M momentum variables. This model, with built-in quenched disorder, is closer to an earlier description of fluids due to Kraichnan (1959a). However, unlike p-spin models, the nonlinearities in the equations of motion here belong to the reversible part of the dynamics. Even in the limit $N \to \infty$ no sharp transition is seen in the toy model. There is thus a fundamental difference between the two kinds of systems with and without reversible mode coupling (Kim and Kawasaki, 2002). The ideal glass transition is only recovered in this model when the number N of density variables is chosen to be different from the number of momentum components (M) (with $N>M$).

Notwithstanding these differences, the analogy of (a) the p-spin interaction spin-glass model equations with the mode-coupling equations for structural glasses, and (b) the off-equilibrium solutions of the spherical model with MD simulation data on aging, strongly indicate a dynamic similarity between the two types of systems with and without intrinsic disorder. The existence of the dynamic transition at T_d in the disordered multispin models is in general associated with the appearance of many metastable minima and breaking of ergodicity at this temperature. This has also been confirmed through computer simulations (Thirumalai *et al.*, 1989). Due to the existence of an exponentially large number of metastable states, the system gets trapped for infinitely long times, preventing it from reaching the true equilibrium state. It is worth noting here that the dynamic transition predicted for the p-spin models is removed in finite dimensions due to nucleation processes or activation over finite free-energy barriers (Kirkpatrick and Thirumalai, 1989; Parisi *et al.*, 1999; Drossel *et al.*, 2000). This is similar to what happens in the mode-coupling theory of structural glasses where finally ergodicity is maintained and no dynamic transition occurs.

Landscape studies of prototype fragile liquids have further strengthened the analogy between structural glasses and the p-spin model. A number of observations have been made in different studies. For example, a finite energy-density interval where local minima dominate overwhelmingly over saddles occurs in mean-field models (Cavagna *et al.*, 1998) as in the case of simple atomic systems (described in Sec. X.B). Moreover, the number of negative eigenvalues of the Hessian is not zero at the dynamic transition point in the p-spin models (Biroli, 1999), analogous to the instantaneous normal-mode studies of structural glasses (see Sec. X.B). Finally, the equivalence of temperatures $T_{\rm int}$ and $T_{\rm eff}$, respectively, defined from landscape descriptions and the extension of fluctuation-dissipation studies (see Sec. X.C) is supported by analytical predictions (Franz and Virasoro, 2000) for the p-spin models. The above described analogies between the different types of glassy systems are somewhat reminiscent of the idea of universality classes indicating similar asymptotic behavior of widely different systems near the critical point. In the renormalization-group approach to critical phenomena this universality is naturally explained from the nature of the fixed points in the coupling constant space of the corresponding Hamiltonian. Similarities in the landscape properties of different disordered systems is significant in this respect. However, one has to be careful in drawing an analogy with the concept of universality

classes in the context of critical phenomena. Unlike critical phenomena, the exponents in mode-coupling theory are not universal.

XII. CONCLUSIONS AND OUTLOOK

We have reviewed here the various approaches, techniques, and approximations in the theory of strongly interacting liquids. These developments started with the discovery of a dynamic feedback mechanism following a self-consistent treatment of the mode-coupling approach already known in the literature. The model was formulated starting from equations of generalized hydrodynamics. In the most basic form, mode-coupling theory predicts a two-step-relaxation scenario: first, power-law decay on the time scale below τ_β, crossing over to von-Schweidler decay with a positive exponent below the time scale τ_α. Second, for times beyond τ_α, the α relaxation is described by a master function which resembles a stretched exponential with temperature-independent exponent. Both time scales τ_β and τ_α appear to diverge as a power of the temperature, as the ideal glass transition is approached from the liquid side. In the nonergodic phase, the long-time limit of the density correlation function is nonzero. Going beyond the simplest approximation, the sharp dynamic transition of the simple theory is not found and ergodic behavior is maintained over the longest time scales.

The appeal of the basic mode-coupling theory has generated strong interest. It is, however, worth noting here that the model and the cited evidence in its support so far from experiments or simulations, are not without weaknesses. In most cases, especially for systems like CKN or OTP, the crucial inputs of the mode-coupling model are treated as free fit parameters. The typical adjustable quantities used are the time scale of transients t_o, the nonergodicity parameter f, the amplitude h, the transition point T_c, the prefactor of the α-relaxation time scale C, and the exponent parameter λ—there can be as many as six such adjustable parameters. In the extended mode-coupling theory with the ergodicity-restoring processes, there is one more adjustable parameter δ, controlling the final time scales of relaxation. Most of the tested relaxation behaviors are predictions from the theory at the leading order, in the close vicinity of the transition. Often this requires careful adjustment of the time range or temperature range in order to be able to observe the predicted effect. Thus, for example, the predicted factorization property (see Sec. V.A.2) is valid only close to the transition and during the time window of the power-law relaxation. It is not valid over the longer time of α relaxation. Similarly, the predicted temperature independence of the stretching exponent β (and hence time/temperature superposition) is only expected to hold when the liquid is neither too close to T_c (so that the ergodicity-restoring mechanisms do not intervene) nor too far from the transition (in which case the leading-order behavior would not hold). Additional correction terms to the leading-order results for both β scaling and α scaling become important (Hinze *et al.*, 2000) as the distance from the transition increases. To decide on their quantitative implications, one has to evaluate a set of correction amplitudes analogous to the exponent parameter λ for the leading-order results (see Sec. IX.B). However, this will require knowledge of the mode-coupling functionals for the corresponding system. Such a calculation has not yet been undertaken for a complicated glass-forming system. Indeed, in view of the importance of the correction terms, it sometimes seems as if the strong agreement of the experimental data with the leading-order results is better than what one would expect. Furthermore, it is not even clear that the cutoff mechanism is weak enough that the system can get really close to the ideal transition, which is finally smoothed off.

On the issue of locating the transition point, mode-coupling theory is often compared with the theory of critical phenomena. But in contrast to the case of critical phenomena the divergence is not real in mode-coupling theory and hence its identification is more difficult. The critical exponents are completely system dependent and cannot be classified into universality classes. In fact, experiment has never really shown a direct signature of T_c. Only after fitting to some model predictions could people say that it was there. So there is at least a substantial blurring or rounding of the transition, which masks it. Assuming this, fitting the experimental data with scaling assumptions is usually possible, within some error around the rounded "singularity." Taking even the most stringent point of view, the experimental data are not inconsistent with the existence of scaling in a limited range. The fitting procedure which seeks consistency between the two steps of relaxation also identifies, indirectly, the location of a dynamic transition point. On the other hand, using the static structure factor of the liquid as an input, one can solve the corresponding mode-coupling equations to obtain the location of the dynamic transition point. This is a first-principles calculation without any adjustable parameter. However, the transition density thus obtained from the mode-coupling theory for a simple hard-sphere system does not seem to agree well with the corresponding control parameter value, at which a possible structural arrest is interpreted in the simulations or experiments. This is presumably linked with the low-order perturbative nature of the mode-coupling theory, in which the one-loop model is used to obtain the renormalized transport coefficient.

In spite of its limitations, mode-coupling theory is the only microscopic theory for supercooled liquids in the initial stages of viscous slowdown. With the development of better experimental tools and faster computers, it has now become possible to probe the liquid-state dynamics over a wide range of time scales, ranging up to 18 decades (see Sec. VII). This has revealed a rich set of hitherto unknown dynamics features of the supercooled state. It is here that a microscopic theory like mode coupling has provided clues to understanding the experimental (laboratory or computer) observations. The main achievement of mode-coupling theory has been to iden-

tify from a microscopic approach the existence of a crossover temperature T_c in the supercooled liquid that is greater than the calorimetric glass transition temperature T_g. T_c signifies a dynamic transition in the liquid, and in its close vicinity interesting scaling behavior has been seen over varying length and time scales. For the supercooled liquids, mode-coupling theory now plays the same role as van der Waals theory did for the theories of the phase transition at the mean-field level (Kawasaki and Miyazima, 1997).

The theory, at least in its present form, is not suitable for understanding the laboratory glass transition associated with the rise of viscosity by 14 orders of magnitude (equivalent to time scales of the order of 10^2 or so). In fact, different workers in the field have varying opinions even on the relevance of this issue. One point of view is, we quote, "if there is anything like a liquid-to-glass transition it should show up in the anomaly of the structural relaxation spectra in the mesoscopic frequency range specified by time scales between, say, 10^{-7} s and 10^2 s" (Götze, 1991). Others have a different point of view, e.g., we quote, "Some of us are not convinced that focusing on the initial stages of viscous slowdown will eventually lead to an adequate description of the laboratory glass transition" (Ediger, Angell, and Nagel, 1996). More sobering is the fact that, while the actual perturbation expansion is systematic, it is in terms of a dimensionless parameter that is not small. Therefore, although the theoretical predictions here are qualitatively correct, they are not quantitatively accurate and cannot be considered definitive. For example, it is tempting to speculate that the universal scaling predicted by Nagel and co-workers, especially over the higher-frequency range, should follow from a microscopic theory like mode-coupling theory for the dense liquids in a natural way.

In mode-coupling theory, the dynamics of the liquid are considered in a stationary state below its freezing point, and it is simply assumed that crystallization does not occur. A complete theory of the glass transition should include in the theoretical analysis the competition of the supercooled liquid state with the crystalline state. This will involve treating the nonequilibrium problem of finite quench from a stable liquid state to a supercooled glassy state and studying the time evolution of a quenched liquid. The kinetics of the fluid near the crystallization transition of course is an old problem. The growth of a nucleus to macroscopic size in the bulk of a liquid was studied theoretically at the phenomenological level by Turnbull and Fischer (1949). Subsequently the problem was studied with a field theory of nucleation (Langer, 1967, 1969; see also Grant and Gunton, 1985 and Langer, 1992). More recently the problem was addressed using Langevin dynamics (Bagchi, 1987b; Oxtoby, 1991) and dynamic density-functional theory (Marconi and Tarazona, 1999, 2000). However, the competition of crystallization with formation of the glassy state has not been studied from such a microscopic approach. A unified description of the amorphous and crystalline state is justified from the existing conservation laws, which hold irrespective of the nature of the thermodynamic phase. In this regard it is interesting to note that the revised Enskog theory for a fluid, generally applicable to the disordered fluid state of a dense hard-sphere system, can also describe the ordered crystalline state (Kirkpatrick *et al.*, 1990). The revised Enskog theory reduces to an exact density-functional description of the solid state. The inhomogeneous density profile in the ordered state can be as good a solution to the kinetic equations as the uniform liquid state. A deterministic version of the equation for density fluctuations in a liquid can also be obtained from the nonlinear revised Enskog equation [Résibois, 1978a, 1978b; Munakata, 1978; see also Eq. (A25)]. Stationary solutions of this equation are specified by densities that must satisfy $\nabla\{\delta F[\rho]/\delta\rho(\mathbf{x})\}=0$. Assuming that fluctuating forces do not change this result, the gradient of the generalized pressure in the Langevin equation must be zero in a metastable state. The standard equilibrium density-functional theory (Singh, 1991), on the other hand, finds the equilibrium density profile from solutions of $\delta F[\rho]/\delta\rho(\mathbf{x})=0$. The static and dynamic theories lead to identical descriptions of the inhomogeneous state (Kirkpatrick and Wolynes, 1987). The choice of the free-energy functional plays an important role here, and one can formulate the dynamics by taking into account the nature of the amorphous state (Turski, 1986). In Sec. IX we have discussed the time evolution of the system in the free-energy landscape going beyond the mode-coupling description. It is also interesting to note in this respect that local minima exist (Singh *et al.*, 1985; Kaur and Das, 2001; Kim and Munakata, 2003) for the same density functional that determines the equilibrium states. A unified description of the dynamics supporting both the fluid and the crystal phases still remains a challenge.

The development of the mode-coupling theory from the equations of statistical mechanics for a classical N-particle system have almost exclusively focused on the equilibrium problem. Relaxation in a metastable liquid is studied here in terms of correlation functions averaged over the equilibrium ensemble. There has been some progress on the nonequilibrium problem, as discussed in Sec. XI, for the p-spin interaction models of spin glasses. While the basic equations of the multispin models are very similar to those of mode-coupling theory for structural glasses, important differences remain with respect to the origin of the mode-coupling terms in these two cases (see Sec. XI). In this regard interesting similarities have been found in potential-energy landscape studies of these two types of systems. In recent years, extensive studies of the potential-energy landscape have identified a temperature T_{th} that marks the crossover of the liquid from nonactivated dynamics ($T>T_{\text{th}}$) to hopping between minima through activated processes below T_{th}. Simulations with model systems consisting of a small number of particles strongly suggest that T_{th} is close to the mode-coupling T_c. It is important to note here that the temperature T_c is often identified with mode coupling in such comparisons is where the extrapolated power-law behavior of the diffusion coeffi-

cient (itself obtained from computer simulations) goes to zero. From a theoretical standpoint, however, using the present form of MCT of one-loop order the dynamic transition point obtained is very different. Simulation studies have also shown a self-diffusion different from the predictions of simple mode-coupling theory (see Sec. X.A). Clearly a better understanding of the role of mode couplings in tagged-particle diffusion is needed.

The dramatic changes seen in a supercooled liquid near T_g when it is cooled at a finite rate raise the question of whether an underlying thermodynamic phase transition occurs in the liquid when it is cooled infinitely slowly. This of course remains mainly speculative, since such a situation cannot be realized in practice. It is, however, important for our understanding of the process of glass transformation. Over the last few years, a microscopic approach to the study of the structural glass transition has been developed by Mézard and Parisi (Mézard, 1999; Mézard and Parisi, 1999a, 1999b, 2000). Here the ideas developed for spin glasses were applied to the structural glasses. The starting point of such a theory is the microscopic Hamiltonian of m identical replicas of the system. The free energy of the system is computed by combining the ideas of liquid-state theory with the replica approach. The configurational entropy obtained from the theory vanishes at a temperature T_f ($<T_c$ for mode-coupling theory) where a static transition should occur. This is identified with the glass transition. This theoretical approach is reminiscent of the application of density-functional theories to the freezing transition. The idea of replicas in the structural glasses void of quenched disorder is applied with the understanding that frustration plays the crucial role. In principle one would expect a purely dynamical approach to give similar results. An approach that combined purely dynamical theories applicable at higher temperature with theories applicable for low-temperature glasses might offer us a better understanding of how the frustration is self-generated at the microscopic level. That would make the subject of a new review; our present review is ended here.

ACKNOWLEDGMENTS

I acknowledge the guidance of Gene Mazenko during my years at the University of Chicago. I am deeply grateful to him for introducing me to the theory of liquids. I have also greatly benefited from working with J. Dufty, M. H. Ernst, T. R. Kirkpatrick, and F. Mezei. I thank my students, R. Alhuwalia, U. Harbola, C. Kaur, S. P. Singh, and S. Srivastava, who have worked with me on related topics in recent years. I acknowledge past and ongoing research collaborations with J-L. Barrat, R. Kühn, and R. Schilling. I am grateful to all those who permitted me to reprint figures from their articles. Finally thanks to N. Banerjee, U. Harbola, C. Kaur, R. N. Saini, P. Sen, and S. P. Singh for their help in the preparation of the manuscript.

APPENDIX: DEDUCTION OF THE SELF-CONSISTENT MODEL

1. Analysis of the memory function

We analyze here Eq. (3.10) for the non-Markovian transport coefficient in the equations of motion [Eq. (3.8)] corresponding to a specific set of collective modes. The generalized force corresponding to density, $K_i = \mathcal{Q}\mathcal{L}g_i$, is expressed (Götze, 1991) in terms of its projection on the coupled hydrodynamic modes $\mathcal{C}(\mathbf{k}p\cdots)$ say, following definition (3.7) as

$$K_i = \sum_{kp}^{k'p'} \langle K_i|\mathcal{C}(\mathbf{k}'p')\chi^{-1}(\mathbf{k}p,\mathbf{k}'p')\mathcal{C}(\mathbf{k}p), \tag{A1}$$

where χ^{-1} is the inverse of the correlation matrix $\langle\mathcal{C}(\mathbf{k}p)\mathcal{C}(\mathbf{k}'p')\rangle$. Substituting Eq. (A1) in Eq. (3.10), one obtains the memory function mainly in terms of time correlation functions like $\langle\mathcal{C}(\mathbf{k}p)\exp(-i\mathcal{Q}\mathcal{L}\mathcal{Q})\mathcal{C}(\mathbf{k}'p')\rangle$ and $\langle\mathcal{C}(\mathbf{k}p)\mathcal{C}\mathcal{L}g_i\rangle$. These are further simplified with two crucial approximations described below.

(a) Near the glass transition, density fluctuations are assumed to be most dominant, leading to the simple choice $\mathcal{C}(\mathbf{k}p)=\delta\rho(\mathbf{k})\delta\rho(\mathbf{p})$. Corresponding to this the equal-time correlation matrix is obtained as $\chi^{-1}(\mathbf{k}'p')=\delta_{\mathbf{k}k'}\delta_{\mathbf{p}p'}/[\beta N^2 S(k)S(p)]$.

(b) The next important approximation involves equating four-point correlations of density fluctuations evolving in time with the generator $\mathcal{Q}\mathcal{L}\mathcal{Q}$ with corresponding two-point correlations evolving in time with $\mathcal{L}$,

$$\langle\delta\rho(\mathbf{k})\delta\rho(\mathbf{p})e^{-iQLQ}\delta\rho(\mathbf{k}')\delta\rho(\mathbf{p}')\rangle \simeq \langle\delta\rho(\mathbf{k},t)^*\delta\rho(\mathbf{k}')\rangle\langle\delta\rho(\mathbf{p},t)^*\delta\rho(\mathbf{p}')\rangle. \tag{A2}$$

This reduction has been termed the Gaussian approximation or the Kawasaki approximation in the mode-coupling literature.

The memory function is now obtained in the form

$$m^L(q,t) \simeq (1/n^2N)\sum_{\mathbf{k}} |\langle(\hat{\mathbf{q}}\cdot\mathbf{K})\mathcal{C}(\mathbf{k}\mathbf{k}_1)\rangle|^2 S(k) \times S(k_1)\phi(k,t)\phi(k_1,t), \tag{A3}$$

where $\mathbf{k}_1=\mathbf{q}-\mathbf{k}$. The equilibrium averages $\langle K_i\mathcal{C}(\mathbf{k}\mathbf{k}_1)\rangle\equiv\langle\rho(\mathbf{k})\rho(\mathbf{k}_1)\mathcal{L}g_i\rangle$ are evaluated using classical Poisson bracket relations between ρ and $\mathbf{g}$ to obtain the mode-coupling kernel (4.4).

A somewhat more systematic approach for computing the memory function, due to Zaccarelli *et al.* (2001b), considers the equation for $\rho_{\mathbf{q}}$ [the Fourier transform of density $\rho(\mathbf{x},t)$] in the form of a linear equation,

$$\ddot{\rho}_{\mathbf{q}} + \Omega_q^2\rho_{\mathbf{q}}(t) + \int_o^t L_{\mathbf{q}}(t-s)\dot{\rho}_{\mathbf{q}}(s)ds = f_{\mathbf{q}}(t). \tag{A4}$$

A self-consistent expression for the memory function $L_{\mathbf{q}}$ is obtained in terms of nonlinear functions of $\rho_{\mathbf{q}}$ exploiting the proper fluctuation-dissipation relation. The final

form (4.4) is reached here by assuming that the noise $f_{\mathbf{q}}$ is an additive Gaussian process. The same approach was used by Wu and Cao (2003) for obtaining the memory kernel for a linear molecular liquid. A simple deduction of the self-consistent mode-coupling model was also given by Kawasaki (1995).

2. The field-theoretic formulation

This field-theoretic formalism, referred to as the Martin-Siggia-Rose field theory, is particularly useful for studying the full implications of nonlinearities in the equations of generalized hydrodynamics introduced in Sec. IV. In the functional-integral formulation of mode-coupling theory (Bausch *et al.*, 1976; de Dominicis, 1978; de Dominicis and Pelti, 1978; Janssen, 1979; Jensen, 1981), the renormalized expressions for the transport coefficients appear in a self-consistent manner. Let us consider the equation of motion for the field $\psi_i(\mathbf{x},t)$ as

$$\frac{\partial \psi_i(\mathbf{x},t)}{\partial t} + \mathcal{V}_i[\psi] = \theta_i(\mathbf{x},t), \tag{A5}$$

where $\mathcal{V}_i[\psi]$ is the nonlinear functional of the slow variables ψ_i. The average correlation of the noise θ is given in terms of the bare damping matrix L^o,

$$\langle \theta(\mathbf{x},t)\theta(\mathbf{x}',t')\rangle = 2k_BTL^o(\mathbf{x},\mathbf{x}')\delta(t-t'). \tag{A6}$$

The correlation of the slow variables averaged over the noise is computed from the functional derivatives of the generating functional Z_U obtained in terms of an action functional A_U as

$$Z_U = I_o \int D\psi \int D\hat{\psi} \exp[-A_U(\psi,\hat{\psi})], \tag{A7}$$

with I_o being a constant. The deduction of the Martin-Siggia-Rose action functional A_U involves introduction of hatted fields; for more details, the interested reader is referred to Das and Mazenko (1986). In order to facilitate a discussion of the renormalization scheme, the action functional is written in polynomial form,

$$\begin{aligned} A_U[\Psi] = {} & \frac{1}{2}\sum_{1,2} \Psi(1)G_o^{-1}(1,2)\Psi(2) \\ & + \frac{1}{3}\sum_{1,2,3} U(1,2,3)\Psi(1)\Psi(2)\Psi(3) \\ & - \sum_{1} \Psi(1)U(1). \end{aligned} \tag{A8}$$

In writing Eq. (A8) we have adopted a compact notation in which the index for the specific slow variable ψ_1, the spatial coordinate $\mathbf{x}_1$, and the time t_1 are all incorporated into one index 1 and the hatted and unhatted fields are both denoted by one vector field $\Psi(1)$. The vertex functions $U(1,2,3)$ are defined such that they are symmetric under the exchange of the indices. We have included vertices only up to cubic order in the action (A8) for simplicity. The more generalized treatment is available elsewhere (Das and Mazenko, 1986).

For the specific case of compressible liquids, we have a set of slow variables $\{\rho,\mathbf{g},\mathbf{V}\}$. The action A_U is expressed as a functional of the fields and their hatted counterparts characteristic of the Martin-Siggia-Rose theory. Usually the hatted field $\hat{\psi}$ enters the action functional due an integral representation of the Gaussian distribution for the noise f present in the corresponding stochastic equation for ψ. In the case of liquids, the momentum densities g_i's each satisfy a Langevin equation with a noise. However, the equation for the density ρ, that is, the continuity equation (4.12), is without any noise. The hatted field $\hat{\rho}$ is introduced through the integral representation of the delta function $\delta[\partial\rho(1)/\partial t_1 + \nabla_1\cdot\mathbf{g}(1)]$. Similarly the nonlinear constraint $\mathbf{g}=\rho\mathbf{V}$ is also taken in the form of a delta function $\int D(\mathbf{V})\Pi_{\mathbf{x}}\,\delta[\mathbf{g}-\rho\mathbf{V}]$ and is represented in terms of another conjugate field $\hat{\mathbf{V}}$ as $i\int d1\hat{V}_i(1)[g_i(1)-\rho(1)V_i(1)]$. The Martin-Siggia-Rose action functional A_U written explicitly in terms of the hatted fields is

$$\begin{aligned} A = \int dt \int d\mathbf{x} \Bigg\{ & \sum_{i,j} \hat{g}_i\beta^{-1}L^o\hat{g}_j + i\sum_i \hat{g}_i \Bigg[\frac{\partial g_i}{\partial t} + \rho\nabla_i\frac{\delta F_u}{\delta\rho} \\ & + \sum_j \nabla_j(\rho V_iV_j) - \sum_j L^o_{ij}V_j \Bigg] + i\hat{\rho}\left[\frac{\partial\rho}{\partial t} + \nabla\cdot\mathbf{g}\right] \\ & + i\sum_i \hat{V}_i[g_i-\rho V_i] \Bigg\}, \end{aligned} \tag{A9}$$

where we have set the linear term involving the currents U_i explicitly to zero. Using the transformation $\hat{\psi} \to \hat{\psi}/\sqrt{\beta}$ and $\psi\to\psi\sqrt{\beta}$, we see that the Gaussian terms are $O(1)$ while nonlinear terms of nth order in the ψ's in the action are $O[(k_BT)^{(n-1)/2}]$. Thus the perturbative corrections to the linear theory are formally expressed in $O(k_BT)$ [see Eq. (A12) below].

a. The renormalized perturbation theory

The renormalized theory, which takes into account the role of the nonlinearities (beyond Gaussian terms) is obtained using the standard Feynman-graph method of field theory (Amit, 1999). The one-point function $G(1)=\langle\Psi(1)\rangle$ is obtained from the generating function Z_U with the derivative $\delta/\delta U(1)[\ln Z_U]$. If we include the density variable in the set of slow variables Ψ as $\delta\rho(1)=\rho(1)-\langle\rho(1)\rangle$ then it follows directly that $G(1)$ vanishes as $U\to 0$. The two-point function $G(12)$ is given by

$$G(12) = \frac{\delta}{\delta U(2)}G(1) = \langle\delta\Psi(1)\delta\Psi(2)\rangle, \tag{A10}$$

where $\delta\Psi(1)=\Psi(1)-\langle\Psi(1)\rangle\equiv\Psi(1)$. The inverse of the two-point correlation matrix $G(12)$ is defined through the relation $G^{-1}(13)G(32)=\delta(12)$. $G(12)$ is identical to the $G_o(12)$ for a Gaussian action without any cubic or higher-order terms in the action. The role of the nonlinearities is expressed in terms of the so-called "self-energy matrix" Σ through the Dyson equation,

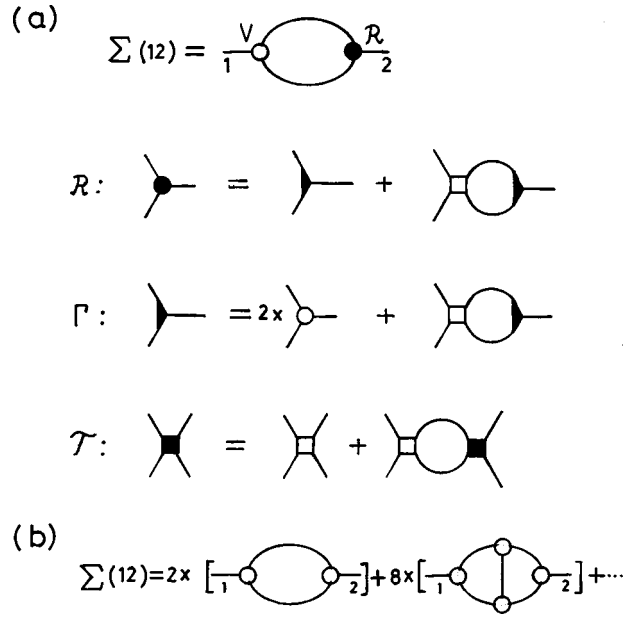

FIG. 14. Diagrammatic expansion for the self-energy Σ. The self-consistent expressions are given by Eqs. (A12)–(A14); ○, $V(123)$; ●, $\mathcal{R}(123)$; solid triangles with three attached legs, $\Gamma(123)$. □, $U(1234)$; ■, $\mathcal{T}(1234)$. The lines joining at both ends with the vertices represent fully renormalized correlation or response functions. (b) Expansion for the self-energy given in part (a) up to second order in (k_BT).

$$G^{-1}(12) = G_o^{-1}(12) - \Sigma(12). \tag{A11}$$

The self-energy matrix Σ for the action (A8) with cubic vertex is obtained from the self-consistent equation (Das and Mazenko, 1986)

$$\Sigma(12) = V(1\bar{6}\bar{3})G(\bar{3}\bar{4})G(\bar{6}\bar{5})R(\bar{4}\bar{5}2). \tag{A12}$$

The renormalized three-point vertex function denoted by $\mathcal{R}(123)$ in Eq. (A12) is determined from the self-consistent integral equations

$$\mathcal{R}(123) = \Gamma(123) + \mathcal{T}(1\bar{4}\bar{5}3)G(\bar{4}\bar{6})G(\bar{5}\bar{7})\Gamma(\bar{7}\bar{6}2),$$

$$\Gamma(123) = 2V(123) + U(1\bar{4}\bar{5}3)G(\bar{4}\bar{6})G(\bar{5}\bar{7})\Gamma(\bar{7}\bar{6}2). \tag{A13}$$

The four-point kernel $\mathcal{T}(1234)$ is to be determined from the integral equation

$$\mathcal{T}(1234) = U(1234) + U(1\bar{2}\bar{3}4)G(\bar{2}\bar{4})G(\bar{3}\bar{5})\mathcal{T}(\bar{5}\bar{4}23), \tag{A14}$$

where we have used the definition $U(1234) = \delta\Sigma(12/\delta G(34)$. To lowest order $U(1234) = 4V(12\bar{3})G(\bar{3}\bar{4})V(34\bar{4})$. The bare vertex function $V(123)$ is controlled by the nonlinearities in the equations of motion for the collective modes. The standard set of graphs representing the coupled equations (A12) and (A13) is shown in Fig. 14(a). A graphical expansion for Σ in terms of the bare vertices V and the full correlation functions G can be obtained to any arbitrary order in principle. In Fig. 14(b) the diagrammatic expansion up to second order in k_BT is shown. In practice the renormalization has been considered only up to one-loop order, as discussed below.

The Martin-Siggia-Rose field theory outlined above involves a large number of correlation functions between the different fields. These broadly belong to two categories: correlation functions $G_{\psi\psi}$ and "response" functions $G_{\psi\hat{\psi}}$. The correlation between a hatted and an unhatted field is the linear-response function corresponding to an equivalent field and is time retarded for maintaining causality. The response functions satisfy the relation $G_{\alpha\hat{\beta}}(q,\omega) = -G^*_{\hat{\beta}\alpha}(q,\omega)$. From the Dyson equation (A11) it then follows that the self-energy matrix elements satisfy $\Sigma_{\alpha\hat{\beta}}(q,\omega) = -\Sigma^*_{\hat{\beta}\alpha}(q,\omega)$. From the construction of the action and causality (Mazenko and Yeo, 1994) the matrix elements $G^{-1}_{\alpha\beta}$ between two unhatted fields are zero, and hence the inverse $G_{\hat{\alpha}\hat{\beta}}$ elements between two hatted fields are zero.

For an isotropic liquid our discussion is somewhat simplified by the fact that we can treat the transverse and longitudinal parts of the vector fields, that is, $\mathbf{g}, \mathbf{V}$ and their hatted counterparts, separately. The transverse components of the vector fields do not couple into the density or its hatted conjugate $\hat{\rho}$. The self-energy matrix $\Sigma_{\alpha_i\beta_j}$ is also expressed as

$$\Sigma_{\alpha_i\beta_j}(q,\omega) = \hat{q}_i\hat{q}_j\Sigma^L_{\alpha\beta}(q,\omega) + (\delta_{ij} - \hat{q}_i\hat{q}_j)\Sigma^T_{\alpha\beta}(q,\omega) \tag{A15}$$

in terms of the longitudinal and transverse parts, denoted by $\Sigma^L_{\alpha\beta}$ and $\Sigma^T_{\alpha\beta}$, respectively. The structure of the nonlinearities in the field theory outlined above obeys the following fluctuation-dissipation relations between correlation and response functions (Deker and Hakke, 1975; Deker, 1979; Das and Mazenko, 1986):

$$G_{V_i\alpha}(q,\omega) = -2k_BT\mathrm{Im}G_{\hat{g}_i\alpha}(q,\omega), \tag{A16}$$

where the index α correspond to an unhatted variable.

b. Nonperturbative results

A number of results for renormalization of the linear theory are obtained exploiting the fluctuation-dissipation relation (A16) in a nonperturbative manner. The renormalized theory takes a simpler form in the hydrodynamic limit of small wave number and frequency. In the transverse case where the hydrodynamic modes are diffusive the self-energy $\Sigma^T(q,\omega)$ is analyzed for $\omega \sim q^2$ in the limit of small q. From symmetry and conservation laws, explicit factors of q and ω in the different elements of the self-energy matrix are identified in this limit, e.g., $\Sigma^{L,T}_{\hat{g}v} = -iq^2\gamma^{L,T}_{\hat{g}v}$, $\Sigma^{L,T}_{\hat{g}\hat{g}} = -q^2\gamma^{L,T}_{\hat{g}\hat{g}}$, and $\Sigma^{L,T}_{\hat{g}\hat{v}} = -iq^2\gamma^{L,T}_{\hat{g}\hat{v}}$. The matrix elements between one vector field ($\mathbf{g}$ or $\mathbf{V}$) and ρ are accompanied with a single power of wave number $\Sigma^L_{\rho\hat{V}} = q\gamma_{\rho\hat{V}}$ or $\Sigma_{\rho\hat{g}} = q\gamma_{\rho\hat{g}}$. Using the fluctuation-dissipation relation (A16), we obtain the transverse current correlation function in the hydrodynamic limit

$$C_{gg}(q,z)=\frac{\chi^T_{gg}(q)}{z+i\eta^R(q,z)}, \tag{A17}$$

with the renormalized shear viscosity in the hydrodynamic limit expressed as

$$\eta^R=\tilde{\eta}_o+\frac{\beta}{2\rho_T}\gamma^T_{\hat{g}\hat{g}}(0,0), \tag{A18}$$

where $\tilde{\eta}_o$ is the bare viscosity divided by the density. The longitudinal case is somewhat more complicated than the transverse one, since here we have to deal with three fields $\{\rho,\mathbf{g},\mathbf{V}\}$ in both the hatted and unhatted sets. In this case there are traveling modes, and hence the self-energies Σ^L are analyzed in the limit $\omega\sim q$ as $q\to 0$. The density correlation function, which is the central quantity in the mode-coupling theory, is also computed from the corresponding response function in the hydrodynamic limit,

$$G_{\rho\rho}(q,\omega)=+2\beta^{-1}\chi_{\rho\rho}(q)\mathrm{Im}G_{\hat{\rho}\rho}(q,\omega), \tag{A19}$$

where $\chi_{\rho\rho}(q)$ is the Fourier transform of the equal-time correlation function. The Laplace transform of the density autocorrelation function normalized to its equal-time value is obtained by inverting the G^{-1} matrix as

$$\phi(q,z)=\frac{z+iq^2\Gamma^R}{z^2-\Omega_q^2+iq^2\Gamma^R[z+i\gamma(q,z)]}, \tag{A20}$$

where $\Omega_q^2=q^2c^2$ with the renormalized sound speed given by $c^2=c_o^2-\gamma'_{\rho\hat{g}}(0,0)$. Since $\Sigma''_{\rho\hat{g}}(0,0)$ is zero in the hydrodynamic limit, the renormalized quantity c is real. The renormalization of the longitudinal viscosity is computed in terms of the corresponding self-energies as

$$\Gamma^R=\tilde{\Gamma}_o+\frac{\beta}{2\rho_L}\gamma^L_{\hat{g}\hat{g}}(0,0), \tag{A21}$$

where $\tilde{\Gamma}_o$ is the corresponding bare viscosity divided by the density. The expression (A20) reduces to the more conventional equation (3.17) for the density correlation function if $\gamma(q,z)$ in the denominator is ignored. The latter is expressed as $\gamma(q,z)=q\Sigma_{\rho\hat{V}}(q,z)$ in terms of the self-energy $\Sigma_{\rho\hat{V}}$. This is a consequence of the nonlinear term involving the $\hat{V}$ field in the Martin-Siggia-Rose action (A9) and originates from the nonlinear constraint (4.14) introduced to deal with the $1/\rho$ nonlinearity in the hydrodynamic equations. To leading order in wave numbers, $\gamma(q,0)$ is approximated as $q^2\tilde{\gamma}$, and is expressed in terms of the self-energy $\Sigma^L_{\hat{V}\hat{V}}$ (Das and Mazenko, 1986). This involves using the nonperturbative relation $\Sigma^L_{\hat{V}\hat{V}}(0,0)=(2\rho_L/\beta c^2)\gamma'_{\rho\hat{V}}(0,0)$ that follows from Eq. (A16).

c. One-loop results

For practical calculations of the self-consistent model with a dynamic transition, the relevant self-energies are computed to one-loop order. Using the vertex functions defined in Eq. (4.18) and the one loop diagrams for $\Sigma^L_{\hat{g}\hat{g}}$ involving the coupling of density fluctuations, we obtain the result (4.4) for the mode-coupling model. Note that here a large number of diagrams due to other nonlinearities are ignored assuming that they give relatively weak contribution that can be absorbed in the definition of the bare transport coefficients. The cutoff function γ is also obtained self-consistently in terms of the hydrodynamic correlation functions. We state the results in terms of the kernel in time $\gamma(q,t)$, where $\gamma(q,z)=\int_o^\infty dte^{izt}\gamma(q,t)$. It is expressed as the sum of two parts, γ_L and γ_T, respectively, referring to the longitudinal and transverse parts in the isotropic fluid. From the one-loop diagrams of the self-energy diagrams (Das and Mazenko, 1986),

$$\gamma_L(q,t)=\frac{1}{2n_o}\int\frac{d\mathbf{k}}{(2\pi)^3}\frac{u}{k}\left[\frac{u}{k}+\frac{u_1}{k_1}\right]\times\frac{S(k)S(k_1)}{S(q)}\dot{\phi}(k_1,t)\dot{\phi}(k,t),$$

$$\gamma_T(q,t)=\frac{1}{2n_o}\int\frac{d\mathbf{k}}{(2\pi)^3}(1-u^2)\frac{S(k_1)}{S(q)}\phi(k_1,t)\phi_T(\vec{k},t), \tag{A22}$$

where $\dot{\phi}$ is the time derivative of the function ϕ and $\mathbf{k}_1\equiv\mathbf{q}-\mathbf{k}$. $u=\hat{\mathbf{q}}\cdot\hat{\mathbf{k}}$ and $u_1=\hat{\mathbf{q}}\cdot\mathbf{k}_1$ where the hatted quantity denotes the corresponding unit vector.

d. Simplified model in terms of the ρ field

An equivalent description of the mode-coupling theory, at least of the simple model with a sharp dynamic transition, is possible in terms of only the density variable rho. By integrating out the momentum density field $\mathbf{g}$, one formulates the dynamics in terms of the density field ρ and its hatted counterpart $\hat{\rho}$. Let us consider the equation of motion for $\mathbf{g}$ in the form

$$\upsilon^{-1}\mathbf{g}+\mathbf{f}_\rho=\theta, \tag{A23}$$

where we have defined $\upsilon^{-1}=\partial_t+L_o\rho^{-1}$, the force $\mathbf{f}_\rho=\rho\nabla\delta F_U[\rho]/\delta\rho(\mathbf{r})$, and θ is the Gaussian white noise. The convective nonlinearity term $\nabla_j[g_ig_j/\rho]$ in Eq. (4.13) has been ignored in Eq. (A23). The momentum field is formally integrated out of the problem by performing a trivial Gaussian integral, and the the action $A[\rho,\hat{\rho}]$ is now simplified to the form

$$A[\rho,\hat{\rho}]=-\int d1\left[\frac{D_o}{2}\rho(\nabla\hat{\rho})^2+i\hat{\rho}\{\dot{\rho}+\beta\nabla\cdot D_o\mathbf{f}_\rho\}\right], \tag{A24}$$

where the bare transport coefficient is $D_o=\tau/\beta$, the particle mass being taken to be unity. In order to reach the above result we have assumed that the momentum density relaxes so fast that the operator υ^{-1} can be replaced by $L_o\rho^{-1}\equiv\tau^{-1}$. The form of the action (A24) indicates that the dynamics can be described in terms of density fluctuations only with the simple equation of motion,

$$\frac{\partial \rho}{\partial t} = D_o \nabla \cdot \left[\rho \nabla \frac{\delta F_U}{\delta \rho} \right] + \theta_\rho, \tag{A25}$$

where θ_ρ is the Gaussian noise with correlation related to D_o. The renormalization to D_o^{-1} is obtained either from the self-energy $\Sigma_{\hat{\rho}\hat{\rho}}$ or from the response self-energy $\Sigma_{\hat{\rho}\rho}$. These two self-energies are related through the fluctuation-dissipation relation $\Sigma'_{\hat{\rho}\rho}(\omega) = \omega/(2\rho_o q^2)\Sigma_{\hat{\rho}\hat{\rho}}(\omega) = -\Sigma_{\rho\hat{\rho}}(\omega)^*$ (Kawasaki and Miyazima, 1997). The nonlinearities in the right-hand side of Eq. (A25) can result even if F_U is completely Gaussian in its density fluctuations.

REFERENCES

Abramowitz, M., and I. A. Stegun, 1965, Eds., *Handbook of Mathematical Functions* (Dover, New York).

Adichtchev, S. V., St. Benkhof, Th. Blochowicz, V. N. Novikov, E. Rössler, Ch. Tschirwitz, and J. Wiedersich, 2002, Phys. Rev. Lett. **88**, 055703.

Ahluwalia, R., and S. P. Das, 1998, Phys. Rev. E **57**, 5771.

Ailawadi, N. K., A. Rahman, and R. Zwanzig, 1971, Phys. Rev. A **4**, 1616.

Akcasu, A. Z., and E. Daniels, 1970, Phys. Rev. A **2**, 962.

Alba-Simionesco, C., and M. Krauzman, 1995, J. Chem. Phys. **102**, 6574.

Alder, B. J. and T. E. Wainright, 1967, Phys. Rev. Lett. **18**, 988.

Alder, B. J., and T. E. Wainright, 1970, Phys. Rev. A **1**, 18.

Allen, M. P., and D. J. Tildesley, 1987, *Computer Simulation of Liquids* (Clarendon, Oxford).

Alley, W. E., B. J. Alder, and S. Yip, 1983, Phys. Rev. A **27**, 3174.

Amit, D., 1999, *Field Theory, The Renormalization Group and Critical Phenomena*, 2nd revised ed. (World Scientific, Singapore).

Amit, D. J., and D. V. I. Roginsky, 1979, J. Phys. A **12**, 689.

Andersen, H. C., 2000, J. Math. Phys. **41**, 1979.

Angelani, L., R. Di Leonardo, G. Parisi, and G. Ruocco, 2001, Phys. Rev. Lett. **87**, 0555021.

Angelani, L., R. Di Leonardo, G. Ruocco, A. Scala, and F. Sciortino, 2000, Phys. Rev. Lett. **85**, 5356.

Angelani, L., R. G. Parisi, G. Ruocco, and G. Viliani, 1998, Phys. Rev. Lett. **81**, 4648.

Angell, C. A., 1984, in *Relaxations in Complex Systems*, edited by K. L. Ngai and G. B. Wright (National Technical Information Service, U.S. Department of Commerce, Springfield, VA), p. 1.

Angell, C. A., J. H. R. Clarke, and L. V. Woodcock, 1981, Adv. Chem. Phys. **48**, 397.

Arnol'd, V. I., 1992, *Catastrophe Theory*, 3rd ed. (Springer, Berlin).

Ashcroft, N. W., and C. David Langreth, 1967, Phys. Rev. **156**, 685.

Ashcroft, N. W., and J. Lekner, 1966, Phys. Rev. **145**, 83.

Bagchi, B., 1987a, Physica A **145**, 273.

Bagchi, B., 1987b, Phys. Lett. A **121**, 29.

Bagchi, B., and S. Bhattacharyya, 2001, Adv. Chem. Phys. **116**, 67.

Bagchi, B., and A. Chandra, 1990, Adv. Chem. Phys. **80**, 1.

Barker, J. A., and D. Henderson, 1976, Rev. Mod. Phys. **48**, 587.

Barrat, J-L., and M. L. Klein, 1991, Annu. Rev. Phys. Chem. **42**, 23.

Barrat, J-L., and W. Kob, 1999, J. Phys.: Condens. Matter **11**, A247.

Barrat, J-L., and A. Latz, 1990, J. Phys.: Condens. Matter **2**, 4289.

Bausch, R., H. Janssen, and H. Wagner, 1976, Z. Phys. B **24**, 113.

Belitz, D., and W. Schirmacher, 1983, J. Phys. C **16**, 913.

Bembenek, S. D., and B. B. Laird, 1995, Phys. Rev. Lett. **74**, 936.

Bengtzelius, U., W. Götze, and A. Sjölander, 1984, J. Phys. C **17**, 5915.

Bergenholtz, J., M. Fuchs, and T. Voigtmann, 2000, J. Phys.: Condens. Matter **12**, 6575.

Berne, B. J., and R. Pecora, 1976, *Dynamic Light Scattering* (Wiley Interscience, New York).

Bernu, B., J. P. Hansen, Y. Hiwatari, and G. Pastore, 1987, Phys. Rev. A **36**, 4891.

Bernu, B., Y. Hiwatari, and J. P. Hansen, 1985, J. Phys. C **18**, L371.

Bhattacharjee, J. K., 1996, Europhys. Lett. **34**, 525.

Bhattacharya, K. K., K. Broderix, R. Kree, and A. Zippelius, 1999, Europhys. Lett. **47**, 449.

Binder, K., and A. P. Young, 1986, Rev. Mod. Phys. **58**, 801.

Birge, N. O., and S. R. Nagel, 1985, Phys. Rev. Lett. **54**, 2674.

Biroli, G. 1999, J. Phys. A **32**, 8365.

Bodeaux, D., and P. Mazur, 1973, Phys. Lett. **43A**, 401.

Böhmer, R., M. Maglione, P. Lunkenheimer, and A. Loidl, 1989, J. Appl. Phys. **65**, 901.

Böhmer, R., K. L. Ngai, C. A. Angell, and D. J. Plazek, 1993, J. Chem. Phys. **99**, 4201.

Boon, J., and S. Yip, 1991, *Molecular Hydrodynamics* (Dover, New York).

Börjesson, L., M. Elmroth, and L. M. Torell, 1990, Chem. Phys. **149**, 209.

Bosse, J., and J. S. Thakur, 1987, Phys. Rev. Lett. **59**, 998.

Bouchaud, J-P., and D. S. Dean, 1995, J. Phys. I **5**, 265.

Bouchaud, J-P., L. F. Cugliandolo, J. Kurchan, and M. Mézard, 1996, Physica A **226**, 243.

Bouchaud, J-P., L. F. Cugliandolo, J. Kurchan, and M. Mézard, 1997, in *Spin Glasses and Random Fields*, edited by A. P. Young (World Scientific, Singapore), p. 161.

Bouchaud, J-P., and M. Mézard, 1994, J. Phys. I **4**, 1109.

Bray, A., 1974, Phys. Rev. Lett. **32**, 1413.

Broderix, K., K. K. Bhattacharya, A. Cavagna, A. Zippelius, and I. Giardina, 2000, Phys. Rev. Lett. **85**, 5360.

Brodin, A., L. Börjesson, D. Engberg, L. M. Torell, and A. P. Sokolov, 1996, Phys. Rev. B **53**, 11 511.

Brodin, A., M. Frank, S. Wiebel, G. Shen, J. Wuttke, and H. Z. Cummins, 2002, Phys. Rev. E **65**, 051503.

Buchner, S., and A. Heuer, 1999, Phys. Rev. E **60**, 6507.

Carnahan, N. F., and K. E. Starling, 1969, J. Chem. Phys. **51**, 635.

Carr, H. Y., and E. M. Purcell, 1954, Phys. Rev. **94**, 630.

Cavagna, A., I. Giardina, and G. Parisi, 1998, Phys. Rev. B **57**, 11 251.

Chamberlin, R. V., 1999, Phys. Rev. Lett. **82**, 2520.

Chandra, P., M. V. Feigel'man, and L. B. Ioffe, 1996, Phys. Rev. Lett. **76**, 4805.

Chandra, P., L. B. Ioffe, and D. Sherrington, 1995, Phys. Rev. Lett. **75**, 713.

Chapmann, S., and T. G. Cowling, 1970, *The Mathematical*

Theory of Non-Uniform Gases (Cambridge University, Cambridge, England).
Chen, S-H., W-R. Chen, and F. Mallamace, 2003, Science **300**, 619.
Chong, S.-H., and M. Fuchs, 2002, Phys. Rev. Lett. **88**, 185702.
Chong, S.-H., and W. Götze, 2002a, Phys. Rev. E **65**, 041503.
Chong, S.-H., and W. Götze, 2002b, Phys. Rev. E **65**, 051201.
Chong, S.-H., W. Götze, and A. P. Singh, 2001, Phys. Rev. E **63**, 011206.
Chong, S.-H., and F. Hirata, 1998, Phys. Rev. E **58**, 6188.
Chung, C. H., and S. Yip, 1969, Phys. Rev. **182**, 323.
Cohen, C., P. D. Fleming, and J. H. Gibbs, 1976, Phys. Rev. B **13**, 866.
Cohen, M. H., and G. S. Grest, 1979, Phys. Rev. B **20**, 1077.
Cole, K. S., and R. H. Cole, 1941, J. Chem. Phys. **9**, 341.
Coluzzi, B., G. Parisi, and P. Verrocchio, 2000, Phys. Rev. Lett. **84**, 306.
Crisanti, A.H. Horner, and H. J. Sommers, 1993, Z. Phys. B: Condens. Matter **92**, 257.
Crisanti, A., and H. J. Sommers, 1992, Z. Phys. B: Condens. Matter **87**, 341.
Cugliandolo, L. F., 2003, in *Slow Relaxations and Nonequilibrium Dynamics in Condensed Matter*, Session LXXVII, 2002 of Les Houches Summer Schools of Theoretical Physics, edited by J-L. Barrat, M. Feigel'man, J. Kurchan, and J. Dalibard (Springer, Berlin), p. 371.
Cugliandolo, L. F., and J. Kurchan, 1993, Phys. Rev. Lett. **71**, 173.
Cugliandolo, L. F., J. Kurchan, R. Monasson, and G. Parisi, 1996, J. Phys. A **29**, 1347.
Cugliandolo, L. F., J. Kurchan, G. Parisi, and F. Ritort, 1995, Phys. Rev. Lett. **74**, 1012.
Cugliandolo, L. F., J. Kurchan, and L. Pelti, 1997, Phys. Rev. E **55**, 3898.
Cugliandolo, L. F., and P. Le Doussal, 1996, Phys. Rev. E **53**, 1525.
Cummins, H. Z., W. M. Du, M. Fuchs, W. Götze, S. Hildebrand, A. Latz, G. Li, and N. J. Tao, 1993, Phys. Rev. E **47**, 4223.
Cummins, H. Z., G. Li, W. M. Du, Y. H. Hwang, and G. Q. Shen, 1997, Prog. Theor. Phys. Suppl. **126**, 21.
Curkier, R. I., and J. R. Mehaffey, 1978, Phys. Rev. A **18**, 1202.
Das, S. P., 1987, Phys. Rev. A **36**, 211.
Das, S. P., 1990, Phys. Rev. A **42**, 6116.
Das, S. P., 1993, J. Chem. Phys. **98**, 3328.
Das, S. P., 1996, Phys. Rev. E **54**, 1715.
Das, S. P., 1999, Phys. Rev. E **59**, 3870.
Das, S. P., 2000, Phys. Rev. E **62**, 1670.
Das, S. P., and J. W. Dufty, 1992, Phys. Rev. A **46**, 6371.
Das, S. P., and G. F. Mazenko, 1986, Phys. Rev. A **34**, 2265.
Das, S. P., G. F. Mazenko, S. Ramaswamy, and J. Toner, 1985a, Phys. Rev. A **32**, 3139.
Das, S. P., G. F. Mazenko, S. Ramaswamy, and J. Toner, 1985b, Phys. Rev. Lett. **54**, 118.
Das, S. P., and R. Schilling, 1994, Phys. Rev. E **50**, 1265.
Dasgupta, C., 1992, Europhys. Lett. **20**, 131.
Dasgupta, C., and O. T. Valls, 1994, Phys. Rev. E **50**, 3916.
Dasgupta, C., and O. T. Valls, 1996, Phys. Rev. E **53**, 2603.
Dasgupta, C., and O. T. Valls, 1999, Phys. Rev. E **59**, 3123.
Dasgupta, C., and O. T. Valls, 2003, Phys. Rev. E **67**, 063501.
Dattagupta, S., and L. A. Turski, 1985, Phys. Rev. Lett. **54**, 2399.
Dattagupta, S., and L. A. Turski, 1993, Phys. Rev. E **47**, 1222.
Davidson, D. W., and R. H. Cole, 1951, J. Chem. Phys. **19**, 1484.
Dawson, K., G. Foffi, M. Fuchs, W. Götze, F. Sciortino, M. Sperl, P. Tartaglia, Th. Voigtmann, and E. Zaccarelli, 2001, Phys. Rev. E **63**, 011401.
De, P., R. Pelcovits, E. Vogel, and J. Vogel, 1993, Phys. Rev. E **47**, 1824.
de Dominicis, C., 1978, Phys. Rev. B **18**, 4913.
de Dominicis, C., and L. Pelti, 1978, Phys. Rev. B **18**, 353.
de Gennes, P. G., 1959, Physica (Amsterdam) **25**, 825.
Deker, U., 1979, Phys. Rev. A **19**, 846.
Deker, U., and F. Haake, 1975, Phys. Rev. A **11**, 2043.
Dendzik, Z., M. Paluch, Z. Gburski, and J. Ziolo, 1997, J. Phys.: Condens. Matter **9**, L339.
Denny, R. A., D. R. Reichman, and J.-P. Bouchaud, 2003, Phys. Rev. Lett. **90**, 0255031.
de Schepper, I., and E. G. D. Cohen, 1980, Phys. Rev. A **22**, 287.
de Schepper, I., and E. G. D. Cohen, 1982, J. Stat. Phys. **27**, 223.
de Schepper, I., A. F. E. M. Haffmans, and H. van Beijeren, 1986, Phys. Rev. Lett. **57**, 1715.
Di Leonardo, R., L. Angelani, G. Parisi, and G. Ruocco, 2000, Phys. Rev. Lett. **84**, 6054.
Dixon, P. K., N. Menon, and S. R. Nagel, 1994, Phys. Rev. E **50**, 1717.
Dixon, P. K., and S. R. Nagel, 1988, Phys. Rev. Lett. **61**, 341.
Dixon, P. K., L. Wu, S. R. Nagel, B. D. Williams, and J. P. Carini, 1990, Phys. Rev. Lett. **65**, 1108.
Doliwa, B., and A. Heuer, 2003, Phys. Rev. E **67**, 031506.
Donati, C., J. F. Douglas, W. Kob, S. J. Plimpton, P. H. Poole, and S. C. Glotzer, 1998, Phys. Rev. Lett. **80**, 2338.
Donati, C., S. C. Glotzer, and P. H. Poole, 1999, Phys. Rev. Lett. **82**, 5064.
Donati, C., F. Sciortino, and P. Tartaglia, 2000, Phys. Rev. Lett. **85**, 1464.
Dorfman, J. R., and E. G. D. Cohen, 1972, Phys. Rev. A **6**, 776.
Dorfman, J. R., and E. G. D. Cohen, 1975, Phys. Rev. A **12**, 292.
Drossel, B., H. Bokil, and M. A. Moore, 2000, Phys. Rev. E **62**, 7690.
Du, W. M., G. Li, H. Z. Cummins, M. Fuchs, J. Toulouse, and L. A. Knauss, 1994, Phys. Rev. E **49**, 2192.
Due, D., and A. D. J. Haymet, 1995, J. Chem. Phys. **103**, 2625.
Due, D., and D. Henderson, 1996, J. Chem. Phys. **104**, 6742.
Dzyaloshinskii, I. E., and G. E. Volovick, 1980, Ann. Phys. (N.Y.) **125**, 67.
Eckert, T., and E. Bartsch, 2002, Phys. Rev. Lett. **89**, 125701.
Ediger, M. D., C. A. Angell, and S. R. Nagel, 1996, J. Phys. Chem. **100**, 13200.
Edwards, S. F., 1964, J. Fluid Mech. **18**, 239.
Elmroth, M., L. Börjesson, and L. M. Torell, 1992, Phys. Rev. Lett. **68**, 79.
Engberg, D. A., A. Wischnewski, U. Buchenau, L. Börjesson, A. J. Dianoux, A. P. Sokolov, and L. M. Torell, 1998, Phys. Rev. B **58**, 9087.
Ernst, M. H., and J. R. Dorfman, 1976, J. Stat. Phys. **12**, 311.
Ernst, M. H., L. K. Haines, and J. R. Dorfman, 1969, Rev. Mod. Phys. **41**, 296.
Ernst, M. H., E. H. Hauge, and J. M. J. van Leeuwen, 1971, Phys. Rev. A **4**, 2055.
Ernst, M. H., E. H. Hauge, and J. M. J. van Leeuwen, 1976, J. Stat. Phys. **15**, 23.

Erpenbeck, J. J., and W. W. Wood, 1981, J. Stat. Phys. **24**, 455.
Evans, D. J. 1980, J. Stat. Phys. **22**, 81.
Eyink, G. L., 1994, Phys. Rev. E **49**, 3990.
Fabbian, L., W. Götze, F. Sciortino, P. Tartaglia, and F. Thiery, 1999, Phys. Rev. E **59**, R1347; **60**, 2430(E).
Fabbian, L., A. Latz, R. Schilling, F. Sciortino, P. Tartaglia, and C. Theis, 1999, Phys. Rev. E **60**, 5768.
Fischer, E. W., 1993, Physica A **201**, 183.
Fischer, K. H., and J. A. Hertz, 1991, *Spin Glasses* (Cambridge University, Cambridge, England).
Fixman, M. 1962, J. Chem. Phys. **36**, 310.
Fleming, P. D., III, and C. Cohen, 1976, Phys. Rev. B **13**, 500.
Foffi, G., W. Götze, F. Sciortino, P. Tartagila, and Th. Voigtmann, 2003, Phys. Rev. Lett. **91**, 085701.
Foffi, G., F. Sciortino, E. Zaccarelli, F. Lo Verso, L. Reatto, K. A. Dawson, and C. N. Likos, 2003, Phys. Rev. Lett. **90**, 238301.
Forster, D., 1975, *Hydrodynamic Fluctuations, Broken Symmetry and Correlation Functions* (Benjamin, Reading, MA).
Forster, D., D. R. Nelson, and M. Stephen, 1977, Phys. Rev. A **16**, 732.
Franosch, T., M. Fuchs, W. Götze, M. R. Mayr, and A. P. Singh, 1997a, Phys. Rev. E **56**, 5659.
Franosch, T., M. Fuchs, W. Götze, M. R. Mayr, and A. P. Singh, 1997b, Phys. Rev. E **57**, 5833.
Franz, S., and J. Hertz, 1995, Phys. Rev. Lett. **74**, 2114.
Franz, S., and M. Mézard, 1994a, Physica A **209**, 1.
Franz, S., and M. Mézard, 1994b, Europhys. Lett. **26**, 209.
Franz, S., M. Mézard, G. Parisi, and L. Pelti, 1998, Phys. Rev. Lett. **81**, 1758.
Franz, S., and G. Parisi, 1997, Phys. Rev. Lett. **79**, 2486.
Franz, S., and M. A. Virasoro, 2000, J. Phys. A **33**, 891.
Frick, B., B. Farago, and D. Richter, 1990, Phys. Rev. Lett. **64**, 2921.
Frick, B., and D. Richter, 1993, Phys. Rev. B **47**, 14 795.
Fuchizaki, K., and K. Kawasaki, 1998a, J. Phys. Soc. Jpn. **67**, 1505.
Fuchizaki, K., and K. Kawasaki, 1998b, J. Phys. Soc. Jpn. **67**, 2158.
Fuchizaki, K., and K. Kawasaki, 1999, Physica A **266**, 400.
Fuchizaki, K., and K. Kawasaki, 2002, J. Phys.: Condens. Matter **14**, 12203.
Fuchs, M., and M. E. Cates, 2002, Phys. Rev. Lett. **89**, 248304.
Fuchs, M., W. Götze, S. Hildebrand, and A. Latz, 1992, Z. Phys. B: Condens. Matter **87**, 43.
Fuchs, M., W. Götze, S. Hofacker, and A. Latz, 1991, J. Phys.: Condens. Matter **3**, 5047.
Fuchs, M., W. Götze, and M. R. Mayr, 1998, Phys. Rev. E **58**, 3384.
Fuchs, M., I. Hofacker, and A. Latz, 1992, Phys. Rev. A **45**, 898.
Fuchs, M., and A. Latz, 1993, Physica A **201**, 1.
Gallo, P., F. Sciortino, P. Tartaglia, and S.-H. Chen, 1996, Phys. Rev. Lett. **76**, 2730.
Gezelter, J. D., E. Rabani, and B. J. Berne, 1997, J. Chem. Phys. **107**, 4618.
Geszti, T. 1983, J. Phys. C **16**, 5805.
Glauber, R. 1963, J. Math. Phys. **4**, 294.
Gleim, T., W. Kob, and K. Binder, 1998, Phys. Rev. Lett. **81**, 4404.
Goldstein, M., 1969, J. Chem. Phys. **51**, 3728.
Götze, W. 1985, Z. Phys. B: Condens. Matter **60**, 195.
Götze, W., 1991, in *Liquids, Freezing and the Glass Transition, Proceedings of the Les Houches Summer School, Course LI*, edited by J. P. Hansen, D. Levesque, and J. Zinn-Justin (Elsevier, New York), p. 287.
Götze, W., 1999, J. Phys.: Condens. Matter **11**, A1.
Götze, W., and R. Haussmann, 1988, Z. Phys. B: Condens. Matter **72**, 403.
Götze, W., and A. Latz, 1989, J. Phys.: Condens. Matter **1**, 4169.
Götze, W., E. Leutheusser, and S. Yip, 1981a, Phys. Rev. A **23**, 2634.
Götze, W., E. Leutheusser, and S. Yip, 1981b, Phys. Rev. A **24**, 1008.
Götze, W., and M. Lücke, 1975, Phys. Rev. A **11**, 2173.
Götze, W., and M. R. Mayr, 2000, Phys. Rev. E **61**, 587.
Götze, W., and L. Sjögren, 1987, Z. Phys. B: Condens. Matter **65**, 415.
Götze, W., and L. Sjögren, 1992, Rep. Prog. Phys. **55**, 241.
Götze, W., and L. Sjögren, 1995, Transp. Theory Stat. Phys. **24**, 801.
Götze, W., and L. Sjögren, 1996, Chem. Phys. **212**, 47.
Götze, W., and M. Sperl, 2002, Phys. Rev. E **66**, 011405.
Götze, W., and T. Voigtmann, 2000, Phys. Rev. E **61**, 4133.
Götze, W., and T. Voigtmann, 2003, Phys. Rev. E **67**, 021502.
Grant, M., and J. D. Gunton, 1985, Phys. Rev. B **32**, 7299.
Gray, C. G., and K. E. Gubbins, 1984, *Theory of Molecular Liquid* (Clarendon, Oxford), Vol. 1.
Grest, G. S., and M. H. Cohen, 1981, Adv. Chem. Phys. **48**, 455.
Grigera, S., A. Cavagna, I. Giardina, and G. Parisi, 2002, Phys. Rev. Lett. **88**, 055502.
Grimsditch, M., R. Bhadra, and L. M. Torell, 1989, Phys. Rev. Lett. **62**, 2616.
Halalay, I. C., Y. Yang, and K. A. Nelson, 1994, J. Non-Cryst. Solids **172-174**, 175.
Hansen, J-P., and J. R. McDonald, 1986, *Theory of Simple Liquids*, 2nd ed. (Academic, London).
Harbola, U., and S. P. Das, 2001, Phys. Rev. E **64**, 046122.
Harbola, U., and S. P. Das, 2002, Phys. Rev. E **65**, 036138.
Harbola, U., and S. P. Das, 2003a, Int. J. Mod. Phys. B **17**, 2395.
Harbola, U., and S. P. Das, 2003b, J. Stat. Phys. **112**, 1131.
Henderson, D., and E. W. Grundke, 1975, J. Chem. Phys. **63**, 601.
Hinze, G., D. D. Brace, S. D. Gottke, and M. D. Fayer, 2000, Phys. Rev. Lett. **84**, 2437.
Hohenberg, P. C., and B. I. Halperin, 1977, Rev. Mod. Phys. **49**, 435.
Hoover, W. G., and F. H. Ree, 1968, J. Chem. Phys. **49**, 3609.
Janssen, H. J., 1976, Z. Phys. B **23**, 377.
Janssen, H. J., 1979, in *Dynamical Critical Phenomena an Related Topics*, edited by C. P. Enz (Springer-Verlag, New York), p. 26.
Jensen, R. V., 1981, J. Stat. Phys. **25**, 183.
Jeong, Y. H., 1987, Phys. Rev. A **36**, 766.
Jeong, Y. H., S. R. Nagel, and S. Bhattacharya, 1986, Phys. Rev. A **34**, 602.
Jonsson, H., and H. C. Anderson, 1988, Phys. Rev. Lett. **60**, 2295.
Kadanoff, L. P., and P. C. Martin, 1963, Ann. Phys. (N.Y.) **24**, 419.
Kadanoff, L. P., and J. Swift, 1968, Phys. Rev. **166**, 89.
Kämmerer, S., W. Kob, and R. Schilling, 1997, Phys. Rev. E **56**, 5450.
Kämmerer, S., W. Kob, and R. Schilling, 1998a, Phys. Rev. E **58**, 2131.

Kämmerer, S., W. Kob, and R. Schilling, 1998b, Phys. Rev. E **58**, 2141.
Kanaya, T., T. Kawaguchi, and K. Kaji, 1994, J. Non-Cryst. Solids **172-174**, 327.
Kartini, E., M. F. Collins, B. Collier, F. Mezei, and E. C. Svensson, 1996, Phys. Rev. B **54**, 6292.
Kaur, C., and S. P. Das, 2001, Phys. Rev. Lett. **86**, 2062.
Kaur, C., and S. P. Das, 2002, Phys. Rev. Lett. **89**, 085701.
Kaur, C., and S. P. Das, 2003a, Phys. Rev. E **67**, 051505.
Kaur, C., and S. P. Das, 2003b, J. Phys.: Condens. Matter **15**, 4657.
Kawasaki, K., 1966a, Phys. Rev. **145**, 224.
Kawasaki, K., 1966b, Phys. Rev. **150**, 291.
Kawasaki, K., 1970a, Phys. Lett. **32A**, 379.
Kawasaki, K., 1970b, Ann. Phys. (N.Y.) **61**, 1.
Kawasaki, K., 1971, Phys. Lett. **34A**, 12.
Kawasaki, K., 1994, Physica A **208**, 35.
Kawasaki, K., 1995, Transp. Theory Stat. Phys. **24**, 755.
Kawasaki, K., 1997, Physica A **243**, 25.
Kawasaki, K., 1998, J. Stat. Phys. **93**, 527.
Kawasaki, K., and K. Fuchizaki, 1998, J. Non-Cryst. Solids **235**, 57.
Kawasaki, K., and Bongsoo Kim, 2001, Phys. Rev. Lett. **86**, 3582.
Kawasaki, K., and Bongsoo Kim, 2002, J. Phys. C **14**, 2265.
Kawasaki, K., and S. Miyazima, 1997, Z. Phys. B: Condens. Matter **103**, 423.
Kawasaki, K., and I. Oppenheim, 1965, Phys. Rev. **139**, A1763.
Keyes, T., 1997, J. Phys. Chem. A **101**, 2921.
Keyes, T., 2000, Phys. Rev. E **62**, 7905.
Kim, B., and A. Latz, 2001, Europhys. Lett. **53**, 660.
Kim, B., and G. F. Mazenko, 1990, Adv. Chem. Phys. **78**, 129.
Kim, B., and G. F. Mazenko, 1991, J. Stat. Phys. **64**, 631.
Kim, B., and G. F. Mazenko, 1992, Phys. Rev. A **45**, 2393.
Kim, Bongsoo, 1992, Phys. Rev. A **46**, 1992.
Kim, Bongsoo, and K. Kawasaki, 2002, J. Phys.: Condens. Matter **14**, 1627.
Kim, K., and T. Munakata, 2003, Phys. Rev. E **68**, 021502.
Kirkpatrick, T. R., 1984, Phys. Rev. Lett. **53**, 1735.
Kirkpatrick, T. R., 1985a, Phys. Rev. A **31**, 939.
Kirkpatrick, T. R., 1985b, Phys. Rev. A **32**, 3130.
Kirkpatrick, T. R., S. P. Das, M. H. Ernst, and J. Piasecki, 1990, J. Chem. Phys. **92**, 3768.
Kirkpatrick, T. R., and J. C. Nieuwoudt, 1986a, Phys. Rev. A **33**, 2651.
Kirkpatrick, T. R., and J. C. Nieuwoudt, 1986b, Phys. Rev. A **33**, 2658.
Kirkpatrick, T. R., and D. Thirumalai, 1987a, Phys. Rev. Lett. **58**, 2091.
Kirkpatrick, T. R., and D. Thirumalai, 1987b, Phys. Rev. B **36**, 5388.
Kirkpatrick, T. R., and D. Thirumalai, 1989, J. Phys. A **22**, L149.
Kirkpatrick, T. R., and P. G. Wolynes, 1987, Phys. Rev. B **35**, 3072.
Kob, W., 2003, in *Slow Relaxations and Nonequilibrium Dynamics in Condensed Matter*, Session LXXVII, 2002 of Les Houches Summer Schools of Theoretical Physics, edited by J-L. Barrat, M. Feigelman, J. Kurchan, and J. Dalibard (Springer, Berlin), p. 199.
Kob, W., and H. C. Andersen, 1994, Phys. Rev. Lett. **73**, 1376.
Kob, W., and H. C. Andersen, 1995a, Phys. Rev. E **51**, 4626.
Kob, W., and H. C. Andersen, 1995b, Phys. Rev. E **52**, 4134.
Kob, W., and J.-L. Barrat, 1997, Phys. Rev. Lett. **79**, 3660.
Kob, W., and J.-L. Barrat, 1999, Europhys. Lett. **46**, 637.
Kob, W., and J.-L. Barrat, 2000, Eur. Phys. J. B **13**, 319.
Kob, W., C. Donati, S. Plimpton, P. H. Poole, and S. C. Glotzer, 1997, Phys. Rev. Lett. **79**, 2827.
Kob, W., M. Nauroth, and F. Sciortino, 2002, J. Non-Cryst. Solids **307-310**, 181.
Kob, W., F. Sciortino, and P. Tartaglia, 2000, Europhys. Lett. **49**, 590.
Kojima, S., and V. N. Novikov, 1996, Phys. Rev. B **54**, 222.
Kraichnan, R., 1959a, J. Fluid Mech. **5**, 32.
Kraichnan, R., 1959b, J. Fluid Mech. **5**, 497.
Kraichnan, R., 1961a, J. Math. Phys. **2**, 124.
Kraichnan, R. 1961b, J. Fluid Mech. **7**, 124.
Kraichnan, R., and S. Chen, 1989, Physica D **37**, 160.
Kree, R., L. A. Turski, and A. Zippelius, 1987, Phys. Rev. Lett. **58**, 1656.
Krieger, U., and J. Bosse, 1987, Phys. Rev. Lett. **59** 1601.
Kühn, R., and U. Horstmann, 1997, Phys. Rev. Lett. **78**, 4067.
Landau, L. D., and E. M. Lifshitz, 1963, *Fluid Mechanics* (Pergamon, London).
Langer, J. S., 1967, Ann. Phys. (N.Y.) **41**, 108.
Langer, J. S., 1969, Ann. Phys. (N.Y.) **54**, 258.
Langer, J. S., 1992, in *Solids Far from Equilibrium*, edited by C. Godréche (Cambridge University, Cambridge, England), p. 297.
Langer, J. S., and L. Turski, 1973, Phys. Rev. A **8**, 3230.
Latz, A., 2000, J. Phys.: Condens. Matter **12**, 6353.
Latz, A., and M. Letz, 2001, Eur. Phys. J. B **19**, 323.
Latz, A., and R. Schmitz, 1996, Phys. Rev. E **53**, 2624.
Lebowitz, J. L., 1964, Phys. Rev. **133**, A895.
Leslie-Pelecky, D. L., and N. O. Birge, 1994, Phys. Rev. Lett. **72**, 1232.
Leutheusser, E., 1984, Phys. Rev. A **29**, 2765.
Levine, H. B., and G. Birnbaum, 1968, Phys. Rev. Lett. **20**, 439.
Li, G., W. M. Du, X. K. Chen, H. Z. Cummins, and N. J. Tao, 1992a, Phys. Rev. A **45**, 3867.
Li, G., W. M. Du, J. Hernandez, and H. Z. Cummins, 1993, Phys. Rev. E **48**, 1192.
Li, G., W. M. Du, A. Sakai, and H. Z. Cummins, 1992b, Phys. Rev. A **46**, 3343.
Li, W., and T. Keyes, 1999, J. Chem. Phys. **111**, 5503.
Liu, C. Z., and I. Oppenheim, 1997, Physica A **235**, 369.
Lovesey, S. W., 1984, *Theory of Neutron Scattering from Condensed Matter* (Clarendon, Oxford).
Löwen, H., J.-P. Hansen, and J.-N Roux, 1991, Phys. Rev. A **44**, 1169.
Lunkenheimer, P., A. Pimenov, M. Dressel, G. Yu Goncharov, R. Böhmer, and A. Loidl, 1996, Phys. Rev. Lett. **77**, 318.
Lunkenheimer, P., A. Pimenov, M. Dressel, B. Schiener, U. Schneider, and A. Loidl, 1997, Prog. Theor. Phys. Suppl. **126**, 123.
Lunkenheimer, P., A. Pimenov, and A. Loidl, 1997, Phys. Rev. Lett. **78**, 2995.
Lundgren, L., P. Svedlindh, P. Norblad, and O. Beckman, 1983, Phys. Rev. Lett. **51**, 911.
Lust, L. M., O. T. Valls, and C. Dasgupta, 1993, Phys. Rev. E **48**, 1787.
Lutsko, J. F., J. W. Dufty, and S. P. Das, 1989, Phys. Rev. A **39**, 1311.
Ma, J., D. V. Bout, and M. Berg, 1996, Phys. Rev. E **54**, 2786.
Ma, S. K., 1976, *Modern Theory of Critical Phenomena* (Benjamin, New York).

Ma, S. K., and G. F. Mazenko, 1975, Phys. Rev. B **11**, 4077.
Ma, S. K., and J. Rudnick, 1978, Phys. Rev. Lett. **40**, 589.
Madan, B., and T. Keyes, 1993, J. Chem. Phys. **98**, 3342.
Madden, P., and D. Kivelson, 1984, Adv. Chem. Phys. **56**, 467.
Mallamace, F., P. Gambadauro, N. Micali, P. Tartaglia, C. Liao, and S.-H. Chen, 2000, Phys. Rev. Lett. **84**, 5431.
Manno, M., and I. Oppenheim, 1999, Physica A **265**, 520.
Marchetti, M. C., 1986, Phys. Rev. A **33**, 3363.
Marconi, U. M. B., and P. Tarazona, 1999, J. Chem. Phys. **110**, 8032.
Marconi., U. M. B., and P. Tarazona, 2000, J. Phys.: Condens. Matter **12**, A413.
Marinari, E., G. Parisi, and F. Ritort, 1994a, J. Phys. A **27**, 7615.
Marinari, E., G. Parisi, and F. Ritort, 1994b, J. Phys. A **27**, 7647.
Martin, P. C., O. Parodi, and P. S. Pershan, 1972, Phys. Rev. A **6**, 2401.
Martin, P. C., E. D. Siggia, and H. A. Rose, 1973, Phys. Rev. A **8**, 423.
Mazenko, G. F., 1973a, Phys. Rev. A **7**, 209.
Mazenko, G. F., 1973b, Phys. Rev. A **7**, 222.
Mazenko, G. F., 1974, Phys. Rev. A **9**, 360.
Mazenko, G. F., S. Ramaswamy, and John Toner, 1983, Phys. Rev. A **28**, 1618.
Mazenko, G. F., and J. Yeo, 1994, J. Stat. Phys. **74**, 1017.
Mazenko, G. F., and S. Yip, 1977, in *Statistical Mechanics: Part B, Time Dependent Processes*, edited by B. J. Berne (Plenum, New York), pp. 181–231.
McComb, W. D., 1990, *The Physics of Fluid Turbulence* (Oxford Science, Oxford).
Menon, N., and S. R. Nagel, 1993, Phys. Rev. Lett. **71**, 4095.
Menon, N., and S. R. Nagel, 1995, Phys. Rev. Lett. **74**, 1230.
Menon, N., S. R. Nagel, and D. C. Venerus, 1994, Phys. Rev. Lett. **73**, 963.
Menon, N., K. P. O'Brien, P. K. Dixon, L. Wu, S. R. Nagel, B. D. Williams, and J. P. Carini, 1992, J. Non-Cryst. Solids **141**, 61.
Mézard, M., 1999, Physica A **265**, 352.
Mézard, M., and G. Parisi, 1999a, J. Chem. Phys. **111**, 1076.
Mézard, M., and G. Parisi, 1999b, Phys. Rev. Lett. **82**, 747.
Mézard, M., and G. Parisi, 2000, J. Phys.: Condens. Matter **12**, 6655.
Mézard, M., G. Parisi, and M. A. Virasoro, 1987, *Spin Glass Theory and Beyond*, Lecture Notes in Physics Vol. 9 (World Scientific, Singapore).
Mezei, F., 1980, Ed., *Neutron Spin Echo: Proceedings* (Springer, Heidelberg/New York).
Mezei, F., 1989, in *Dynamics of Disordered Materials*, edited by D. Richter, A. J. Dianoux, W. Petry, and J. Teixeira (Springer Verlag, Berlin, 1989), p. 164.
Mezei, F., W. Knaak, and B. Farago, 1987, Phys. Rev. Lett. **58**, 571.
Mezei, F., and M. Russina, 1999, J. Phys.: Condens. Matter **11**, A341.
Miyazaki, K., and D. R. Reichman, 2002, Phys. Rev. E **66**, 0505011.
Moore, M. A., and B. Drossel, 2002, Phys. Rev. Lett. **89**, 217202.
Mopsik, F. I., 1984, Rev. Sci. Instrum. **55**, 79.
Mori, H., 1965a, Prog. Theor. Phys. **33**, 423.
Mori, H., 1965b, Prog. Theor. Phys. **34**, 399.
Morkel, Chr., Chr. Gronemeyer, W. Gläser, and J. Bosse, 1987, Phys. Rev. Lett. **58**, 1873.
Mountain, R. D., 1997, J. Chem. Phys. **102**, 5408.
Munakata, T., 1978, J. Phys. Soc. Jpn. **45**, 749.
Munakata, T., 1989, J. Phys. Soc. Jpn. **58**, 2434.
Munakata, T., 1990, J. Phys. Soc. Jpn. **59**, 1299.
Munakata, T., and A. Igarashi, 1977, Prog. Theor. Phys. **58**, 1345.
Munakata, T., and A. Igarashi, 1978, Prog. Theor. Phys. **60**, 45.
Mydosh, J. A., 1993, *Spin-Glasses: An Experimental Introduction* (Taylor & Francis, London).
Nauroth, M., and W. Kob, 1997, Phys. Rev. E **55**, 657.
Nielsen, J. K., and J. C. Dyre, 1996, Phys. Rev. B **54**, 15 754.
Norblad, P., P. Svedlindh, L. Lundgren, and L. Sandlund, 1986, Phys. Rev. B **33**, 645.
Odagaki, T., 1995, Phys. Rev. Lett. **75**, 3701.
Odagaki, T., and Y. Hiwatari, 1990, Phys. Rev. A **41**, 929.
Odagaki, T., T. Yoshidome, T. Tao, and A. Yoshimori, 2002, J. Chem. Phys. **117**, 10151.
Odagaki, T., and A. Yoshimori, 2000, J. Phys.: Condens. Matter **12**, 6509.
Onsager, L., 1931a, Phys. Rev. **37**, 405.
Onsager, L., 1931b, Phys. Rev. **38**, 2265.
Oxtoby, D. W., 1986, J. Chem. Phys. **85**, 1549.
Oxtoby, D. W., 1991, in *Liquids, Freezing and the Glass Transition*, edited by J. P. Hansen, D. Levesque, and J. Zinn-Justin (Elsevier, New York), p. 145.
Parisi, G., 1997, Phys. Rev. Lett. **79**, 3660.
Parisi, G., M. Picco, and F. Ritort, 1999, Phys. Rev. E **60**, 58.
Percus, J. K., and G. J. Yevick, 1958, Phys. Rev. **110**, 1.
Pham, K. N., A. M. Puertas, J. Bergenholtz, S. U. Egelhaaf, A. Moussaïd, P. N. Pusey, A. B. Schofield, M. E. Cates, M. Fuchs, and W. C. K. Poon, 2002, Science **296**, 104.
Phythian, R., 1975, J. Phys. A **8**, 1423.
Phythian, R., 1976, J. Phys. A **9**, 269.
Phythian, R., 1977, J. Phys. A **10**, 777.
Pimenov, A., P. Lunkenheimer, H. Rall, R. Kohlhass, A. Loidl, and R. Böhmer, 1996, Phys. Rev. E **54**, 676.
Pitard, E., and E. I. Shakhnovich, 2001, Phys. Rev. E **63**, 0415011.
Pomeau, Y., and P. Résibois, 1975, Phys. Rep., Phys. Lett. **19**, 63.
Puertas, A. M., M. Fuchs, and M. E. Cates, 2002, Phys. Rev. Lett. **88**, 098301.
Pusey, P. N., 1991, in *Liquids, Freezing and the Glass Transition*, edited by J. P. Hansen, D. Levesque, and J. Zinn-Justin (Elsevier, New York), p. 763.
Rahman, A., 1964, Phys. Rev. **136**, A405.
Ramakrishnan, T. V., and M. Yussouff, 1979, Phys. Rev. B **19**, 2775.
Résibois, P., 1978a, J. Stat. Phys. **19**, 593.
Résibois, P., 1978b, Physica A **94A**, 1.
Résibois, P., and M. de Leener, 1977, *Classical Kinetic Theory of Fluids* (Wiley Interscience, New York).
Ribeiro, M. C. C., and P. A. Madden, 1998, J. Chem. Phys. **108**, 3256.
Rogers, F. J., and D. A. Young, 1984, Phys. Rev. A **30**, 999.
Roux, J.-N., J-L. Barrat, and J.-P. Hansen, 1989, J. Phys.: Condens. Matter **1**, 7171.
Roux, J.-N., J-L. Barrat, and J.-P. Hansen, 1990, Chem. Phys. **149**, 197.
Sachdev, S., 1986, Phys. Rev. B **33**, 6395.
Sanyal, S., and A. K. Sood, 1995, Phys. Rev. E **52**, 4154 (Part I); **52**, 4168 (Part II).

Sanyal, S., and A. K. Sood, 1996, Europhys. Lett. **34**, 361.
Sanyal, S., and A. K. Sood, 1998, Phys. Rev. E **57**, 908.
Sastry, S., P. G. Debenedetti, and F. H. Stillinger, 1998, Nature (London) **393**, 554.
Scala, A., C. Valeriani, F. Sciortino, and P. Tartaglia, 2003, Phys. Rev. Lett. **90**, 115503.
Schilling, R., 2002, Phys. Rev. E **65**, 051206.
Schilling, R., and T. Scheidsteger, 1997, Phys. Rev. E **56**, 2932.
Schmitz, R., J. W. Dufty, and P. De, 1993, Phys. Rev. Lett. **71**, 2066.
Schneider, U., P. Lunkenheimer, R. Brand, and A. Loidl, 1999, Phys. Rev. E **59**, 6924.
Schönhals, A., F. Kremer, A. Hofmann, E. W. Fischer, and E. Schlosser, 1993, Phys. Rev. Lett. **70**, 3459.
Schönhals, A., F. Kremer, and E. Sclosser, 1991, Phys. Rev. Lett. **67**, 999.
Schröder, T. B., S. Sastry, J. Dyre, and S. C. Glotzer, 2000, J. Chem. Phys. **112**, 9834.
Sciortino F., L. Fabbian, S. H. Chen, and P. Tartaglia, 1997, Phys. Rev. E **56**, 5397.
Sciortino, F., L. Fabbian, and P. Tartaglia, 1999, Nuovo Cimento D **20**, 2135.
Sciortino, F., P. Gallo, P. Tartaglia, and S. H. Chen, 1996, Phys. Rev. E **54**, 6331.
Sciortino, F., and W. Kob, 2001, Phys. Rev. Lett. **86**, 648.
Sciortino, F., W. Kob, and P. Tartaglia, 1999, Phys. Rev. Lett. **83**, 3214.
Sciortino, F., and P. Tartaglia, 1997, Phys. Rev. Lett. **78**, 2385.
Sciortino, F., and P. Tartaglia, 2001, Phys. Rev. Lett. **86**, 107.
Siggia, E., 1985, Phys. Rev. A **32**, 3135.
Singh, Y., 1991, Phys. Rep. **207**, 351.
Singh, Y., J. P. Stoessel, and P. G. Wolynes, 1985, Phys. Rev. Lett. **54**, 1059.
Sinha, S., and M. C. Marchetti, 1992, Phys. Rev. A **46**, 4942.
Sjögren, L., 1986, Phys. Rev. A **33**, 1254.
Sjögren, L., 1990, Z. Phys. B: Condens. Matter **79**, 5.
Sjögren, L., and A. Sjölander, 1978, Ann. Phys. (N.Y.) **110**, 122.
Smolej, F., and H. H. Hahn, 1993, Physica A **201**, 164.
Sokolov, A., A. Kisliuk, D. Quitmann, A. Kudlik, and E. Rössler, 1994, J. Non-Cryst. Solids **172-174**, 138.
Sompolinsky, H., and A. Zippelius, 1981, Phys. Rev. Lett. **47**, 359.
Sompolinsky, H., and A. Zippelius, 1982, Phys. Rev. B **25**, 6860.
Srivastava, S., and S. P. Das, 2001, Phys. Rev. E **63**, 011505.
Srivastava, S., and S. P. Das, 2002, J. Chem. Phys. **116**, 2529.
Srivastava, S., U. Harbola, and S. P. Das, 2002, Phys. Rev. E **65**, 051506.
Stillinger, F. H., 1995, Science **267**, 1935.
Stillinger, F. H., and T. A. Weber, 1982, Phys. Rev. A **25**, 978.
Stillinger, F. H., and T. A. Weber, 1984, Science **225**, 983.
Struik, L. C. E., 1978, *Physical Aging in Amorphous Polymers and Other Materials* (Elsevier, Amsterdam).
Szamel, G., and H. Löwen, 1991, Phys. Rev. A **44**, 8215.
Taborek, P., R. N. Kleiman, and D. J. Bishop, 1986, Phys. Rev. B **34**, 1835.
Thakur, J. S., and J. Bosse, 1991a, Phys. Rev. A **43**, 4378.
Thakur, J. S., and J. Bosse, 1991b, Phys. Rev. A **43**, 4388.
Theenhaus, T., R. Schilling, A. Latz, and M. Letz, 2001, Phys. Rev. E **64**, 051505.
Thirumalai, D., R. D. Mountain, and T. R. Kirkpatrick, 1989, Phys. Rev. A **39**, 3563.
Tokuyama, M., and I. Oppenheim, 1997, Physica A **216**, 85.
Tölle, A., H. Schober, J. Wuttke, and F. Fujara, 1997, Phys. Rev. E **56**, 809.
Tölle, A., J. Wuttke, H. Schober, O. G. Randl, and F. Fujara, 1998, Eur. Phys. J. B **5**, 231.
Torell, L. M., L. Börjesson, and A. P. Sokolov, 1995, Transp. Theory Stat. Phys. **24**, 1097.
Torre, R., P. Bartolini, and R. M. Pick, 1998, Phys. Rev. E **57**, 1912.
Toulouse, J., G. Coddens, and R. Pattnaik, 1993, Physica A **201**, 305.
Toulouse, J., R. Pick, and C. Dreyfus, 1996, in *Disordered Materials and Interfaces*, edited by H. E. Stanley, H. Z. Cummins, D. J. Durian, and D. L. Johnson, MRS Symposia Proceedings No. 407 (Materials Research Society, Pittsburgh), p. 161.
Turnbull, D., and J. C. Fisher, 1949, J. Chem. Phys. **17**, 71.
Turski, L. A., 1986, Phys. Scr. **T13**, 259.
Ullo, J. J., and S. Yip, 1985, Phys. Rev. Lett. **54**, 1509.
Ullo, J. J., and S. Yip, 1989, Phys. Rev. A **39**, 5877.
Valls, O. T., and G. F. Mazenko, 1991, Phys. Rev. A **44**, 2596.
Valls, O. T., and G. F. Mazenko, 1992, Phys. Rev. A **46**, 7756.
van Beijeren, H., and M. H. Ernst, 1973, Physica (Amsterdam) **68**, 437.
van Leeuwen, J. M. J., J. Groeneveld, and J. de Boer, 1959, Physica (Amsterdam) **25**, 792.
van Megen, W., 1995, Transp. Theory Stat. Phys. **24**, 1017.
van Megen, W., T. C. Mortensen, S. R. Williams, and J. Müller, 1998, Phys. Rev. E **58**, 6073.
van Megen, W., and S. M. Underwood, 1993a, Phys. Rev. Lett. **70**, 2766.
van Megen, W., and S. M. Underwood, 1993b, Phys. Rev. E **47**, 248.
van Megen, W., and S. M. Underwood, 1994, Phys. Rev. E **49**, 4206.
Verlet, L., and J. J. Weiss, 1972, Phys. Rev. A **5**, 939.
Vincent, E., J. Hammann, and M. Ocio, 1992, in *Recent Progress in Random Magnets*, edited by D. H. Ryan (World Scientific, Singapore), pp. 207-236.
Vincent, E., J. Hammann, M. Ocio, J.-P Bouchaud, and L. F. Cugliandolo, 1997, in *Complex Behaviour of Glassy Systems: Proceedings of the XIV Sitges Conference, Barcelona, 1996*, edited by J. M. Rubi and Conrado Perez-Vicente, Lecture Notes in Physics Vol. 492 (Springer, Berlin), pp. 184–219.
von-Schweidler, E., 1907, Ann. Phys. (Leipzig) **24**, 711.
Williams, G., and D. C. Watts, 1970, Trans. Faraday Soc. **66**, 80.
Woodcock, L. V., 1981, Ann. N.Y. Acad. Sci. **371**, 274.
Woodcock, L. V., and C. A. Angell, 1981, Phys. Rev. Lett. **47**, 1129.
Wu, J., and J. Cao, 2003, Phys. Rev. E **67**, 061116.
Wu, L., 1991, Phys. Rev. B **43**, 9906.
Wu, L., P. K. Dixon, S. R. Nagel, B. D. Williams, and J. P. Carini, 1991, J. Non-Cryst. Solids **131**, 32.
Wuttke, J., J. Hernandez, G. Li, G. Goddens, H. Z. Cummins, F. Fujara, W. Petry, and H. Sillescu, 1994, Phys. Rev. Lett. **72**, 3052.
Wuttke, J., M. Kiebel, E. Bartsch, F. Fujara, W. Petry, and H. Sillescu, 1993, Z. Phys. B: Condens. Matter **91**, 357.
Wuttke, J., M. Ohl, M. Goldammer, S. Roth, U. Schneider, P. Lunkenheimer, R. Kahn, B. Rufflé, R. Lechner, and M. A. Berg, 2000, Phys. Rev. E **61**, 2730.
Yan, Y.-X., and K. A. Nelson, 1987a, J. Chem. Phys. **87**, 6240.
Yan, Y.-X., and K. A. Nelson, 1987b, J. Chem. Phys. **87**, 6257.
Yang, Y., L. J. Muller, and K. A. Nelson, 1996, in *Disordered*

Materials and Interfaces, edited by H. E. Stanley, H. Z. Cummins, D. J. Durian, and D. L. Johnson, MRS Symposia Proceedings No. 407 (Materials Research Society, Pittsburgh), p. 145.
Yang, Y., and K. A. Nelson, 1995, Phys. Rev. Lett. **74**, 4883.
Yang, Y., and K. A. Nelson, 1996, J. Chem. Phys. **104**, 5429.
Yeo, J., 1995, Phys. Rev. E **52**, 853.
Yeo, J., and G. F. Mazenko, 1994, J. Non-Cryst. Solids **172-174**, 1.
Yeo, J., and G. F. Mazenko, 1995, Phys. Rev. E **51**, 5752.
Young, A. P., 1997, Ed., *Spin Glasses and Random Fields* (World Scientific, Singapore).
Zaccarelli, E., G. Foffi, K. A. Dawson, F. Sciortino, and P. Tartaglia, 2001a, Phys. Rev. E **63**, 031501.
Zaccarelli, E., G. Foffi, F. Sciortino, P. Tartaglia, and K. A. Dawson, 2001b, Europhys. Lett. **55**, 157.
Zaccarelli, E., H. Löwen, P. P. F. Wessels, F. Sciortino, P. Tartaglia, and C. N. Likos, 2004, Phys. Rev. Lett. **92**, 225703.
Zeng, Xiao-Chen, D. Kivelson, and G. Tarjus, 1994, Phys. Rev. E **50**, 1711.
Zerah, G., and J. P. Hansen, 1986, J. Chem. Phys. **84**, 2336.
Zippelius, A., B. I. Halperin, and D. R. Nelson, 1980, Phys. Rev. B **22**, 2514.
Zubarev, D. N., V. Morozov, and G. Röpke, 1997, *Statistical Mechanics of Nonequilibrium Processes* (Wiley, New York), Vol. II.
Zwanzig, R., 1961, in *Lectures in Theoretical Physics*, edited by W. E. Britton, B. W. Downs, and J. Down (Wiley-Interscience, New York), Vol. III, p. 135.
Zwanzig, R., 1963, Phys. Rev. **129**, 486.
Zwanzig, R., 1972, in *Statistical Mechanics*, edited by S. A. Rice, K. F. Freed, and J. C. Light (University of Chicago, Chicago).
Zwanzig, R., 1988, J. Chem. Phys. **88**, 5831.
Zwanzig, R., and M. Bixon, 1970, Phys. Rev. A **2**, 2005.